CENTRIFUGAL DISTORTION IN ASYMMETRIC TOP MOLECULES

A Thesis Submitted
In partial Fulfilment of the Requirements
for the Degree of
DOCTOR OF PHILOSOPHY

By
VIJAY KUMAR KAUSHIK

to the

DEPARTMENT OF PHYSICS
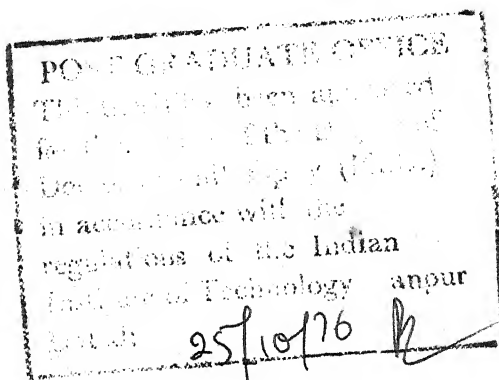# INDIAN INSTITUTE OF TECHNOLOGY KANPUR

TO

MY PARENTS

CERTIFICATE

Certified that the work presented in the thesis entitled 'Centrifugal Distortion in Asymmetric Top Molecules' is the original work of Mr. Vijay Kumar Kaushik carried out under my supervision.

This work has not been submitted anywhere else for a degree.

P. Venkateswarlu 22.4.76
(P. Venkateswarlu)
Senior Professor
Department of Physics
Indian Institute of Technology
Kanpur 208016, India

ACKNOWLEDGEMENTS

Financial help provided by the authorities of Indian Institute of Technology, Kanpur and the Council of Scientific and Industrial Research, New Delhi is gratefully acknowledged.

I also wish to thank Mr. Nihal Ahmad for typing the manuscript.

Vijay Kumar Kaushik
22-4-76

VIJAY KUMAR KAUSHIK

CONTENTS

LIST OF TABLES

LIST OF FIGURE

PREFACE

CENTRIFUGAL DISTORTION IN ASYMMETRIC TOP MOLECULES

By

VIJAY KUMAR KAUSHIK
Ph.D.
Department of Physics
Indian Institute of Technology, Kanpur, India

Centrifugal distortion analysis has been very useful for the complete analysis of the microwave spectrum of a molecule. When high resolution microwave techniques are used to study the pure rotational spectrum of the molecule it is found that the rigid rotator theory is insufficient to describe the observed spectrum. The molecular rotational levels are not predicted exactly by rigid rotator theory but are influenced by the centrifugal distortion. Since the transitions in the conventional microwave region in asymmetric top molecules may occur between states of rather large angular momentum, the shift in energy levels of such molecules due to centrifugal distortion is considerably large compared to that in symmetric top molecules.

The present thesis deals with the calculation of centrifugal distortion constants for inorganic as well as organic molecules. These molecules are Nitric acid (HNO_3 and DNO_3), Tetrafluorohydrazine and Allylamine (NGLG1 and NGLT).

Chapter I deals with the general theory of asymmetric rotators, calculation of rigid rotator energies and calculation of centrifugal distortion constants with different notations, i.e., Nielsen's, Watson's and Kivelson-Wilson's. In the last part of the chapter a-type, b-type and c-type dipole transitions and selection rules are discussed.

Chapter II describes the analysis of the rotational spectrum of HNO_3 and DNO_3 molecules up to J=12 in the frequency region 5-45 GHz. These molecules are nearly oblate with both a and b components of dipole moment and therefore we expect the spectra to consist of a-type as well as b-type transitions. Only twenty-two transitions in HNO_3 and seventeen in DNO_3 have been reported experimentally by earlier workers. Since the molecules are asymmetric tops, we cannot predict the unreported lines accurately unless we apply the centrifugal distortion correction to each transition. We have used the reported spectrum to calculate the rotational and centrifugal distortion constants. Thus, the refined rotational constants and quartic centrifugal distortion constants have been calculated for HNO_3 and DNO_3 molecules. The calculated rotational and centrifugal distortion constants have been used for the prediction of other possible transitions in both the molecules. Different a-type and b-type series have been presented such that the comparative study can be made between the two molecules. Using the earlier constants the difference between the observed and calculated

value was approximately 25 MHz for J=12. Now the calculated values lie within ±0.43 MHz of the experimental values for HNO_3 molecule and within ±0.61 MHz for DNO_3 molecule.

Chapter III describes the analysis of the rotational spectrum of Tetrafluorohydrazine molecule in the frequency region 19-33 GHz up to J=21. This molecule is a near prolate molecule with only c component of dipole moment, so only c-type transitions are expected in the rotational spectrum of the molecule. Only two Q-branch series namely $J_{4,J-3}-J_{5,J-5}$ and $J_{5,J-4}-J_{6,J-6}$ have been reported so far up to J=21 and both these series correspond to $\Delta\tau =3$. The reported spectrum of the tetrafluorohydrazine consists of twenty-five lines. These lines have been used to calculate the refined rotational constants and quartic centrifugal distortion constants. When these calculated rotational and centrifugal distortion constants were used to predict the possible transitions within $\Delta\tau \leq 3$ in the frequency region studied, it was found that even the $J_{4,J-3}J_{5,J-5}$ and $J_{5,J-4}-J_{6,J-6}$ Q-branch series have not been reported completely. Hence we have predicted these series as well as other possible series in the above frequency region completely. The calculated spectrum lies within ±0.41 MHz of the experimental values while the difference between the earlier calculated values and observed values was much larger ranging, for instance, from about 2 MHz for J=10 to 100 MHz for J=21.

Chapter IV of the thesis deals with the analysis of the microwave rotational spectrum of the two isomeric forms of allylamine namely, N-gauche, lone-electron-pair gauche 1 (NGLG1) and N-gauche, lone-electron-pair trans (NGLT) in the frequency region 5-40 GHz up to J=26 and J=29 respectively. The molecule allylamine is near prolate molecule which can have several isomeric forms. As the molecules NGLG1 and NGLT have all the three nonzero dipole components, we expect the rotational spectra of these molecules to be very crowded with all the a-type, b-type and c-type transitions. The reported spectrum of both the forms of the molecule consists of two Q-branch series - $J_{1,J-1}$-$J_{0,J}$ series which is b-type and $J_{1,J}$-$J_{0,J}$ series which is c-type. We have sufficient number of lines to calculate the quartic centrifugal distortion constants of these molecules. The inclusion of centrifugal distortion effect improves the result to such an extent that the ~~lines for which~~ which previously differences between the observed and calculated values were 43.182 MHz for NGLG1 and 430.228 MHz for NGLT, now reduce to within ±0.584 MHz. We have used the rotational and centrifugal distortion constants to predict the other lines of the molecules in the frequency region studied up to the specified J values. One more Q-branch series corresponding to a-type has been predicted with the other possible R-branch series also. at In the end of the chapter a comparative study of Q-branch series of NGLG1 and NGLT has been made.

Recently, after completing the main part of the thesis, the work has been extended to the NF_2H molecule. The spectrum has been analysed up to J=19 in the frequency region 15-36 GHz. The analysis gives refined rotational constants and all quartic distortion constants. The calculated spectrum lies within ±0.06 MHz of the experimental values, while the difference between the earlier calculated values and observed values (even after inclusion of a term of the type $-D_{JK} K_{-1}^2 J(J+1)$) was as high as 33 MHz. The results of analysis are presented in Appendix.

CHAPTER 1

GENERAL THEORY

ABSTRACT

The general theory of asymmetric rotator is given. The calculations for rigid rotator energies are also given and have been extended to nonrigid rotator energies which include the centrifugal distortion correction. Different notations for centrifugal distortion constants, i.e. 'Nielsen, Watson, Kivelson and Wilson' have been discussed and methods of calculation of all these constants have been given. In the end, the three different types of rotational transitions a, b and c types and their selection rules are discussed.

INTRODUCTION

The molecules having unequal moments of inertia about the three principal axes are classified as asymmetric top molecules, i.e. $I_a \neq I_b \neq I_c$.* Those molecules for which $I_a \sim I_b \neq I_c$ are known as near-oblate asymmetric tops while those for which $I_a \neq I_b \sim I_c$ are known as near-prolate asymmetric tops. The degree of symmetry in these types of molecules is considerably less than that of a linear or symmetric top molecule, which complicates the energy level calculations of these molecules.

The two main differences of asymmetric top molecules from symmetric tops are -

(i) In an asymmetric top molecule the projection of J (Total angular momentum) is not constant along any axis fixed in the molecule, i.e. K is not a good quantum number. Thus asymmetry removes the degeneracy of the energy levels, and instead of their being $(J+1)$ levels corresponding to different values of K, each level is now split into $(2J+1)$ sub-levels of different energy values.

(ii) Since the transitions in the conventional microwave region in asymmetric top molecules may occur between states of rather large angular momentum (high J values), the shift in

---

* $I_a < I_b < I_c$.

energy levels of such molecules due to centrifugal distortion is considerably large compared to that observed in symmetric top molecules.

Even though the asymmetric rotator possesses no quantum number comparable to K, the parameter K is retained to label the energy levels in the following manner. Each level is labelled as $J_{K_{-1}K_1}$, the former suffix being the value of K for the particular level in the limiting prolate symmetric top and the latter the value of K in the limiting oblate symmetric top.

CALCULATION OF THE RIGID ROTATOR ENERGY

The energy of a rigid asymmetric top is expressed as:

$$E(I_a, I_b, I_c) = \frac{1}{2}\left(\frac{P_a^2}{I_a} + \frac{P_b^2}{I_b} + \frac{P_c^2}{I_c}\right) \tag{1}$$

where P_a, P_b and P_c are the components of angular momentum along the principal inertial axes a, b and c of the rotator with I_a, I_b and I_c as principal moments of inertia. The rotational constants A, B and C of the molecule can be defined in terms of moments of inertia I_a, I_b and I_c as :

$$A = \hbar^2/2I_a, \quad B = \hbar^2/2I_b \quad \text{and} \quad C = \hbar^2/2I_c \tag{2}$$

So, $$E(A, B, C) = \frac{1}{\hbar^2}\left(AP_a^2 + BP_b^2 + CP_c^2\right) \tag{3}$$

The matrices for P_a, P_b and P_c may be any set of angular momentum matrices which satisfy the Poisson bracket

relations. To examine the general properties of such a set of matrices, let us take a right handed system of Cartesian axes x, y, z fixed in the rotator with the origin at its center of mass. The commutation relations are –

$$P_x P_y - P_y P_x = -i\hbar P_z$$
$$P_y P_z - P_z P_y = -i\hbar P_x \tag{4}$$
and
$$P_z P_x - P_x P_z = -i\hbar P_y$$

A solution of these matrix equations is –

$$\langle JK | P_y | JK+1 \rangle = \langle JK | -iP_x | JK+1 \rangle = \frac{\hbar}{2} [J(J+1) - K(K+1)]^{\frac{1}{2}} \tag{5}$$

$$\langle JK | P_z | JK \rangle = \hbar K$$

The representation used here is that which diagonalizes P_z and $P^2 = P_x^2 + P_y^2 + P_z^2$; and which corresponds to wavefunctions chosen by Wang,[1] Mulliken[2] and Van Vleck.[3] The phase factors of these functions are such that P_y is real and positive, and P_x is imaginary.

It follows from (5) that the squares of the angular momenta which appear in (3) are

$$\langle JK | P_y^2 | JK \rangle = \langle JK | P_x^2 | JK \rangle = \frac{\hbar^2}{2} [J(J+1) - K^2]$$

$$\langle JK | P_y^2 | JK+2 \rangle = -\langle JK | P_x^2 | JK+2 \rangle = \frac{\hbar^2}{4} [\{J(J+1) - K(K+1)\}$$

$$\{J(J+1) - (K+1)(K+2)\}]^{\frac{1}{2}} \tag{6}$$

$$\langle JK \,|\, P_z^2 \,|\, JK \rangle = \hbar^2 k^2$$

and

$$\langle JK \,|\, P^2 \,|\, JK \rangle = \hbar^2 J(J+1) \tag{7}$$

The calculation of energy levels is greatly facilitated by the change in variables made in the following manner as proposed by Ray.[4]

Let σ and ρ be the scalar factors, then –

$$E(\sigma A+\rho,\ \sigma B+\rho,\ \sigma C+\rho) = \frac{1}{\hbar^2} \left[(\sigma A+\rho)\, P_a^2 + (\sigma B+\rho)\, P_b^2 + (\sigma C+\rho)\, P_c^2 \right]$$

$$= \frac{1}{\hbar^2} \left[\sigma (AP_a^2 + BP_b^2 + CP_c^2) + \rho (P_a^2 + P_b^2 + P_c^2) \right]$$

$$= \sigma E(A,B,C) + \rho J(J+1) \tag{8}$$

Ray now chooses

$$\sigma = \frac{2}{A - C} \tag{9}$$

$$\rho = -\frac{A + C}{A - C}$$

so that

$$\sigma A + \rho = 1$$

$$\sigma B + \rho = \frac{2B - A - C}{A - C} \tag{10}$$

$$\sigma C + \rho = -1$$

He then defines the parameters of asymmetry k as

$$k = \frac{2B - A - C}{A - C} \tag{11}$$

so that $-1 \le k \le +1$.

Substituting (9), (10) and (11) into (8) we obtain,

$$E(1,k,-1) = \frac{2}{A-C} E(A,B,C) - \frac{A+C}{A-C} J(J+1)$$

or, $E(k) = \frac{2}{A-C} E(A,B,C) - \frac{A+C}{A-C} J(J+1)$

or, $\frac{A-C}{2} E(k) = E(A,B,C) - \frac{A+C}{2} J(J+1)$

or, $E(A,B,C) = \frac{A+C}{2} J(J+1) + \frac{A-C}{2} E(k)$ (12)

where $E(k)$ is the reduced energy value.[5] Further Ray[4] has shown

$$E_\tau^J(k) = -E_\tau^J(-k)$$ (13)

where $\tau = (K_{-1} - K_1)$.

Equations (12) and (13) show that if the energy levels for the values of k between -1 and 0 are determined, the energy for k between +1 and 0 can be obtained by simple multiplication and addition.[6]

When high resolution microwave techniques are used to study the pure rotational spectrum of the molecule, it was realized that rigid rotator theory is not sufficient to describe the observed spectrum. The molecular energy levels are not predicted exactly by rigid rotator theory but are influenced by perturbations, such as those resulting from rotation-vibration interactions and centrifugal distortion.

CENTRIFUGAL DISTORTION EFFECT

As the bonds between the atoms in a molecule are not rigid, the interatomic distances will vary with the speed of rotation giving rise to centrifugal distortion. The magnitude of the distortion will be dependent on the angular velocity and hence on the rotational energy as well as the location of various off axis atoms.[7]

The theory of centrifugal distortion has been developed by many authors[8-17] for the rotational spectra of asymmetric top molecules. The exact solution of the problem involves the diagonalization of Hamiltonian matrix having off diagonal elements in K only.

The Hamiltonian for a semi-rigid rotator may be expressed as[18] -

$$H = H_0' + H_1'$$

where H_0' = Rigid rotator Hamiltonian

$$= AP_z^2 + BP_x^2 + CP_y^2$$

with $A = \dfrac{\hbar^2}{2I_z}$, $B = \dfrac{\hbar^2}{2I_x}$ and $C = \dfrac{\hbar^2}{2I_y}$

and H_1' = Distortion term

$$= \frac{1}{4} \hbar^4 \sum_{\alpha,\beta,\gamma,\delta} \tau_{\alpha\beta\gamma\delta} \, P_\alpha \, P_\beta \, P_\gamma \, P_\delta$$

where P_α ($\alpha = x, y, z$) is the α-component of angular momentum operator in units of $\hbar$ and $\tau_{\alpha\beta\gamma\delta}$ are the centrifugal distortion

constants independent of the quantum numbers.

So,

$$H = A\, P_z^2 + BP_x^2 + CP_y^2 + \frac{1}{4}\, \hbar^4 \sum_{\alpha\beta\gamma\delta} \tau_{\alpha\beta\gamma\delta}\, P_\alpha\, P_\beta\, P_\gamma\, P_\delta \qquad (1)$$

The Hamiltonian (1) is referred to as Wilson[16] form of Hamiltonian. Because of the non-commutating character of angular momentum components P_α, there are a total of eighty one terms where there are only twenty one different values[19] of τ's in the sum of equation (1). However, the number of constants $\tau_{\alpha\beta\gamma\delta}$ is significantly reduced[19] if the molecule possesses some symmetry. For Orthorhombic molecules for example out of the twenty one coefficients, since many are equal to one another, one is left with only the following nine different quartic distortion constants.

$$\tau_{\alpha\alpha\alpha\alpha}, \; \tau_{\alpha\alpha\beta\beta} = \tau_{\beta\beta\alpha\alpha} \; ; \; \tau_{\alpha\beta\alpha\beta} = \tau_{\alpha\beta\beta\alpha} = \tau_{\beta\alpha\alpha\beta} = \tau_{\beta\alpha\beta\alpha} \qquad (2)$$

with $\alpha \neq \beta$

By using commutation rules governing angular momentum operators, terms of the type $\alpha\beta\alpha\beta$ can be removed from H_1' by choosing the new parameters.

$$A' = A + \frac{1}{4}\, \hbar^4 (3\, \tau_{xyxy} - 2\, \tau_{xzxz} - 2\, \tau_{yzyz})$$

$$B' = B + \frac{1}{4}\, \hbar^4 (3\, \tau_{yzyz} - 2\, \tau_{xyxy} - 2\, \tau_{xzxz})$$

$$C' = C + \frac{1}{4}\, \hbar^4 (3\, \tau_{xzxz} - 2\, \tau_{xyxy} - 2\, \tau_{yzyz})$$

$$\tau'_{\alpha\alpha\alpha\alpha} = \tau_{\alpha\alpha\alpha\alpha}\, \hbar^4 \qquad (3)$$

and $\tau'_{\alpha\alpha\beta\beta} = (\tau_{\alpha\alpha\beta\beta} + 2\tau_{\alpha\beta\alpha\beta}) \hbar^4; \alpha \neq \beta$

The Hamiltonian (1) can then be written as —

$$H = A' P_z^2 + B' P_x^2 + C' P_y^2 + \frac{1}{4} \sum \tau'_{\alpha\alpha\beta\beta} P_\alpha^2 P_\beta^2 \qquad (4)$$

This is the Kivelson-Wilson form of Hamiltonian. Here —

$$\tau'_{\alpha\alpha\beta\beta} = \tau'_{\beta\beta\alpha\alpha} \qquad (5)$$

Expanding (4), we get —

$$H = A' P_z^2 + B' P_x^2 + C' P_y^2 + \frac{1}{4} \tau'_{xxxx} P_x^4 + \frac{1}{4} \tau'_{yyyy} P_y^4$$

$$+ \frac{1}{4} \tau'_{zzzz} P_z^4 + \frac{1}{4} \tau'_{xxyy} (P_x^2 P_y^2 + P_y^2 P_x^2) +$$

$$+ \frac{1}{4} \tau'_{yyzz} (P_y^2 P_z^2 + P_z^2 P_y^2) + \frac{1}{4} \tau'_{zzxx} (P_z^2 P_x^2 + P_x^2 P_z^2)$$

$$\qquad (6)$$

Using the angular momentum relations[18] we get the expectation values of various operators on the right hand side of (6) as —

$$\left\langle P_x^4 \right\rangle = \left(\frac{1}{B'-C'}\right)^2 [C'^2 P^4 + 2C' (A'-C') P^2 \left\langle P_z^2 \right\rangle$$

$$+ (A'-C')^2 \left\langle P_z^4 \right\rangle - 2C' P^2 E_r - 2(A'-C') E_r \left\langle P_z^2 \right\rangle + E_r^2]$$

where $E_r = \left\langle H_r \right\rangle = A' \left\langle P_z^2 \right\rangle + B' \left\langle P_x^2 \right\rangle + C' \left\langle P_y^2 \right\rangle$,

$$\left\langle P_y^4 \right\rangle = \left(\frac{1}{B'-C'}\right)^2 [B'^2 P^4 + 2B' (A'-B') P^2 \left\langle P_z^2 \right\rangle + (A'-B')^2$$

$$\left\langle P_z^4 \right\rangle - 2B' P^2 E_r - 2(A'-B') E_r \left\langle P_z^2 \right\rangle + E_r^2],$$

$$\left\langle P_x^2 P_y^2 + P_y^2 P_x^2 \right\rangle = -2\left(\frac{1}{B'-C'}\right)^2 \left[B'C' \ P^4 + (A'B'+A'C'-2B'C')P^2 \right.$$

$$\left\langle P_z^2 \right\rangle + (A'-B')(A'-C')\left\langle P_z^4 \right\rangle - (B'+C')$$

$$\left. P^2 E_r - (2A'-B'-C') \ E_r \left\langle P_z^2 \right\rangle + E_r^2 \right], \qquad (7)$$

$$\left\langle P_x^2 P_z^2 + P_z^2 P_x^2 \right\rangle = -2\left(\frac{1}{B'-C'}\right)\left[C'P^2 \left\langle P_z^2 \right\rangle + (A'-C')\left\langle P_z^4 \right\rangle - E_r \left\langle P_z^2 \right\rangle \right] \ ,$$

and

$$\left\langle P_y^2 P_z^2 + P_z^2 P_y^2 \right\rangle = \left(\frac{2}{B'-C'}\right)\left[B'P^2 \left\langle P_z^2 \right\rangle + (A'-B')\left\langle P_z^4 \right\rangle - E_r \left\langle P_z^2 \right\rangle \right].$$

[In deriving above relations, the following relations
have been used –

$$P_x^2 = \left[H_r - (A'-C') \ P_z^2 - C'P^2 \right] / \ (B'-C') \qquad (8)$$

$$P_y^2 = \left[H_r - (A'-B') \ P_z^2 - B'P^2 \right] / \ (C'-B') \quad]$$

From these one may construct the desired average value
equations –

$$\left\langle P^4 \right\rangle = J^2 (J+1)^2 \ \hbar^4$$

$$\left\langle H_r^2 \right\rangle = E_r^2$$

$$\left\langle H_r P^2 + P^2 H_r \right\rangle = 2 E_r \ J \ (J+1) \ \hbar^2$$

$$\left\langle H_r P_z^2 + P_z^2 H_r \right\rangle = 2 E_r \left\langle P_z^2 \right\rangle \qquad (9)$$

$$\left\langle P^2 P_z^2 + P_z^2 P^2 \right\rangle = 2J \ (J+1) \left\langle P_z^2 \right\rangle \hbar^2$$

and also $\quad \langle JK | P^2 | JK \rangle = J(J+1) \, \hbar^2 \qquad (10)$

and $\quad \langle JK | P_z | JK \rangle = \hbar K \qquad (11)$

because the basis sets are such that these diagonalize P_z and P^2.

Using the above relations, we get the Nielsen's expression for energy as -

$$E^* = E_r + A_1 E_r^2 + A_2 E_r J(J+1) + A_3 J^2(J+1)^2 +$$

$$A_4 \, J(J+1) \langle P_z^2 \rangle + A_5 \langle P_z^4 \rangle + A_6 E_r \langle P_z^2 \rangle \qquad (12)$$

wherein E_r is the energy of a rigid rotator and

$$A_1 = \frac{16R_6}{(B'-C')^2}$$

$$A_2 = -[\frac{16R_6(B'+C')}{(B'-C')^2} + \frac{4\delta}{(B'-C')}]$$

$$A_3 = - D_J + 2R_6 + \frac{16R_6 B'C'}{(B'-C')^2} + 2\delta \frac{(B'+C')}{(B'-C')}$$

$$A_4 = -[D_{JK} - 2\delta\sigma - 16R_6 \frac{(A'^2-B'C')}{(B'-C')^2} + 4R_6 \, \sigma^2$$

$$+ 4R_5 \frac{(B'+C')}{(B'-C')}] \qquad (13)$$

---

*In the case of symmetric rotator R_5, R_6 and δ vanish and $B=C$. It can also be seen that the factors multiplying R_5, R_6 and δ are finite.[20] With these results and remembering that $\langle P_z^4 \rangle = \langle P_z^2 \rangle^2 = K^4$ in the symmetric rotator limit, one gets (from equation (12))

$$E = E_r - D_J J^2(J+1)^2 - D_{JK} J(J+1) K^2 - D_K K^4$$

which is the result given by Dennison and Slawsky.[21]

$$A_5 = - [D_K + 4R_5 \sigma + 2R_6 - 4R_6 \sigma^2]$$

$$A_6 = \frac{8R_5 - 16R_6\sigma}{(B'-C')}$$

and

$$\sigma = \frac{2A'-B'-C'}{B'-C'}$$

The constants δ, D_J, D_{JK}, D_K, R_5 and R_6 are Nielsen's centrifugal distortion constants and are given in terms of τ's as –

$$\delta = - \frac{1}{16} \hbar^4 [\tau_{xxxx} - \tau_{yyyy}]$$

$$D_J = - \frac{1}{32} \hbar^4 [3\tau_{xxxx} + 3\tau_{yyyy} + 2\tau_{xxyy} + 4\tau_{xyxy}]$$

$$D_K = D_J - \frac{1}{4} \hbar^4 [\tau_{zzzz} - \tau_{zzxx} - \tau_{yyzz} - 2\tau_{xzxz} - 2\tau_{yzyz}]$$

$$D_{JK} = - D_J - D_K - \frac{1}{4} \hbar^4 \tau_{zzzz} \tag{14}$$

$$R_5 = - \frac{1}{32} \hbar^4 [\tau_{xxxx} - \tau_{yyyy} - 2(\tau_{xxzz} + 2\tau_{xzxz})$$

$$+ 2 (\tau_{yyzz} + 2\tau_{yzyz})]$$

and

$$R_6 = \frac{1}{64} \hbar^4 [\tau_{xxxx} + \tau_{yyyy} - 2(\tau_{xxyy} + 2\tau_{xyxy})]$$

Rearrangement of terms in the energy expression (12) gives the energy of semi-rigid rotator as[22-23]

$$E = E_r + E_d$$

where E_r is the energy of a rigid rotator with the following modified rotational constants –

$$\mathcal{A} = A' + 16R_6$$

$$\mathcal{B} = B' - \frac{16R_6 \ (A'-C')}{(B'-C')} \tag{15}$$

$$\mathcal{C} = C' + \frac{16R_6 \ (A'-B')}{(B'-C')}$$

and

$$E_d = -d_J \ J^2(J+1)^2 - d_{JK} \ J(J+1) \left\langle P_z^2 \right\rangle - d_K \left\langle P_z^4 \right\rangle$$

$$-d_{EJ} \ E_r \ J(J+1) - d_{EK} \ E_r \left\langle P_z^2 \right\rangle \tag{16}$$

where d-coefficients are given by Watson[22-23] in terms of the Nielsen's coefficients as -

$$d_J = D_J - \frac{2\delta \ (B'+C')}{(B'-C')} - 2R_6$$

$$d_{JK} = D_{JK} - 2\sigma\delta + 4 \ (R_5 + 2\sigma \ R_6) \frac{B'+C'}{B'-C'} + 12 \ R_6$$

$$d_K = D_K + 4\sigma \ (R_5 + 2\sigma \ R_6) - 10R_6 \tag{17}$$

$$d_{EJ} = \frac{4\delta}{B'-C'}$$

and

$$d_{EK} = - \ \frac{8(R_5 + 2\sigma R_6)}{(B'-C')}$$

The difficulty with the Kivelson-Wilson formalism arises from the fact that the six angular momentum terms appearing in the last term of eqn. (4) are not independent.[26] In order to remove this difficulty, Watson chose the rotational constants as -

$$A'' = A' - \frac{1}{2} \ \tau'_{xxyy}$$

$$B' = B' - \frac{1}{2} \ \tau'_{zzyy}$$

$$C'' = C' - \frac{1}{2} \ \tau'_{zzxx} \tag{18}$$

$$\tau''_{\alpha\alpha\alpha\alpha} = \tau'_{\alpha\alpha\alpha\alpha} \qquad \alpha = x, \ y, \ z$$

$$\tau_1 = \tau'_{xxyy} + \tau'_{yyzz} + \tau'_{zzxx}$$

and

$$\tau_2 = \frac{A'}{S} \ \tau'_{xxyy} + \frac{B'}{S} \ \tau'_{zzyy} + \frac{C'}{S} \ \tau'_{zzxx}$$

where

$$S = A' + B' + C'$$

These eight parameters are Watson's parameters. The angular momentum operators corresponding to these parameters are somewhat arbitrary. This arises because the number of parameters in Watson's[22-25] formulation is one less than the number appearing in Kivelson-Wilson form of Hamiltonian. In order to remove this difficulty it is convenient to define one more parameter. Once this parameter is defined, the transformation from Watson set to Kivelson-Wilson set is well defined and hence the operators corresponding to the Watson parameters also become well defined. A convenient but not a unique choice for this parameter is -

$$\tau_3 = \frac{S}{B'-A'} \ \tau'_{zzxx} + \frac{S}{A'-C'} \ \tau'_{zzyy} + \frac{S}{C'-B'} \ \tau'_{xxyy} \qquad (19)$$

With the above choice of parameters the Hamiltonian can be written as -

$$H = A'' \ P_z^2 + B'' \ P_x^2 + C'' \ P_y^2 + \frac{1}{4} \sum \tau''_{\alpha\alpha\alpha\alpha} \ P_\alpha^4 + \tau_1 P_1^4 + \tau_2 P_2^4 + \tau_3 P_3^4$$

$$(20)$$

where

$$P_1^4 = \frac{1}{3} \left\{ \left[\frac{A'}{A'-C'} - \frac{B'}{C'-B'} \right] \left[\frac{1}{2} P_y^2 + \frac{1}{4} (P_z^2 P_x^2 + P_x^2 P_z^2) \right] + \right.$$

$$\left[\frac{B'}{B'-A'} - \frac{C'}{A'-C'} \right] \left[\frac{1}{2} P_z^2 + \frac{1}{4} (P_x^2 P_y^2 + P_y^2 P_x^2) \right] + \left[\frac{C'}{C'-B'} \right.$$

$$\left. \left. - \frac{A'}{B'-A'} \right] \left[\frac{1}{2} P_x^2 + \frac{1}{4} (P_z^2 P_y^2 + P_y^2 P_z^2) \right] \right\} \, ,$$

$$P_2^4 = \frac{S}{3} \left\{ \left[\frac{1}{C'-A'} + \frac{1}{C'-B'} \right] \left[\frac{1}{2} P_y^2 + \frac{1}{4} (P_z^2 P_x^2 + P_x^2 P_z^2) \right] + \left[\frac{1}{A'-B'} \right. \right.$$

$$\left. + \frac{1}{A'-C'} \right] \left[\frac{1}{2} P_z^2 + \frac{1}{4} (P_x^2 P_y^2 + P_y^2 P_x^2) \right] + \left[\frac{1}{B'-C'} + \frac{1}{B'-A'} \right]$$

$$\left. \left[\frac{1}{2} P_x^2 + \frac{1}{4} (P_z^2 P_y^2 + P_y^2 P_z^2) \right] \right\},$$

$$P_3^4 = \frac{1}{3S} \left\{ [B'-A'] \left[\frac{1}{2} P_y^2 + \frac{1}{4} (P_z^2 P_x^2 + P_x^2 P_z^2) \right] + [C'-B'] \right.$$

$$\left[\frac{1}{2} P_z^2 + \frac{1}{4} (P_x^2 P_y^2 + P_y^2 P_x^2) \right] + [A'-C'] \left[\frac{1}{2} P_x^2 + \frac{1}{4} (P_z^2 P_y^2 + P_y^2 P_z^2) \right] \right\}$$

(21)

with

$$S = A' + B' + C'$$

For a planar molecule the value of τ_3 may be conventionally fixed by using planarity conditions

$$\tau_{zzyy} = \left(\frac{C^2}{A^2} \right) \tau_{zzzz} + \left(\frac{C^2}{B^2} \right) \tau_{zzxx}$$

$$\tau_{xxyy} = \left(\frac{C^2}{B^2} \right) \tau_{xxxx} + \left(\frac{C^2}{A^2} \right) \tau_{zzxx}$$

$$\tau_{yyyy} = \left(\frac{C^2}{A^2} \right) \tau_{zzyy} + \left(\frac{C^2}{B^2} \right) \tau_{xxyy}$$

(22)

and then it can be shown that for planar molecules

$$\tau_3 = \frac{3}{2} \left(\frac{B'-C'}{A'-C'}\right) \left(\frac{S}{A'+B'}\right) \tau'_{zzzz} - \frac{3}{2} \left(\frac{A'-C'}{B'-C'}\right) x$$

$$\left(\frac{S}{A'+B'}\right) \tau'_{xxxx} - \frac{1}{2} \left(\frac{S}{A'-B'}\right) \left(\frac{A'}{A'-C'} + \frac{B'}{B'-C'}\right) \tau_1$$

$$+ \frac{1}{2} \left(\frac{S}{A'-B'}\right) \left(\frac{S}{A'-C'} + \frac{S}{B'-C'}\right) \tau_2 \qquad (23)$$

Equation (20) represents Watson's form of Hamiltonian modified by Kirchhoff.[26]

In Kirchhoff's notation the Hamiltonian of eqn. (20) is written as

$$H = A'' P_a^2 + B'' P_b^2 + C'' P_c^2 + \frac{1}{4} \sum \tau'_{\alpha\alpha\alpha\alpha} P_\alpha^4 + \tau_1 P_1^4 + \tau_2 P_2^4 + \tau_3 P_3^4$$

and the Hamiltonian of equantion (4) as –

$$H = A' P_a^2 + B' P_b^2 + C' P_c^2 + \frac{1}{4} \sum \tau'_{\alpha\alpha\beta\beta} P_\alpha^2 P_\beta^2$$

where a, b, c stand for z, x and y respectively. Discussion of the spectra will be given using Kirchhoff's notations.

SPECIAL CASE OF DOUBLET SPLITTING

A much simpler method of calculating Q-branch transitions between K-doublet levels, is to expand the matrices to first order in distortion parameters.[27,28] This method is referred to as HSKW[29] method. Now, if the equation

$$\Delta^1 (J_K) = 2KJ(J+1) \frac{\delta}{H} + (K-1) J(J+1) \frac{D_{JK}}{G-F}$$

$$- \frac{4}{3} K (K^2+2) \frac{R_5}{H} + \frac{2}{3} K(K-1)(2K-1) \frac{D_K}{G-F}$$

$$+ \frac{8}{3} K (K^2-1) \frac{(G-F)}{H^2} R_6 \qquad (24)$$

be the first order approximation to the reduced* distortion
correction, then to the first order, the transition frequency
is given by –

$$\nu^1 (J_K) = \nu^R (J_K) [1 + \Delta^1 (J_K)] \tag{25}$$

where $\nu^R(J_K)$ is the calculated rigid rotator frequency.
This is, in effect, the HSKW formula in terms of reduced
distortion constants.*

HIGHER ORDER TREATMENT

Equation (4) for the rotational energy includes terms
up to the fourth order in angular momentum. However, for
very light molecules the following additional terms in the
sixth order in angular momentum will also be considered.
These are first given by Pierce[30] as

$$H_J J^3 (J+1)^3 + H_{JK} J^2 (J+1)^2 \left\langle P_z^2 \right\rangle + H_{KJ} J(J+1) \left\langle P_z^4 \right\rangle$$

$$+ H_K \left\langle P_z^6 \right\rangle \tag{26}$$

where H_J, H_{JK}, H_{KJ} and H_K are sextic distortion constants.
Similarly equation (20) includes centrifugal distortion cor-
rection only up to fourth order of angular momentum as –

---

*Actual distortion constants are equal to $\frac{A-C}{2}$ times the reduced
distortion constants.

$$H = A'' P_z^2 + B'' P_x^2 + C'' P_y^2 + \tfrac{1}{4} \sum_{\alpha=x,y,z} \tau'_{\alpha\alpha\alpha\alpha} P_\alpha^4 + \tau_1 P_1^4$$

$$+ \tau_2 P_2^4 + \tau_3 P_3^4 \tag{27}$$

and Watson's[25] theory to sixth order in angular momentum gives the following additional terms to the above equation

$$H_J P^6 + H_{JK} P^4 P_z^2 + H_{KJ} P_z^4 P^2 + H_K P_z^6 + h_J{}^* P^4 (P_x^2 - P_y^2)$$

$$+ h_{JK} P^2 \cdot [P_z^2 (P_x^2 - P_y^2) + (P_x^2 - P_y^2) P_z^2]$$

$$+ h_K [P_z^4 (P_x^2 - P_y^2) + (P_x^2 - P_y^2) P_z^4] \tag{28}$$

where H_J, H_{JK}, H_{KJ}, H_K, h_J, h_{JK} and h_k are sextic distortion constants.

SELECTION RULES AND DIFFERENT TYPES OF TRANSITIONS

The selection rules for J are $\Delta J = 0, \pm 1$. $\Delta J = 0$ specifies the Q-branch while $\Delta J = -1$ and $\Delta J = +1$ specify the P and R branches respectively. The selection rules for pseudo-quantum numbers K_{-1} and K_1 are, however, derived from the symmetry considerations.[6,31] Numerical evaluation shows that, in general, the most intense transitions are those for which K_{-1} and K_1 change by 0 or ± 1. However, nonzero matrix elements are obtained for $|\Delta K_{\pm 1}| = 2,3,4\ldots$ also, but their magnitude falls off rapidly with increasing $|\Delta K_{\pm 1}|$.

---

*Watson used $2h_J$ for this parameter.

The spectrum of an asymmetric rotator is complicated by three different types of transitions. These are of a, b or c-type depending upon which component of the dipole moment makes the transition possible.

SYMMETRY CLASSIFICATION OF ASYMMETRIC ROTATOR TRANSITIONS

It is to be noted that the asymmetric rotator Hamiltonian commutes with all the operations of the four group (D_2 or V) of the Table 1.1. The proof of this can be given as follows —

We know that the Hamiltonian for a rigid rotator is —

$$H_r = \frac{2\pi}{\hbar} [A \, P_a^2 + B \, P_b^2 + C \, P_c^2] \tag{1}$$

Clearly H_r commutes with the identity operation E. As H_r is invariant with respect to a cyclic change $a \to b \to c$, if we prove that H_r commutes with C_2^a, the commutation with C_2^b and C_2^c would follow. Performing the operation C_2^a we obtain,

$$C_2^a \, a \, C_2^a = a$$

$$C_2^a \, b \, C_2^a = -b \tag{2}$$

$$C_2^a \, c \, C_2^a = -c \tag{3}$$

Table 1.1. Character table for D_2 (or V) group in asymmetric rotator notations

D_2(V)	E	C_2^a	C_2^b	C_2^c		
A	1	1	1	1	ee	
B_c	1	1	-1	-1	oe	ϕ_{cF}
B_b	1	-1	1	-1	oo	ϕ_{bF}
B_a	1	-1	-1	1	eo	ϕ_{aF}

so that

$$C_2^a \, b^2 = b^2 \tag{4}$$

$$C_2^a \, c^2 = c^2 \tag{5}$$

which shows that

$$C_2^a \, A = A \tag{6}$$

Similarly

$$C_2^a \, B = B \tag{7}$$

and

$$C_2^a \, C = C \tag{8}$$

Entirely similar reasoning leads to –

$$C_2^a \, P_a^2 = P_a^2$$
$$C_2^a \, P_b^2 = P_b^2 \tag{9}$$

and

$$C_2^a \, P_c^2 = P_c^2$$

Substitution of (6), (7), (8) and (9) into equation (1) gives –

$$C_2^a \, H_r C_2^a = H_r \tag{10}$$

which implies[32] that –

$$C_2^a \, H_r - H_r \, C_2^a = 0 \tag{11}$$

Similarly we can show that –

$$C_2^b \, H_r - H_r \, C_2^b = 0 \tag{12}$$

and

$$C_2^c \, H_r - H_r \, C_2^c = 0$$

i.e., H_r commutes with C_2^a, C_2^b and C_2^c. The importance of this result is that it tells us that the stationary states of the asymmetric rotator can be classified by irreducible representations or symmetry species of the $V(D_2)$ point group, A, B_a, B_b and B_c. The correlation of asymmetric rotator eigen-state $|JK_{-1}K_1\rangle$ with these representations requires rather tedious[33] investigation of the symmetry properties of the eigenfunctions.

It is found, for example, that states for which $|JK_{-1}K_1\rangle$ = $|J$ even even$\rangle$ transform like the representation A or symbolically -

$$|J \text{ even even}\rangle \rightarrow A \tag{13}$$

where the terms even and odd refer to the evenness or oddness of the prolate and oblate K values of the asymmetric rotator states. Similarly -

$$
\begin{aligned}
|J \text{ even odd}\rangle &\rightarrow B_a \\
|J \text{ odd even}\rangle &\rightarrow B_c \\
|J \text{ odd odd}\rangle &\rightarrow B_b
\end{aligned}
\tag{14}
$$

and

These are indicated in the above table by the abbreviations ee, eo, oe and oo and it is to be noted that we have used, King, Hainer and Cross[6] and not the Dennison's[34] notations.

The dipole matrix element is given by[32]

$$|\langle JK_{-1}K_1 |\mu| JK_{-1}K_1\rangle|^2 = \sum_{g,F} \mu_g^2 \cdot \{\langle JK_{-1}K_1 | \phi_{gF} |J' K'_{-1}K'_1\rangle\}^2 \tag{15}$$

g-type (g=a,b,c) transitions occur only if

$$\Gamma \times \Gamma_{\phi_{gF}} \times \Gamma' \rightarrow \Gamma_A \qquad (16)$$

where Γ, Γ_{gF}, Γ' and Γ_A are species of $|JK_{-1}K_1\rangle$, ϕ_{gF}, $|J'K'_{-1}K'_{+1}\rangle$ and the totally symmetric representation A, respectively. Since ϕ_{gF} transform like simple vectors, the correlation is $\phi_{aF} \rightarrow B_a$, $\phi_{bF} \rightarrow B_b$ and $\phi_{cF} \rightarrow B_c$ as shown in the above table.

The a-type transitions are found by performing all the triple products $\Gamma \times \Gamma_{\phi_{aF}} \times \Gamma'$. For example, the character of representation formed by $\Gamma_{ee} \times \Gamma_{aF} \times \Gamma_{eo}$ for the operator $\tilde{R}$ is obtained by the character table by performing the product.

$$\chi(R) = \chi^{ee}(R) \ \chi^{aF}(R) \ \chi^{eo}(R) \qquad (17)$$

which gives -

$$\chi(E) = \chi(C_2^a) = \chi(C_2^b) = \chi(C_2^c) = 1 \qquad (18)$$

which in turn shows -

$$\Gamma_{ee} \times \Gamma_{aF} \times \Gamma_{eo} \rightarrow \Gamma_A \qquad (19)$$

Investigating another triple product representation, $\Gamma_{ee} \times \Gamma_{aF} \times \Gamma_{oo}$, we find the characters to be -

$$\chi(E) = 1, \ \chi(C_2^a) = -1, \ \chi(C_2^b) = -1, \ \chi(C_2^c) = 1 \qquad (20)$$

so that

$$\Gamma_{ee} \times \Gamma_{aF} \times \Gamma_{oo} \rightarrow \Gamma_{B_a} \qquad (21)$$

Similarly we find

$$\Gamma_{ee} \times \Gamma_{aF} \times \Gamma_{oe} \rightarrow \Gamma_{B_b}$$

$$\Gamma_{oo} \times \Gamma_{aF} \times \Gamma_{eo} \rightarrow \Gamma_{B_b}$$

$$\Gamma_{oo} \times \Gamma_{aF} \times \Gamma_{oe} \rightarrow \Gamma_A \qquad\qquad (22)$$

and

$$\Gamma_{eo} \times \Gamma_{aF} \times \Gamma_{oe} \rightarrow \Gamma_{B_c}$$

which completes all the possibilities for the ϕ_{aF} matrix elements. Thus, it can be seen that the a-type transitions can occur only when the $K_{-1}K_1$ labels obey the selection rules ee $\leftrightarrow$ eo or oo $\leftrightarrow$ oe.

In a similar fashion the b and c-type selection rules can be established and these have been listed in Table 1.2. It is to be noted that the selection rules are exclusive, that is, those permitted by a-type rules are not permitted by b- or c-type selection rules, etc.

Table 1.2. Symmetry selection rules for asymmetric rotator transitions

Dipole component	Permitted transitions
a	ee $\leftrightarrow$ eo, oo $\leftrightarrow$ oe
b	ee $\leftrightarrow$ oo, eo $\leftrightarrow$ oe
c	ee $\leftrightarrow$ oe, oo $\leftrightarrow$ eo

As a result of these selection rules the number of allowed transitions are considerably reduced for molecules having one or two nonzero dipole moment components.

CHAPTER 2

CENTRIFUGAL DISTORTION CONSTANTS OF NITRIC ACID

ABSTRACT

The rotational spectra of HNO_3 and DNO_3 molecules have been analysed up to $J=12$ in the frequency region 5000-45000 MHz. Both a and b-type transitions are analysed. The analysis gives refined rotational constants and all quartic centrifugal distortion constants.

INTRODUCTION

The first microwave study of nitric acid was made by Millen and Morton[35] who observed the HNO_3 transitions up to J=3. Subsequently, the same authors extended this study[36] up to J=12 in the frequency region 8-35 GHz and also to some of the isotopic species of HNO_3. They also calculated the structure parameters of nitric acid. Later, Cox and Riveros[37] further extended the study of this molecule. Recently the far infrared spectrum of nitric acid vapor has been reported by Fleming.[38] He has found that the transition frequencies calculated using rigid rotator model differ from the observed frequencies. He attributes this difference to the centrifugal distortion in the molecule.

The molecules HNO_3 and DNO_3 are near oblate symmetric rotators with μ_a = 1.99 D and μ_b = 0.83D[36] and so they involve both a and b-type transitions. In order to improve our knowledge of these molecules and for the better analysis of the microwave spectrum in their ground vibrational states we have in the present work calculated the centrifugal distortion constants guided by the behaviour of the frequencies calculated theoretically.

ANALYSIS OF THE SPECTRUM

The observed spectrum was fitted to the model of Watson[22-25] using the techniques described by Kirchhoff.[26]

To start with, the rigid rotator energies were calculated using the rigid rotator constants A, B and C (which are calculated using the observed frequencies of low J transitions). The differences between the observed and calculated energies were used to find the rotational and centrifugal distortion constants δA, δB, δC, τ'_{aaaa}, τ'_{bbbb}, τ'_{cccc}, τ_1, τ_2 and τ_3 of eqn. (1) below, by linear least square fitting* giving unit weighting to all the transitions.

$$H = (A + \delta A)\, P_a^2 + (B + \delta B)\, P_b^2 + (C + \delta C)\, P_c^2 + \frac{1}{4} \sum_{\alpha = a,b,c} \tau'_{\alpha\alpha\alpha\alpha} \times P_\alpha^4 + \tau_1 P_1^4 + \tau_2 P_2^4 + \tau_3 P_3^4$$

or,

$$H - (A P_a^2 + B P_b^2 + C P_c^2) = \delta A P_a^2 + \delta B P_b^2 + \delta C P_c^2 + \frac{1}{4} \sum_{\alpha = a,b,c} \tau'_{\alpha\alpha\alpha\alpha} \times P_\alpha^4 + \tau_1 P_1^4 + \tau_2 P_2^4 + \tau_3 P_3^4 \qquad (1)$$

where $A P_a^2 + B P_b^2 + C P_c^2$ is the rigid rotator energy, and

$$A'' = A + \delta A, \quad B'' = B + \delta B \quad \text{and} \quad C'' = C + \delta C.$$

Rotational and centrifugal distortion parameters thus determined were inserted in the Hamiltonian given in equation

---

*Given in detail in Chapter 4.

of Chapter 1 and used to calculate the transition energies. The differences between the observed and calculated values were refitted and the iteration process was continued until the variation of rotational and centrifugal distortion constants were insignificant.

Because nitric acid is a planar molecule, the planarity conditions are used to calculate the undeterminable parameter τ_3 at each step of iteration. Once τ_3 has been set, the Kivelson-Wilson parameters A', B', C', τ'_{bbcc}, τ'_{ccaa} and τ'_{aabb} may be calculated.[26] The calculated parameters are given in Tables 2.3 and 2.4. The quality of the fit can be seen from Tables 2.1 and 2.2.

GENERAL DISCUSSION

Different series of transitions have been seen in the frequency region chosen and up to J=12 for both the molecules. These series can be divided as -

1. Q-branch, a-type

2. R-branch, a-type

3. Q-branch, b-type

4. R-branch, b-type

1. Q-Branch, a-type Transitions

Nine Q-branch, a-type series have been predicted in the frequency region studied. Out of these nine, five correspond to $\Delta\tau = 1$ and four correspond to $\Delta\tau = 3$.

Series corresponding to $\Delta\tau = 1$

The frequencies of lines belonging to all the five series of this class decrease with the increase in J and centrifugal distortion (C.D.) corrections are always negative and increase with the increase in J.

(i) $J_{J-1,1}-J_{J-1,2}$ series - Except $8_{7,1}-8_{7,2}$ line of HNO_3 and $6_{5,1}-6_{5,2}$ line of DNO_3 all the transitions of this series have been reported[35,36] earlier. For HNO_3, the lines of interest in this series lie between 17517.547 MHz corresponding to J=2 and 5984.009 MHz corresponding to J=8 and for DNO_3 between 15833.097 MHz corresponding to J=2 and 5093.385 MHz corresponding to J=6. The frequencies and C.D. corrections for lines belonging to this series are shown in Table 2.5.

(ii) $J_{J-2,2}-J_{J-2,3}$ series - All the transitions of this series except lines corresponding to J=3 and J=4 of HNO_3 and corresponding to J=9 of DNO_3 have already been reported.[36] As can be seen from Table 2.6, for HNO_3 the lines of interest lie between 31046.613 MHz corresponding to J=3 and 9245.560 MHz

corresponding to J=12, while for DNO_3 between 29138.535 MHz corresponding to J=3 and 7743.580 MHz corresponding to J=9.

(iii) $J_{J-3,3}-J_{J-3,4}$ series — Only transitions from J=8 to J=12 of DNO_3 belonging to this series have been reported[36] so far, but none for HNO_3. As can be seen from Table 2.7 for HNO_3 the lines of interest lie between 43854.755 MHz corresponding to J=4 and 29478.368 MHz corresponding to J=12, while for DNO_3 between 41965.824 MHz corresponding to J=4 and 10486.600 MHz corresponding to J=12.

(iv) $J_{J-4,4}-J_{J-4,5}$ series — This series has only been reported for DNO_3 and no line of HNO_3 molecule lies in the frequency region studied. The results for these lines are shown in Table 2.8.

(v) $J_{J,0}-J_{J,1}$ series — The lines belonging to this series have been predicted at low frequencies. Only two lines corresponding to J=1 and J=2 have been predicted for HNO_3 and the single line corresponding to J=1 for DNO_3. The results for these lines are shown in Table 2.9.

Series Corresponding to $\Delta \tau = 3$

Out of the four series which belong to this class only one series has so far been reported and that too only for HNO_3 molecule. These series are as follows.

(i) $J_{J,1}-J_{J-2,2}$ series - Only the line $3_{3,1}-3_{1,2}$ belonging to this series of HNO_3 has been reported[35] so far. As can be seen from Table 2.10. the lines of interest in this series lie between 20349.458 MHz corresponding to J=2 and 41625.914 MHz corresponding to J=7 for HNO_3, while for DNO_3 between 21139.455 MHz corresponding to J=2 and 40403.673 MHz corresponding to J=5. The frequencies of these transitions increase with the J and C.D. corrections are such that their contributions are negative for all these DNO_3 transitions. For HNO_3 C.D. Corrections are negative up to J=4 and after that these become positive and increase with J.

(ii) $J_{5,J-4}-J_{3,J-3}$ series - The C.D. corrections for the transitions of this series increase with the J. Only three lines of this series have been predicted for both the molecules. For the line corresponding to J=5 the centrifugal distortion correction is very small but beyond J=5 it increases fast with the increase in J value. The frequencies and C.D. corrections of transitions belonging to this series are shown in Table 2.11.

(iii) $J_{J-2,3}-J_{J-4,4}$ series - The C.D. corrections increase with increase in J value for this series also but its effect is such that the nonrigid rotator frequencies are always less than the rigid rotator frequencies. The frequencies and C.D. corrections for these lines are shown in Table 2.12.

(iv) $J_{J-1,2}-J_{J-3,3}$ series - No line belonging to this series has been observed for either of the molecules. As can be seen from Table 2.13 the lines of interest in this series lie between 31538.456 MHz corresponding to J=3 and 43064.440 MHz corresponding to J=9 for HNO_3, while for DNO_3 between 30765.712 MHz corresponding to J=3 and 38451.077 MHz corresponding to J=6. The frequencies of these lines increase with J. The C.D. corrections of lines belonging to this series are such that their values are negative and increase with the J up to J=7 and after that decrease with J. Since no line was found for DNO_3 after J=6, we expect lines corresponding to J=7,8 and 9 beyond 45 GHz such that the centrifugal distortion correction for the line corresponding to J=7 will be larger than 10.132 MHz in magnitude and will decrease afterward with the increase in J value.

2. R-branch, a-type Transitions

All the three predicted R-branch, a-type series correspond to $\Delta\tau=1$. Out of these three series only one transition $2_{1,2}-1_{1,1}$ of $J_{1,J}-J-1_{1,J-1}$ series has so far been reported[36] for DNO_3. For series $J_{1,J}-J-1_{1,J-1}$ and $J_{0,J}-J-1_{0,J-1}$ a pair of lines corresponding to J=2 and J=3, separated by about 12 GHz have been predicted to lie in the region of interest for both the molecules. The frequencies and C.D. corrections for these

lines are shown in Tables 2.14 and 2.15. For the third series $J_{J-1,1}-J-1_{J-1,0}$ only one line has been predicted whose frequency and centrifugal distortion correction is shown in Table 2.16.

Other Transitions

One transition $1_{0,1}-0_{0,0}$ which was observed experimentally[35,36] for both the molecules have been predicted. For DNO_3* the frequency and C.D. correction are 17347.705 MHz and -0.095 MHz and for HNO_3 are 18360.507 MHz and -0.066 MHz.

3. Q-branch, b-type Transitions

All the eight predicted Q-branch, b-type series correspond to $\Delta\tau =2$. Out of these eight, only three series have so far been reported for HNO_3. These three series are as follows:

(i) $J_{J-1,1}-J_{J-2,2}$ series - Only two lines corresponding to J=2 and 3 of this series have so far been reported[35] for HNO_3 molecule. The frequencies of the lines belonging to this series increase with J from J=5 onwards for HNO_3 and from J=4 onwards for DNO_3. The C.D. corrections, however, increase up to J=6 and then decrease up to J=8 beyond which they continue to increase after a change in sign for J=9. All the lines of this series up to J=12 have been predicted for HNO_3 but for DNO_3 those up to J=9 only have been predicted. The results for these lines are shown in Table 2.17.

---

*This line was observed with hyperfine components.

(ii) $J_{J,0}-J_{J-1,1}$ series - Only one line; $3_{3,0}-3_{2,1}$ of HNO_3 belonging to this series has so far been reported.[35] As is clear from Table 2.18, for HNO_3 the lines of interest lie between 6750.378 MHz corresponding to J=1 and 42017.282 MHz corresponding to J=10, while for DNO_3 between 6935.585 MHz corresponding to J=1 and 39882.383 MHz corresponding to J=7. The frequencies of lines belonging to this series increase with the increase in J. The C.D. corrections increase up to J=2 and then decrease and ultimately change sign and then again increase with J.

(iii) $J_{J,1}-J_{J-1,2}$ series - Only one line; $3_{3,1}-3_{2,2}$ of HNO_3 belonging to this series was observed[35] experimentally. The lines of interest lie between 20250.954 MHz corresponding to J=2 and 44639.642 MHz corresponding to J=10 for HNO_3 and between 20806.571 MHz corresponding to J=2 and 42710.910 MHz corresponding to J=7 for DNO_3. As can be seen from Table 2.19, the frequency of a transition in this series increase with the J. The C.D. corrections first increase with the J and then decrease, ultimately change sign, and finally again increase with the increase in rotational quantum number.

The next two series of this class which have not so far been reported are such that their C.D. corrections increase with the J. These two series are -

(i) $J_{J-3,3}-J_{J-4,4}$ series - For HNO_3 the lines of interest of this series lie between 43855.133 MHz corresponding to J=4 and 33403.574 MHz corresponding to J=12, while for DNO_3 between 41970.360 MHz corresponding to J=4 and 33989.150 MHz corresponding to J=12. The frequencies and centrifugal distortion corrections corresponding to different J are given in Table 2.20.

(ii) $J_{J-4,4}-J_{J-5,5}$ series - Lines of this series occur in the frequency region of interest only for DNO_3. No line was, however, observed experimentally because both the predicted lines occur at frequencies above 35 GHz (the region above 35 GHz has not yet been studied). The frequencies and C.D. corrections for these lines are shown in Table 2.21.

The remaining three series of this class have not yet been reported. These series are -

(i) $J_{J-2,2}-J_{J-3,3}$ series - The HNO_3 series starts at 31053.313 MHz corresponding to J=3 and the frequencies decrease with the J up to J=10 for which the frequency is 23827.704 MHz, but further ahead in the series the frequencies increase with the J. The DNO_3 series starts at 29181.311 MHz corresponding to J=3 and the frequencies decrease with the J up to J=7 for which the frequency is 22721.662 MHz, but further ahead frequencies increase with the J. The frequencies and C.D. corrections for these lines are shown in Table 2.22.

(ii) $J_{J-1,2}-J_{J-2,3}$ series – The lines of interest of this series lie between 31531.755 MHz corresponding to J=3 and 43935.530 MHz corresponding to J=11 for HNO_3 and between 30722.936 MHz corresponding to J=3 and 42881.985 MHz corresponding to J=8 for DNO_3. As can be seen from Table 2.23, the frequencies of transitions for both the molecules increase with the J but the C.D. corrections first increase and then decrease with the J.

(iii) $J_{J-2,3}-J_{J-3,4}$ series – All the predicted lines belonging to this series lie in the frequency region 40-45 GHz, which has not yet been studied experimentally. The frequencies of these lines first decrease and then increase with the J. The frequencies and C.D. corrections for these lines are shown in Table 2.24.

4. R-branch, b-type Transitions

Both the predicted R-branch, b-type series correspond to $\Delta\tau = 2$. Out of these series $J_{1,J}-J-1_{0,J-1}$ and $J_{0,J}-J-1_{0,J-1}$, only two transitions of HNO_3 and DNO_3* have so far been reported[35,36] which belong to $J_{1,J}-J-1_{0,J-1}$ series. As can be seen from Tables 2.25 and 2.26 the frequencies as well as C.D. corrections for these lines increase with the J.

---

*Line $1_{1,1}-0_{0,0}$ was observed with hyperfine components.

Other Transitions

Only one b-type transition $2_{2,1}-1_{1,0}$ for DNO_3 has been
predicted at 44946.933 MHz with the centrifugal distortion
correction as +0.133 MHz.

It is clear from above discussion that the spectra of
the two isotopes HNO_3 and DNO_3 show nearly similar behaviour
as far as the centrifugal distortion correction is concerned.
However, for some of the series the centrifugal distortion
corrections do not vary in the same manner for the two
molecules. The reason for this discrepancy could be that some
of the seventeen observed transitions for DNO_3 might be in
significant error in their measurement, which is reflected in
the overall fit of the transitions. Elimination of such faulty
transitions could perhaps give us a better fit but due to
small number of transitions available such a procedure could
not be adopted. Hence there is still room for refinement in
the constants of DNO_3 molecule. Because of the availability
of relatively large number of observed transition frequencies,
the analysis is more complete for the HNO_3 molecule and conse-
quently the constants obtained for this molecule are more
refined.

Table 2.1.   The microwave spectrum of HNO_3

Std. dev = 0.078 MHz

Transition	Calculated freq. MHz	Observed freq.* MHz	Centrifugal corr. MHz
$1_{0,1}-0_{0,0}$	18360.507	18360.53	-0.066
$1_{1,1}-0_{0,0}$	19271.623	19271.60	-0.060
$2_{1,1}-2_{1,2}$	17517.547	17517.49	-0.302
$2_{1,1}-2_{0,2}$	17616.051	17616.03	-0.317
$2_{1,2}-1_{0,1}$	31792.800	31792.80	-0.173
$3_{3,1}-3_{1,2}$	22161.087	22161.00	-0.503
$3_{2,1}-3_{2,2}$	16215.648	16215.64	-0.809
$3_{2,1}-3_{1,2}$	16700.791	16700.74	-0.843
$3_{3,1}-3_{2,2}$	21675.945	21676.16	-0.469
$3_{3,0}-3_{2,1}$	9448.053	9447.97	-0.018
$4_{3,1}-4_{3,2}$	14534.252	14534.25	-1.553
$5_{3,2}-5_{3,3}$	29175.275	29175.32	-3.554
$5_{4,1}-5_{4,2}$	12540.993	12540.98	-2.565
$6_{4,2}-6_{4,3}$	27369.731	27369.67	-5.693
$6_{5,1}-6_{5,2}$	10344.191	10344.23	-3.818
$7_{5,2}-7_{5,3}$	24993.477	24993.51	-8.504
$7_{6,1}-7_{6,2}$	8097.546	8097.58	-5.167
$8_{6,2}-8_{6,3}$	22147.431	22147.00	-11.616
$9_{7,2}-9_{7,3}$	18969.572	18969.56	-15.867
$10_{8,2}-10_{8,3}$	15628.213	15628.19	-19.927
$11_{9,2}-11_{9,3}$	12317.350	12317.35	-23.546
$12_{10,2}-12_{10,3}$	9245.560	9245.56	-25.945

*The observed transition frequencies are corresponding to the observations of Millen and Morton.[35,36]

Table 2.2. The microwave spectrum of DNO_3

Std. dev = 0.347 MHz

Transition	Calculated freq. MHz	Observed freq* MHz	Centrifugal corr. MHz
$2_{1,1}-2_{1,2}$	15833.097	15832.83	-0.304
$2_{1,2}-1_{1,1}$	29417.497	29417.40	-0.303
$2_{1,2}-1_{0,1}$	31075.302	31075.40	-0.298
$3_{1,2}-3_{1,3}$	29138.535	29138.41	-0.908
$3_{2,1}-3_{2,2}$	13579.431	13579.09	-0.895
$4_{2,2}-4_{2,3}$	27215.912	27215.84	-2.274
$4_{3,1}-4_{3,2}$	10808.330	10807.99	-1.575
$5_{3,2}-5_{3,3}$	24229.789	24229.63	-3.865
$5_{4,1}-5_{4,2}$	7834.196	7833.96	-2.283
$6_{4,2}-6_{4,3}$	20396.234	20396.03	-5.506
$7_{5,2}-7_{,5,3}$	16065.609	16065.29	-7.020
$8_{5,3}-8_{5,4}$	32137.295	32137.90	-13.630
$8_{6,2}-8_{6,3}$	11680.132	11680.10	-8.262
$9_{6,3}-9_{6,4}$	26938.561	26938.68	-16.464
$10_{7,3}-10_{7,4}$	21229.817	21229.43	-18.712
$11_{8,3}-11_{8,4}$	15554.033	15553.69	-20.143
$12_{9,3}-12_{9,4}$	10486.600	10487.08	-20.433

*The observed transition frequencies are corresponding to the observations of Millen and Morton.[36]

Table 2.3. Rotational and centrifugal distortion constants of HNO_3

Watson's determinable parameters	Kivelson-Wilson's derived parameters[c]
$A'' = 13011.038$ MHz	$A' = 13011.029$ MHz
$B'' = 12099.928$ MHz	$B' = 12099.922$ MHz
$C'' = 6260.645$ MHz	$C' = 6260.608$ MHz
$\tau_1 = -102.55411$ KHz	$\tau'_{bbcc} = -18.30795$ KHz
$\tau_2 = -26.46419$ KHz	$\tau'_{ccaa} = -11.05978$ KHz
$\tau_3 = 2.56693$ MHz[b]	$\tau'_{aabb} = -73.18636$ KHz
$\tau'_{aaaa} = -48.38137$ KHz	
$\tau'_{bbbb} = -68.71805$ KHz	
$\tau'_{cccc} = 11.72386$ KHz	

The Ground State Moments of Inertia

$$I_a = 38.832096 \text{ amu Å}^2 \text{[a]}$$
$$I_b = 41.766860 \text{ amu Å}^2$$
$$I_c = 80.722672 \text{ amu Å}^2$$
$$\Delta = 0.113716 \text{ amu Å}^2 \text{[d]}$$

[a] The conversion factor = 505376 MHz amu Å^2

[b] The value of τ_3 is set using the planarity condition and is not, strictly speaking, a determinable parameter.

[c] These parameters are calculated from A'', B'', C'', τ_1, τ_2 and τ_3 and thus obey the planarity conditions used to calculate τ_3.

[d] Inertia defect $\Delta = I_c - I_a - I_b$.

Table 2.4. Rotational and centrifugal distortion constants
of DNO_3

Watson's determinable parameters		Kivelson-Wilson's derived parameters[c]	
A''	= 12970.60 MHz	A'	= 12970.594 MHz
B''	= 11312.80 MHz	B'	= 11312.801 MHz
C''	= 6035.00 MHz	C'	= 6034.925 MHz
τ_1	= -158.24591 KHz	τ'_{bbcc}	= -10.76288 KHz
τ_2	= -33.67339 KHz	τ'_{ccaa}	= 1.65556 KHz
τ_3	= 2.79656 MHz[b]	τ'_{aabb}	= -149.13858 KHz
τ'_{aaaa}	= -52.43154 KHz		
τ'_{bbbb}	= -72.45680 KHz		
τ'_{cccc}	= 8.52115 KHz		

The Ground State Moments of Inertia

$$I_a = 38.963193 \text{ amu } Å^2 \text{ [a]}$$
$$I_b = 44.672936 \text{ amu } Å^2$$
$$I_c = 83.740845 \text{ amu } Å^2$$
$$\Delta = 0.104715 \text{ amu } Å^2 \text{ [d]}$$

---

[a] The conversion factor = 505376 MHz amu $Å^2$

[b] The value of τ_3 is set using the planarity condition and is not, strictly speaking, a determinable parameter.

[c] These parameters are calculated from A'', B'', C'', τ_1, τ_2 and τ_3 and thus obey the planarity conditions used to calculate τ_3.

[d] Inertia defect $\Delta = I_c - I_a - I_b$

Table 2.5.   Transitions of the $J_{J-1,1}-J_{J-1,2}$ series

Transition	HNO$_3$		DNO$_3$	
	Calculated freq.. MHz	C.D. Correction MHz	Calculated freq. MHz	C.D. Correction MHz
$2_{1,1}-2_{1,2}$	17517.547*	-0.302	15833.097*	-0.304
$3_{2,1}-3_{2,2}$	16215.648*	-0.809	13579.431*	-0.895
$4_{3,1}-4_{3,2}$	14534.252*	-1.553	10808.330*	-1.575
$5_{4,1}-5_{4,2}$	12540.993*	-2.565	7834.196*	-2.283
$6_{5,1}-6_{5,2}$	10344.191*	-3.818	5093.385	-2.868
$7_{6,1}-7_{6,2}$	8097.546*	-5.167		
$8_{7,1}-8_{7,2}$	5984.009	-6.325		

*Observed transitions.

Table 2.6. Transitions of the $J_{J-2,2}-J_{J-2,3}$ series

Transition	HNO$_3$		DNO$_3$	
	Calculated freq. MHz	C.D. Correction MHz	Calculated freq. MHz	C.D. Correction MHz
$3_{1,2}-3_{1,3}$	31046.613	-0.969	29138.535*	-0.908
$4_{2,2}-4_{2,3}$	30378.433	-2.026	27215.912*	-2.274
$5_{3,2}-5_{3,3}$	29175.275*	-3.554	24229.789*	-3.865
$6_{4,2}-6_{4,3}$	27369.731*	-5.693	20396.234*	-5.506
$7_{5,2}-7_{5,3}$	24993.477*	-8.504	16065.609*	-7.020
$8_{6,2}-8_{6,3}$	22147.431*	-11.616	11680.132*	-8.262
$9_{7,2}-9_{7,3}$	18969.572*	-15.867	7743.580	-8.975
$10_{8,2}-10_{8,3}$	15628.213*	-19.927		
$11_{9,2}-11_{9,3}$	12317.350*	-23.546		
$12_{10,2}-12_{10,3}$	9245.560*	-25.945		

*Observed transitions.

Table 2.6. Transitions of the $J_{J-2,2}-J_{J-2,3}$ series

Transition	HNO$_3$		DNO$_3$	
	Calculated freq. MHz	C.D. Correction MHz	Calculated freq. MHz	C.D. Correction MHz
$3_{1,2}-3_{1,3}$	31046.613	-0.969	29138.535*	-0.908
$4_{2,2}-4_{2,3}$	30378.433	-2.026	27215.912*	-2.274
$5_{3,2}-5_{3,3}$	29175.275*	-3.554	24229.789*	-3.865
$6_{4,2}-6_{4,3}$	27369.731*	-5.693	20396.234*	-5.506
$7_{5,2}-7_{5,3}$	24993.477*	-8.504	16065.609*	-7.020
$8_{6,2}-8_{6,3}$	22147.431*	-11.616	11680.132*	-8.262
$9_{7,2}-9_{7,3}$	18969.572*	-15.867	7743.580	-8.975
$10_{8,2}-10_{8,3}$	15628.213*	-19.927		
$11_{9,2}-11_{9,3}$	12317.350*	-23.546		
$12_{10,2}-12_{10,3}$	9245.560*	-25.945		

*Observed transitions.

Table 2.7. Transitions of the $J_{J-3,3}-J_{J-3,4}$ series

Transition	HNO$_3$		DNO$_3$	
	Calculated freq. MHz	C.D. Correction MHz	Calculated freq.. MHz	C.D. Correction MHz
$4_{1,3}-4_{1,4}$	43854.755	-2.268	41965.824	-2.272
$5_{2,3}-5_{2,4}$	43660.351	-4.003	41110.450	-4.771
$6_{3,3}-6_{3,4}$	43259.178	-6.207	39352.270	-7.532
$7_{4,3}-7_{4,4}$	42512.864	-9.093	36369.868	-10.536
$8_{5,3}-8_{5,4}$	41257.375	-13.014	32137.295*	-13.630
$9_{6,3}-9_{6,4}$	39349.932	-18.356	26938.561*	-16.464
$10_{7,3}-10_{7,4}$	36725.955	-25.294	21229.817*	-18.712
$11_{8,3}-11_{8,4}$	33426.375	-33.705	15554.033*	-20.143
$12_{9,3}-12_{9,4}$	29478.368	-43.138	10486.600*	-20.433

*Observed transitions.

Table 2.8. Transitions of the $J_{J-4,4}-J_{J-4,5}$ series

Transition	HNO$_3$		DNO$_3$	
	Calculated freq. MHz	C.D. Correction MHz	Calculated freq. MHz	C.D. Correction MHz
$11_{7,4}-11_{7,5}$			39777.028	-32.640
$12_{8,4}-12_{8,5}$			33346.992	-36.483

Table 2.9. Transitions of the $J_{J,0}-J_{J,1}$ series

Transition	HNO$_3$		DNO$_3$	
	Calculated freq. MHz	C.D. Correction MHz	Calculated Freq. MHz	C.D. Correction MHz
$1_{1,0}-1_{1,1}$	5839.263	-0.020	5277.780	-0.020
$2_{2,0}-2_{2,1}$	5026.548	-0.144		

Table 2.10.   Transitions of the $J_{J,1}-J_{J-2,2}$ series

Transition	HNO$_3$		DNO$_3$	
	Calculated freq. MHz	C.D. Correction MHz	Calculated freq.. MHz	C.D. correction MHz
$2_{2,1}-2_{0,2}$	20349.458	-0.241	21139.455	-0.341
$3_{3,1}-3_{1,2}$	22161.087*	-0.503	25068.187	-0.953
$4_{4,1}-4_{2,2}$	25007.407	-0.518	31418.600	-1.252
$5_{5,1}-5_{3,2}$	29128.227	0.144	40403.673	-0.538
$6_{6,1}-6_{4,2}$	34663.525	2.031		
$7_{7,1}-7_{5,2}$	41625.914	5.708		

* Observed transition.

Table 2.11.   Transitions of the $J_{5,J-4}-J_{3,J-3}$ series

| Transition | HNO$_3$ | | DNO$_3$ | |
	Calculated freq. MHz	C.D. correction MHz	Calculated freq. MHz	C.D. correction MHz
$5_{5,1}-5_{3,2}$	29128.227	0.144	40403.673	-0.538
$6_{5,2}-6_{3,3}$	33630.123	-4.187	38451.077	-10.132
$7_{5,3}-7_{3,4}$	43870.728	-8.711	43710.363	-16.884

Table 2.12.   Transitions of the $J_{J-2,3}-J_{J-4,4}$ series

| Transition | HNO$_3$ | | DNO$_3$ | |
	Calculated freq. MHz	C.D. Correction MHz	Calculated freq. MHz	C.D. Correction MHz
$4_{2,3}-4_{0,4}$	43901.738	-2.290	42262.685	-2.641
$5_{3,3}-5_{1,4}$	43847.743	-4.050	42263.662	-6.048
$6_{4,3}-6_{2,4}$	43815.246	-6.205	42603.867	-10.700
$7_{5,3}-7_{3,4}$	43870.728	-8.711	43710.363	-16.884
$8_{6,3}-8_{4,4}$	44125.072	-11.260		
$9_{7,3}-9_{5,4}$	44741.815	-13.831		

Table 2.13. Transitions of the $J_{J-1,2}-J_{J-3,3}$ series

Transition	HNO$_3$		DNO$_3$	
	Calculated freq. MHz	C.D. Correction MHz	Calculated freq. MHz	C.D. Correction MHz
$3_{2,2}-3_{0,3}$	31538.456	-1.008	30765.712	-1.413
$4_{3,2}-4_{1,3}$	31832.729	-2.000	31831.881	-3.610
$5_{4,2}-5_{2,3}$	32461.677	-3.142	34156.549	-6.603
$6_{5,2}-6_{3,3}$	33630.123	-4.187	38451.077	-10.132
$7_{6,2}-7_{4,3}$	35598.195	-4.635		
$8_{7,2}-8_{5,3}$	38655.764	-3.691		
$9_{8,2}-9_{6,3}$	43064.440	-0.035		

Table 2.14.　Transitions of the $J_{1,J}-J-1_{1,J-1}$ series

Transition	HNO$_3$		DNO$_3$	
	Calculated freq. MHz	C.D. correction MHz	Calculated freq. MHz	C.D. correction MHz
$2_{1,2}-1_{1,1}$	30881.904	0.041	29417.497*	-0.303
$3_{1,3}-2_{1,2}$	43800.313	0.174	42125.962	0.053

*Observed transition.

Table 2.15.　Transitions of the $J_{0,J}-J-1_{0,J-1}$ series

Transition	HNO$_3$		DNO$_3$	
	Calculated freq. MHz	C.D. correction MHz	Calculated freq. MHz	C.D. correction MHz
$2_{0,2}-1_{0,1}$	31694.296	-0.158	30742.419	-0.186
$3_{0,3}-2_{0,2}$	43891.738	-0.216	42415.715	-0.354

Table 2.16. Transitions of the $J_{J-1,1}-J-1_{J-1,0}$ series

| Transition | HNO$_3$ | | DNO$_3$ | |
	Calculated freq. MHz	C.D. correction MHz	Calculated freq. MHz	C.D. Correction MHz
$2_{1,1}-1_{1,0}$	42559.968	-0.460	39972.814	-0.586

Table 2.17. Transitions of the $J_{J-1,1}-J_{J-2,2}$ series

| Transition | HNO$_3$ | | DNO$_3$ | |
	Calculated freq. MHz	C.D. correction MHz	Calculated freq. MHz	C.D. correction MHz
$2_{1,1}-2_{0,2}$	17616.051*	-0.317	16165.980	-0.416
$3_{2,1}-3_{1,2}$	16700.791*	-0.843	15163.833	-1.341
$4_{3,1}-4_{2,2}$	15941.943	-1.506	15131.974	-2.557
$5_{4,1}-5_{3,2}$	15643.387	-2.110	16647.942	-3.869
$6_{5,1}-6_{4,2}$	16065.312	-2.329	20092.142	-4.878
$7_{6,1}-7_{5,2}$	17405.258	-1.712	25579.981	-4.876
$8_{7,1}-8_{6,2}$	19803.955	-0.022	32778.635	-3.150
$9_{8,1}-9_{7,2}$	23326.549	4.273	40953.686	0.642
$10_{9,1}-10_{8,2}$	27911.866	10.373		
$11_{10,1}-11_{9,2}$	33353.217	18.264		
$12_{11,1}-12_{10,2}$	39339.185	27.133		

*Observed transitions.

Table 2.18. Transitions of the $J_{J,0}-J_{J-1,1}$ series

Transition	HNO$_3$		DNO$_3$	
	Calculated freq. MHz	C.D. correction MHz	Calculated freq. MHz	C.D. correction MHz
$1_{1,0}-1_{0,1}$	6750.378	-0.015	6935.585	-0.015
$2_{2,0}-2_{1,1}$	7759.955	-0.068	8926.274	-0.121
$3_{3,0}-3_{2,1}$	9448.053*	-0.018	12431.283	-0.039
$4_{4,0}-4_{3,1}$	11975.078	0.358	17685.192	0.712
$5_{5,0}-5_{4,1}$	15446.947	1.385	24449.718	2.723
$6_{6,0}-6_{5,1}$	19835.863	3.367	32077.034	6.450
$7_{7,0}-7_{6,1}$	24961.729	6.440	39882.383	12.171
$8_{8,0}-8_{7,1}$	30545.682	10.288		
$9_{9,0}-9_{8,1}$	363002.078	15.398		
$10_{10,0}-10_{9,1}$	42017.282	21.017		

*Observed transition.

Table 2.19. Transitions of the $J_{J,1}-J_{J-1,2}$ series

Transition	HNO$_3$		DNO$_3$	
	Calculated freq. MHz	C.D. correction MHz	Calculated freq. MHz	C.D. Correction MHz
$2_{2,1}-2_{1,2}$	20250.954	-0.225	20806.571	-0.229
$3_{3,1}-3_{2,2}$	21675.945*	-0.469	23483.785	-0.506
$4_{4,1}-4_{3,2}$	23599.716	-0.566	27094.956	-0.270
$5_{5,1}-5_{4,2}$	26025.833	-0.311	31589.926	1.050
$6_{6,1}-6_{5,2}$	28942.404	0.542	36850.693	4.090
$7_{7,1}-7_{6,2}$	32318.201	2.252	42710.910	9.455
$8_{8,1}-8_{7,2}$	36103.234	5.056		
$9_{9,1}-9_{8,2}$	40233.690	9.145		
$10_{10,1}-10_{9,2}$	44639.642	14.654		

*Observed transition.

Table 2.20. Transitions of the $J_{J-3,3}-J_{J-4,4}$ series

Transition	HNO$_3$		DNO$_3$	
	Calculated freq. MHz	C.D. Correction MHz	Calculated freq. MHz	C.D. Correction MHz
$4_{1,3}-4_{0,4}$	43855.133	-2.268	41970.360	-2.288
$5_{2,3}-5_{1,4}$	43663.735	-4.007	41150.649	-4.897
$6_{3,3}-6_{2,4}$	43275.976	-6.223	39457.781	-8.083
$7_{4,3}-7_{3,4}$	42573.722	-9.123	37054.311	-12.220
$8_{5,3}-8_{4,4}$	41436.764	-12.882	34043.656	-17.613
$9_{6,3}-9_{5,4}$	39803.553	-18.109	31360.944	-24.128
$10_{7,3}-10_{6,4}$	37743.846	-24.172	29993.635	-31.234
$11_{8,3}-11_{7,4}$	35490.308	-30.296	30723.824	-38.312
$12_{9,3}-12_{8,4}$	33403.574	-34.900	33989.150	-44.602

Table 2.21. Transitions of the $J_{J-4,4}-J_{J-5,5}$ series

Transition	HNO$_3$		DNO$_3$	
	Calculated freq. MHz	C.D. Correction MHz	Calculated freq. MHz	C.D. Correction MHz
$11_{7,4}-11_{6,5}$			42450.257	-42.026
$12_{8,4}-12_{7,5}$			39036.579	-53.109

Table 2.22. Transitions of the $J_{J-2,2} - J_{J-3,3}$ series

Transition	HNO$_3$		DNO$_3$	
	Calculated freq. MHz	C.D. correction MHz	Calculated freq. MHz	C.D. correction MHz
$3_{1,2} - 3_{0,3}$	31053.313	-0.974	29181.311	-0.967
$4_{2,2} - 4_{1,3}$	30425.038	-2.047	27508.237	-2.627
$5_{3,2} - 5_{2,3}$	29359.283	-3.597	25342.802	-5.016
$6_{4,2} - 6_{3,3}$	27909.002	-5.676	23452.320	-8.122
$7_{5,2} - 7_{4,3}$	26290.483	-8.091	22721.662	-11.683
$8_{6,2} - 8_{5,3}$	24835.739	-9.994	23840.909	-15.314
$9_{7,2} - 9_{6,3}$	23907.820	-11.589	27212.520	-18.431
$10_{8,2} - 10_{7,3}$	23827.704	-10.998	32901.718	-20.117
$11_{9,2} - 11_{8,3}$	24832.134	-7.614	40507.843	-19.561
$12_{10,2} - 12_{9,3}$	27071.941	-0.566		

Table 2.23. Transitions of the $J_{J-1,2} - J_{J-2,3}$ series

Transition	HNO$_3$		DNO$_3$	
	Calculated freq. MHz	C.D. correction MHz	Calculated freq. MHz	C.D. correction MHz
$3_{2,2} - 3_{1,3}$	31531.755	-1.003	30722.936	-1.355
$4_{3,2} - 4_{2,3}$	31786.124	-1.978	31539.556	-3.257
$5_{4,2} - 5_{3,3}$	32277.669	-3.099	33043.536	-5.452
$6_{5,2} - 6_{4,3}$	33090.852	-4.204	35394.991	-7.515
$7_{6,2} - 7_{5,3}$	34301.189	-5.048	38676.979	-8.814
$8_{7,2} - 8_{6,3}$	35967.431	-5.313	42881.985	-8.590
$9_{8,2} - 9_{7,3}$	38125.904	-4.636		
$10_{9,2} - 10_{8,3}$	40787.182	-2.654		
$11_{10,2} - 11_{9,3}$	43935.530	0.949		

Table 2.24. Transitions of the $J_{J-2,3} - J_{J-3,4}$ series

| Transition | HNO$_3$ | | DNO$_3$ | |
	Calculated freq. MHz	C.D. Correction MHz	Calculated freq. MHz	C.D. Correction MHz
$4_{2,3} - 4_{1,4}$	43901.360	-2.289	42258.148	-2.625
$5_{3,3} - 5_{2,4}$	43844.359	-4.045	42223.463	-5.922
$6_{4,3} - 6_{3,4}$	43798.449	-6.189	42408.356	-10.149
$7_{5,3} - 7_{4,4}$	43809.870	-8.680	43025.920	-15.199
$8_{6,3} - 8_{5,4}$	43945.708	-11.392	44298.068	-20.682
$9_{7,3} - 9_{6,4}$	44288.172	-14.078		
$10_{8,3} - 10_{7,4}$	44925.446	-16.366		

Table 2.25.   Transitions of the $J_{1,J}-J-1_{0,J-1}$ series

| Transition | HNO$_3$ | | DNO$_3$ | |
	Calculated freq. MHz	C.D. correction MHz	Calculated freq. MHz	C.D. Correction MHz
$1_{1,1}-0_{0,0}$	19271.623*	-0.060	19005.510*	-0.090
$2_{1,2}-1_{0,1}$	31792.800*	-0.173	31075.302*	-0.298
$3_{1,3}-2_{0,2}$	43898.208	-0.451	42458.417	-0.487

*Observed transitions.

Table 2.26.   Transitions of the $J_{0,J}-J-1_{1,J-1}$ series

| Transition | HNO$_3$ | | DNO$_3$ | |
	Calculated freq. MHz	C.D. Correction MHz	Calculated freq. MHz	C.D. Correction MHz
$2_{0,2}-1_{1,1}$	30783.180	-0.163	29084.614	-0.191
$3_{0,3}-2_{1,2}$	43793.233	-0.201	42082.832	-0.242

Table 2.25.   Transitions of the $J_{1,J}-J-1_{0,J-1}$ series

| Transition | HNO$_3$ | | DNO$_3$ | |
	Calculated freq. MHz	C.D. correction MHz	Calculated freq. MHz	C.D. correction MHz
$1_{1,1}-0_{0,0}$	19271.623*	-0.060	19005.510*	-0.090
$2_{1,2}-1_{0,1}$	31792.800*	-0.173	31075.302*	-0.298
$3_{1,3}-2_{0,2}$	43898.208	-0.451	42458.417	-0.487

*Observed transitions.

Table 2.26.   Transitions of the $J_{0,J}-J-1_{1,J-1}$ series

| Transition | HNO$_3$ | | DNO$_3$ | |
	Calculated freq. MHz	C.D. Correction MHz	Calculated freq. MHz	C.D. Correction MHz
$2_{0,2}-1_{1,1}$	30783.180	-0.163	29084.614	-0.191
$3_{0,3}-2_{1,2}$	43793.233	-0.201	42082.832	-0.242

CHAPTER 3

CENTRIFUGAL DISTORTION CONSTANTS OF TETRAFLUOROHYDRAZINE

ABSTRACT

The rotational spectrum of Tetrafluorohydrazine (N_2F_4) has been analysed up to J=21 in the frequency region 19-33 GHz. Only c-type transitions were analysed. The analysis gives refined rotational constants and all quartic centrifugal distortion constants.

INTRODUCTION

So far there has been only one study of the microwave spectrum of N_2F_4, by Lide and Mann.[39]   In this they reported the microwave spectrum of the molecule up to J=21 and rotational constants were found using the rigid rotator model. They have found that for the lines of higher J values the difference between the frequencies calculated using the rigid rotator model and observed frequencies were quite large.   For example, for the line corresponding to J=21 of $J_{5,J-4}$-$J_{6,J-6}$ series the difference between the calculated and observed value is 100.9 MHz.   The authors suggested this difference to be due to centrifugal distortion and they also suggested that the rotational constants could be refined.

N_2F_4 offers a good opportunity for the verification of various theories of centrifugal distortion discussed in Chapter 1 because of the large centrifugal distortion contribution observed for this molecule.

ANALYSIS OF THE SPECTRUM

N_2F_4 is a near prolate symmetric rotator whose inertial axes are oriented such that only c-type transitions occur μ_c being the only nonzero (=0.26D)[39] component of dipole moment. Twenty five transitions in the ground state were measured by

Lide and Mann in the frequency region 19-33 GHz. These twenty five transitions are used for an analysis similar to that discussed in Chapter 2. The results of the analysis are shown in Table 3.1. The rotational and centrifugal distortion parameters are given in Table 3.2.

GENERAL DISCUSSION

The calculations have been made only for Q-branch transitions with $\Delta\tau \leq 3$ and R-branch transitions with $\Delta\tau = 1$ as only these transitions have been reported so far.

Q-branch Transitions

Out of the nine predicted Q-branch transitions three correspond to $\Delta\tau = 1$ and six correspond to $\Delta\tau = 3$.

Series Corresponding to $\Delta\tau = 1$

None of these three series have so far been reported. The frequencies of the lines belonging to these series decrease with the increase in the rotational quantum number, but their centrifugal distortions show different behaviours.

(i) $J_{4,J-4} - J_{5,J-4}$ series – The lines of interest in this series lie between 23088.372 MHz corresponding to $J=5$ and 20063.478 MHz corresponding to $J=13$. The centrifugal distortion corrections for the lines belonging to this series are such that they decrease with J up to $J=7$, but increase afterwards.

The frequencies and C.D. corrections for lines belonging to this series are shown in Table 3.3.

(ii) $J_{5,J-5}-J_{6,J-5}$ series - The lines of interest in this series lie between 28227.687 MHz corresponding to J=6 and 20337.005 MHz corresponding to J=19. The centrifugal distortion corrections for the lines belonging to this series are such that they decrease with J, but increase from J=11 onwards. The frequencies and C.D. corrections for lines belonging to this series are shown in Table 3.4.

(iii) $J_{6,J-6}-J_{7,J-6}$ series - Only nine lines of this series between 32946.062 MHz corresponding to J=13 and 27844.957 MHz corresponding to J=21 lie in the region of interest. The centrifugal distortion correction for the lines belonging to this series is such that it is negative for J=13 but becomes positive at J=14 and then increases with the J. The frequencies and C.D. corrections for these lines are shown in Table 3.5.

Series Corresponding to $\Delta\tau =3$

Out of the six series corresponding to $\Delta\tau =3$, only few transitions belonging to two of these series, i.e. $J_{4,J-3}-J_{5,J-5}$ and $J_{5,J-4}-J_{6,J-6}$ have been reported earlier.

Out of the four new series predicted here, for the first three series, the frequencies as well as C.D. corrections increase with the increase in the J, while the fourth one behaves in a different manner as described later. These four series are as follows.

The frequencies and C.D. corrections for lines belonging to this series are shown in Table 3.3.

(ii) $J_{5,J-5}-J_{6,J-5}$ series - The lines of interest in this series lie between 28227.687 MHz corresponding to J=6 and 20337.005 MHz corresponding to J=19. The centrifugal distortion corrections for the lines belonging to this series are such that they decrease with J, but increase from J=11 onwards. The frequencies and C.D. corrections for lines belonging to this series are shown in Table 3.4.

(iii) $J_{6,J-6}-J_{7,J-6}$ series - Only nine lines of this series between 32946.062 MHz corresponding to J=13 and 27844.957 MHz corresponding to J=21 lie in the region of interest. The centrifugal distortion correction for the lines belonging to this series is such that it is negative for J=13 but becomes positive at J=14 and then increases with the J. The frequencies and C.D. corrections for these lines are shown in Table 3.5.

Series Corresponding to $\Delta\tau = 3$

Out of the six series corresponding to $\Delta\tau = 3$, only few transitions belonging to two of these series, i.e. $J_{4,J-3}-J_{5,J-5}$ and $J_{5,J-4}-J_{6,J-6}$ have been reported earlier.

Out of the four new series predicted here, for the first three series, the frequencies as well as C.D. corrections increase with the increase in the J, while the fourth one behaves in a different manner as described later. These four series are as follows.

(i) $J_{1,J}-J_{2,J-2}$ series - Only three lines belonging to this series between 20556.578 MHz corresponding to J=8 and 28746.369 MHz corresponding to J=10 lie in the region of interest. The frequencies and C.D. corrections for these lines are shown in Table 3.6.

(ii) $J_{2,J-1}-J_{3,J-3}$ series - Only four lines belonging to this series between 20158.742 MHz corresponding to J=10 and 31115.581 MHz corresponding to J=13 lie in the region of interest. The frequencies and C.D. corrections for these lines are shown in Table 3.7.

(iii) $J_{3,J-2}-J_{4,J-4}$ series - Only seven lines belonging to this series between 19690.846 MHz corresponding to J=11 and 32791.470 MHz corresponding to J=16 lie in the region of interest. The frequencies and C.D. corrections for these lines are shown in Table 3.8.

(iv) $J_{6,J-5}-J_{7,J-7}$ series - All the predicted lines from J=13 to J=21 of this series lie in the frequency region 32-33 GHz. The C.D. corrections of these lines always increase with the increase in the J. In the beginning the centrifugal distortion corrections increase slowly but afterwards they increase rapidly with the increase in the J. The frequencies and C.D. corrections for lines belonging to this series are shown in Table 3.9.

The two series reported so far are given below.

(i) $J_{4,J-3} - J_{5,J-5}$ series – Only seven lines from J=9 to J=15 of this series have been reported[39] earlier. All the lines from J=5 to J=18 of this series have been predicted in the frequency region studied. The frequencies of the lines decrease with the increase in the rotational quantum number up to J=11 and then increase with the increase in the rotational quantum number. The C.D. corrections for lines belonging to this series are positive for J=5 and J=6 and decrease with the increase in the rotational quantum number and ultimately change sign at J=7 and then increase with the increase in the rotational quantum number. The frequencies and C.D. corrections for these lines are shown in Table 3.10.

(ii) $J_{5,J-4} - J_{6,J-6}$ series – Eight lines from J=14 to J=21 of this series have been reported[39] earlier. The series starts at J=6 and all the lines up to J=21 lie in the frequency region studied. The frequencies of the lines decrease up to J=15 with the increase in the rotational quantum number and then increase with the increase in the rotational quantum number. The C.D. corrections for these lines are positive for J=6,7 and 8 and decrease with the increase in the J value and finally change sign at J=9 and then increase with the increase in the rotational quantum number. The frequencies and C.D. corrections for these lines are shown in Table 3.11.

R-branch Transitions

Five different R-branch series corresponding to $\Delta\tau = 1$ have been predicted. All the transitions belonging to these series have already been reported.[39] The frequencies as well as C.D. corrections for the transitions belonging to these series increase with the increase in the rotational quantum number, but the effect of centrifugal distortion is always such that the nonrigid rotator energies are less than the rigid rotator energies, i.e. C.D. corrections are negative. The frequencies and C.D. corrections for these series are shown in Tables 3.12, 3.13, 3.14, 3.15 and 3.16 respectively.

It is seen that the centrifugal distortion correction up to J=7 is $\leq$ 0.4 MHz for all the series. So the lines up to J=7 can be expressed by rigid rotator energies within this uncertainty of 0.4 MHz, with the refined rotational constants.

Table 3.1. Microwave spectrum of N_2F_4

Std. dev = 0.177 MHz

Transition	Calculated freq. MHz	Observed freq* MHz	C. D. Correction MHz
$1_{1,0}-2_{2,0}$	19582.824	19582.6	-0.032
$1_{1,1}-2_{2,1}$	19917.968	19917.9	-0.026
$2_{0,2}-3_{1,2}$	21725.032	21725.0	-0.143
$2_{1,1}-3_{2,1}$	25370.167	25370.14	-0.121
$2_{1,2}-3_{2,2}$	26296.681	26297.0	-0.117
$3_{0,3}-4_{1,3}$	28549.845	28549.9	-0.351
$2_{2,0}-3_{3,0}$	30686.339	30868.47	-0.081
$2_{2,1}-3_{3,1}$	30906.577	30906.52	-0.088
$3_{1,2}-4_{2,2}$	31187.477	31187.4	-0.302
$3_{1,3}-4_{2,3}$	32855.793	32856.0	-0.298
$9_{4,6}-9_{5,4}$	22866.911	22866.9	-0.353
$10_{4,7}-10_{5,5}$	22805.773	22805.9	-0.710
$11_{4,8}-11_{5,6}$	22788.290	22788.3	-1.418
$12_{4,9}-12_{5,7}$	22865.476	22865.6	-2.811
$13_{4,10}-13_{5,8}$	23110.412	23110.0	-5.425
$14_{4,11}-14_{5,9}$	23620.014	23620.1	-10.047
$14_{5,10}-14_{6,8}$	27526.494	27526.5	-1.524
$15_{4,12}-15_{5,10}$	24512.452	24512.5	-17.703
$15_{5,11}-15_{6,9}$	27461.573	27461.3	- 3.060

*The observed transition frequencies are corresponding to
the observations of Lide and Mann.[39]

Table 3.1 (...Contd.)

$16_{5,12}$-$16_{6,10}$	27501.610	27501.8	-6.078
$17_{5,13}$-$17_{6,11}$	27722.999	27723.1	-11.594
$18_{5,14}$-$18_{6,12}$	28225.863	28226.0	-21.015
$19_{5,15}$-$19_{6,13}$	29131.571	29131.5	-36.075
$20_{5,16}$-$20_{6,14}$	30572.118	30572.0	-58.532
$21_{5,17}$-$21_{6,15}$	32668.927	32669.0	-89.607

Table 3.2. Rotational and centrifugal distortion constants
of N_2F_4

Watson's determinable parameters

$A'' = 5576.1943$ MHz

$B'' = 3189.4051$ MHz

$C'' = 2813.1758$ MHz

$\tau_1 = -8.00244$ KHz

$\tau_2 = -1.81253$ KHz

$\tau_3 = 153.91927$ KHz[b]

$\tau'_{aaaa} = -2.08513$ KHz

$\tau'_{bbbb} = -7.18058$ KHz

$\tau'_{cccc} = 0.07941$ KHz

Kivelson-Wilson's derived
parameters[c]

$A' = 5576.1939$ MHz

$B' = 3189.4102$ MHz

$C' = 2813.1671$ MHz

$\tau'_{bbcc} = -0.84956$ KHz

$\tau'_{ccaa} = 10.29359$ KHz

$\tau'_{aabb} = -17.44468$ KHz

The Ground State Moments of Inertia

$I_a = 90.630986$ amu $\mathring{A}^2$ [a]

$I_b = 158.454630$ amu $\mathring{A}^2$

$I_c = 179.646074$ amu $\mathring{A}^2$

$\Delta = -69.439542$ amu $\mathring{A}^2$ [d]

---

[a] The conversion factor $= 505376.$ MHz amu $\mathring{A}^2$

[b] The value of τ_3 is set using the planarity condition and is not, strictly speaking, a determinable parameter.

[c] These parameters are calculated from A'', B'', C'', τ_1, τ_2 and τ_3 and thus obey the planarity conditions used to calculate τ_3

[d] Inertia defect $\Delta = I_c - I_a - I_b$.

Table 3.3. Transitions of the $J_{4,J-4}-J_{5,J-4}$ series

Transition	Calculated frequency MHz	C.D. Correction MHz
$5_{4,1}-5_{5,1}$	23088.372	0.170
$6_{4,2}-6_{5,2}$	23047.944	0.092
$7_{4,3}-7_{5,3}$	22978.215	0.042
$8_{4,4}-8_{5,4}$	22860.933	0.076
$9_{4,5}-9_{5,5}$	22667.249	0.309
$10_{4,6}-10_{5,6}$	22352.775	0.943
$11_{4,7}-11_{5,7}$	21857.959	2.287
$12_{4,8}-12_{5,8}$	21114.411	4.705
$13_{4,9}-13_{5,9}$	20063.478	8.486

Table 3.4. Transitions of the $J_{5,J-5}$-$J_{6,J-5}$ series

Transition	Calculated frequency MHz	C.D. Correction MHz
$6_{5,1}$-$6_{6,1}$	28227.687	0.323
$7_{5,2}$-$7_{6,2}$	28196.291	0.197
$8_{5,3}$-$8_{6,3}$	28148.678	0.076
$9_{5,4}$-$9_{6,4}$	28078.787	-0.017
$10_{5,5}$-$10_{6,5}$	27977.770	-0.035
$11_{5,6}$-$11_{6,6}$	27832.127	0.109
$12_{5,7}$-$12_{6,7}$	27620.786	0.576
$13_{5,8}$-$13_{6,8}$	27311.410	1.650
$14_{5,9}$-$14_{6,9}$	26856.955	3.779
$15_{5,10}$-$15_{6,10}$	26195.248	7.577
$16_{5,11}$-$16_{6,11}$	25255.945	13.698
$17_{5,12}$-$17_{6,12}$	23977.911	22.561
$18_{5,13}$-$18_{6,13}$	22332.136	34.055
$19_{5,14}$-$19_{6,14}$	20337.005	47.477

Table 3.5. Transitions of the $J_{6,J-6}-J_{7,J-6}$ series

Transition	Calculated frequency MHz	C.D. Correction MHz
$13_{6,7}-13_{7,7}$	32946.062	-0.099
$14_{6,8}-14_{7,8}$	32777.075	0.218
$15_{6,9}-15_{7,9}$	32551.871	0.980
$16_{6,10}-16_{7,10}$	32247.183	2.525
$17_{6,11}-17_{7,11}$	31828.206	5.404
$18_{6,12}-18_{7,12}$	31245.460	10.439
$19_{6,13}-19_{7,13}$	30434.484	18.687
$20_{6,14}-20_{7,14}$	29322.501	31.199
$21_{6,15}-21_{7,15}$	27844.957	48.540

Table 3.6. Transitions of the $J_{1,J}-J_{2,J-2}$ series

Transition	Calculated frequency MHz	C.D. Correction MHz
$8_{1,8}-8_{2,6}$	20556.578	-5.464
$9_{1,9}-9_{2,7}$	24460.610	-8.267
$10_{1,10}-10_{2,8}$	28746.369	-11.650

Table 3.7. Transitions of the $J_{2,J-1}-J_{3,J-3}$ series

Transition	Calculated frequency MHz	C.D. Correction MHz
$10_{2,9}-10_{3,7}$	20158.742	-10.331
$11_{2,10}-11_{3,8}$	23248.145	-15.900
$12_{2,11}-12_{3,9}$	26927.223	-22.924
$13_{2,12}-13_{3,10}$	31115.581	-31.225

Table 3.6. Transitions of the $J_{1,J}-J_{2,J-2}$ series

Transition	Calculated frequency MHz	C.D. Correction MHz
$8_{1,8}-8_{2,6}$	20556.578	-5.464
$9_{1,9}-9_{2,7}$	24460.610	-8.267
$10_{1,10}-10_{2,8}$	28746.369	-11.650

Table 3.7. Transitions of the $J_{2,J-1}-J_{3,J-3}$ series

Transition	Calculated frequency MHz	C.D. Correction MHz
$10_{2,9}-10_{3,7}$	20158.742	-10.331
$11_{2,10}-11_{3,8}$	23248.145	-15.900
$12_{2,11}-12_{3,9}$	26927.223	-22.924
$13_{2,12}-13_{3,10}$	31115.581	-31.225

Table 3.8.   Transitions of the $J_{3,J-2}-J_{4,J-4}$ series

Transition	Calculated frequency MHz	C.D. Correction MHz
$11_{3,9}-11_{4,7}$	19690.846	-6.926
$12_{3,10}-12_{4,8}$	21038.957	-12.145
$13_{3,11}-13_{4,9}$	22981.737	-19.940
$14_{3,12}-14_{4,10}$	25589.581	-30.627
$15_{3,13}-15_{4,11}$	28874.388	-44.173
$16_{3,14}-16_{4,12}$	32791.470	-60.229

Table 3.9.   Transitions of the $J_{6,J-5}-J_{7,J-7}$ series

Transition	Calculated frequency MHz	C.D. Correction MHz
$13_{6,8}-13_{7,6}$	32965.282	-0.307
$14_{6,9}-14_{7,7}$	32824.248	-0.327
$15_{6,10}-15_{7,8}$	32659.260	-0.343
$16_{6,11}-16_{7,9}$	32476.036	-0.472
$17_{6,12}-17_{7,10}$	32287.604	-0.959
$18_{6,13}-18_{7,11}$	32117.652	-2.258
$19_{6,14}-19_{7,12}$	32004.421	-5.127
$20_{6,15}-20_{7,13}$	32004.665	-10.741
$21_{6,16}-21_{7,14}$	32197.076	-20.802

Table 3.10.   Transitions of the $J_{4,J-3}-J_{5,J-5}$ series

Transition	Calculated frequency MHz	C.D. Correction MHz
$5_{4,2}-5_{5,0}$	23089.816	0.166
$6_{4,3}-6_{5,1}$	23055.157	0.075
$7_{4,4}-7_{5,2}$	23004.539	-0.029
$8_{4,5}-8_{5,3}$	22939.195	-0.158
$9_{4,6}-9_{5,4}*$	22866.911	-0.353
$10_{4,7}-10_{5,5}*$	22805.773	-0.710
$11_{4,8}-11_{5,6}*$	22788,290	-1.418
$12_{4,9}-12_{5,7}*$	22865.476	-2.811
$13_{4,10}-13_{5,8}*$	23110.412	-5.425
$14_{4,11}-14_{5,9}*$	23620.014	-10.047
$15_{4,12}-15_{5,10}*$	24512.452	-17.703
$16_{4,13}-16_{5,11}$	25916.049	-29.502
$17_{4,14}-17_{5,12}$	27947.097	-46.309
$18_{4,15}-18_{5,13}$	30681.921	-68.394

*Observed transitions.

Table 3.11. Transitions of the $J_{5,J-4}-J_{6,J-6}$ series

Transition	Calculated frequency MHz	C.D. Correction MHz
$6_{5,2}-6_{6,0}$	28227.778	0.322
$7_{5,3}-7_{6,1}$	28196.834	0.195
$8_{5,4}-8_{6,2}$	28151.015	0.064
$9_{5,5}-9_{6,3}$	28086.969	-0.061
$10_{5,6}-10_{6,4}$	28002.029	-0.177
$11_{5,7}-11_{6,5}$	27895.856	-0.296
$12_{5,8}-12_{6,6}$	27772.232	-0.464
$13_{5,9}-13_{6,7}$	27641.993	-0.797
$14_{5,10}-14_{6,8}*$	27526.494	-1.524
$15_{5,11}-15_{6,9}*$	27461.573	-3.060
$16_{5,12}-16_{6,10}*$	27501.610	-6.078
$17_{5,13}-17_{6,11}*$	27722.999	-11.594
$18_{5,14}-18_{6,12}*$	28225.863	-21.015
$19_{5,15}-19_{6,13}*$	29131.571	-36.075
$20_{5,16}-20_{6,14}*$	30572.118	-58.532
$21_{5,17}-21_{6,15}*$	32668.927	-89.607

*Observed transitions

Table 3.12. Transitions of the $J-1_{J-1,1}-J_{J,1}$ series

Transition	Calculated frequency MHz	C.D. Correction MHz
$1_{1,1}-2_{2,1}*$	19917.962	-0.026
$2_{2,1}-3_{3,1}*$	30906.577	-0.088

*Observed transition.

Table 3.13. Transitions of the $J-1_{0,J-1}-J_{1,J-1}$ series

Transition	Calculated frequency MHz	C.D. Correction MHz
$2_{0,2}-3_{1,2}*$	21725.032	-0.143
$3_{0,3}-4_{1,3}*$	28549.845	-0.351

*Observed transitions

Table 3.14. Transitions of the $J-1_{1,J-2}-J_{2,J-2}$ series

Transition	Calculated frequency MHz	C.D. Correction MHz
$1_{1,0}-2_{2,0}*$	19582.824	-0.032
$2_{1,1}-3_{2,1}*$	25370.167	-0.121
$3_{1,2}-4_{2,2}*$	31187.477	-0.302

*Observed transitions

Table 3.15. Transitions of the $J-1_{1,J-1}-J_{2,J-1}$ series

Transition	Calculated frequency MHz	C.D. Correction MHz
$1_{1,1}-2_{2,1}*$	19917.962	-0.026
$2_{1,2}-3_{2,2}*$	26296.681	-0.117
$3_{1,3}-4_{2,3}*$	32855.793	-0.298

*Observed transitions

Table 3.16. Transitions of the $J-1_{J-1,0}-J_{J,0}$ series

Transition	Calculated frequency MHz	C.D. Correction MHz
$1_{1,0}-2_{2,0}*$	19582.824	-0.032
$2_{2,0}-3_{3,0}*$	30868.339	-0.081

*Observed transitions

CHAPTER 4

CENTRIFUGAL DISTORTION CONSTANTS OF ALLYLAMINE

ABSTRACT

The microwave spectra of two rotameric forms, i.e., N-gauche lone electron pair gauche 1 (NGLG1) and N-gauche lone electron pair trans (NGLT) of allylamine have been analysed up to J=26 and J=29 respectively in the frequency region 5-40 GHz. Analysis gives all the quartic centrifugal distortion constants of both the forms of the molecule.

INTRODUCTION

Allylic compounds are a class of compounds most of which exhibit the feature of rotational isomerism making the study through microwave spectroscopy very interesting. The compounds 3 fluoropropene,[40] butene-1[41] and 3 chloropropene[42] present cis and gauche forms, whereas allylalcohol[43] and allylmercaptane[44] are observed only in gauche form.

Allylamine has two bond axes, shown as C_2-C_3 and C_3-N in the figure 4.1, several angular positions of which give rise to different potential minima. Hence, the molecule shows rotational isomerism.

The microwave study of allylamine was started by Roussy et al.[45] who characterised the molecule as possessing seven rotameric forms, each rotameric form by virtue of its unique set of rotational constants, giving rise to a distinct rotational spectrum. So far microwave spectra of N-cis, lone-electron pair (lep) trans (NCLT),[45] N-gauche lone-electron pair gauche 1 (NGLG1)[46] and N-gauche lone-electron pair trans (NGLT)[47] have been studied.

In the first study,[45] approximate values of rotational constants, dipole moments and quadrupole coupling constants were calculated for the seven rotamer models with different dihedral angles of the nitrogen lone electron pair direction

with respect to C-C single bond (lep trans and lep gauche).
The separation of the N-gauche positions from the N-cis, and
of the lep-gauche positions from lep-trans, were each assumed
to be 120°.

The microwave spectrum of NCLT[45] was studied up to J=8
in the ground vibrational state and later the study was
extended[47] up to three vibrational states T'_1, T'_2 and E'_1 but
unfortunately these studies were also limited to J values
less than 8.   Therefore due to the fact that the centrifugal
distortion effect is small at low rotational quantum numbers,
the problem of centrifugal distortion constant calculation
of this form of allylamine was not attempted.   Further study
of the microwave spectrum of allylamine was made by Cotskor
et al.[46] who studied the ground state spectrum of NGLG1 form
up to J=26 and also observed and assigned the spectra corres-
ponding to four excited vibrational states (T1, T2, T3 and T4)
of the C-C torsional mode.

The study was continued[47] with NGLT which is studied
up to J=29 in the ground vibrational state along with the
microwave spectrum corresponding to five different (T1, T2,
T3, E1 and T1E1) vibrational states of the C-C, C-N and a
combination of C-C and C-N torsional modes.

Since the molecule is an asymmetric top and the observed
spectrum shows a significant difference from the rigid rotator

values, the calculation of centrifugal distortion constants is essential for further study of these forms of the molecule. We have calculated the quartic centrifugal distortion constants for both the isomeric forms in the ground and the two excited vibrational states of the C-C torsional mode.

ANALYSIS OF THE SPECTRUM

Allylamine molecule is a near prolate symmetric rotator with all the three components of dipole moment being nonzero, hence the spectrum is expected to be a crowded one. A large number of transitions have been observed by Botskor et al.[46,47] in the frequency region 5-40 GHz. These transitions make a complete analysis of its microwave spectrum possible.

An iterative process is used for the calculation of these constants and in the least square fit the difference between the calculated frequency and the observed frequency is considered to be a linear function of the parameters to be determined, i.e. we are fitting an equation of the type

$$Y_i = \sum_{k=1}^{M} C_k X_{ki} \quad i = 1, 2, 3, \ldots N \quad (1)$$

where y_i is the difference between the observed frequency and the calculated frequency of the ith transition, and C_k (k = 1, 2, ...M) are the parameters to be determined (δA, δB, δC, τ'_{aaaa}, τ'_{bbbb}, τ'_{cccc}, τ_1, τ_2 and τ_3)* and X_{ki}, k=1,2,...M

---

* $A'' = A + \delta A$, $B'' = B + \delta B$ and $C''| = C + \delta C$.

are the expectation values of the angular momentum operators
(P_a^2, P_b^2, P_c^2, P_a^4, P_b^4, P_c^4, P_1^4, P_2^4 and P_3^4) associated with C_k
for the ith transition. N indicates the number of transitions
included in the fit. If the uncertainties in the determina-
tion of the frequencies of all the observed transitions are
assumed to be equal*, the following least square matrix
equation is obtained from above set of equations.

$$XC \ = \ Y \tag{2}$$

where C is a column matrix whose elements are C_k and X is a
(MxM) least square matrix whose elements are

$$X_{kl} \ = \ \sum_{i=1}^{N} X_{ki} X_{li} \tag{3}$$

and Y is an M dimensional column vector

$$Y_k \ = \ \sum_{i=1}^{N} X_{ki} Y_i \tag{4}$$

The parameters C_k are given by

$$C = X^{-1} Y \tag{5}$$

The standard deviation of the fit* is given by -

$$S \ = \left[\frac{\sum_{i=1}^{N} (\nu_{obs} - \nu_{cal})^2}{N - M} \right]^{1/2} \tag{6}$$

where ν_{cal} and ν_{obs} are calculated and observed transition
frequencies.

---

* All transitions were given unit weightage.

A particular quantity of interest is the 'standard deviation of the calculated frequency' δ_{yi} given by

$$(\delta_{yi})^2 = \sum_{k=1}^{M} \sum_{l=1}^{M} X_{ki} V_{kl} X_{li} \qquad (7)$$

where V is the variance convergence matrix obtained by multiplying X^{-1} with the square of the standard deviation.

If $\hat{y}_i$ is the calculated frequency of a transition which has not been included in the fit, then δ_{yi} has the property that if ith transition is measured and value of y_i falls within $\pm \delta_{yi}$ of the calculated value $\hat{y}_i$, then inclusion of that transition in the fit will not increase the overall standard deviation of the fit S.

A mismeasured or misassigned transition, when included in the fit, can appear to be well fitted with the error distributed among the remaining transitions. This results from the effects of the correlation and the fact that the parameters can be sensitive to the value of certain individual transitions. If more and more transitions are measured and included in the fit, the badly measured transition will become more obviously mismeasured and eventually can be weeded out.

This procedure is illustrated in the analysis of the T_1 state of NGLG1. On the first calculation, three of the transitions were so poorly fitted that their elimination reduced the standard deviation from 1.952 MHz to 0.540 MHz. On the

second calculation two transitions were found to have large

δ_{yi} and their elimination reduces the standard deviation

from 0.540 MHz to 0.063 MHz, while in the third calculation

one more transition was eliminated and the standard deviation

was finally reduced to 0.036 MHz. A look at Table 4.1 indicates

that out of the six eliminated transitions three could be

almost correctly assigned. The remaining three, i.e.,

$8_{1,7}-8_{0,8}$; $9_{1,9}-9_{0,9}$ and $12_{1,11}-12_{0,12}$ seem to have been

mismeasured which is also evident from the centrifugal

distortion corrections of these transitions in their respec-

tive series.

Similar analysis for different states of NGLT and NGLG1

shows the mismeasurement of a few transitions which are given

in Table 4.2.

When the calculations were done for the ground state of

NGLT, it was not possible to include all the observed transi-

tions in the fit, because of the limitation of the memory

available in the IBM-7044 computer. The system has memory

of 32,000 words which can however be increased by using the

link facility of this computer though only to a limited

extent. Using the link, the program can fit a maximum of

45 transitions.

But on the other hand the memory limitation was found to

give an interesting test to the calculations as below -

The constants obtained by using the maximum possible 45 transitions (randomly chosen out of 77 observed) were used to predict all the possible transitions in the frequency region studied up to J=29. The predicted transitions were compared with the remaining observed values which are not used in the fit and it was found that all the transitions were predicted within ± 1.15 MHz of the observed values as can be seen from Table 4.21 showing frequencies of various transitions for the ground state of NGLT. These results show the excellent capability of the calculations.

The rotational spectra in the T_1 and T_2 states of NGLG1 and NGLT have been observed up to J=15 and J=20 respectively, and up to J=26 and J=29 in the ground state. For comparison purpose another least square fitting is made using the observed transitions up to J=15 of the ground state of NGLG1 and up to J=20 of the ground state of NGLT and transitions up to J=26 of NGLG1 and up to J=29 of NGLT were predicted. The predicted transitions were found to be within ± 2.5 MHz of the observed values for NGLG1 and within ± 7.0 MHz for NGLT. Thus we expect that the uncertainties in the predicted frequencies of transitions with $J \geq 15$ of NGLG1 and $J \geq 20$ of NGLT in their T_1 and T_2 states to be also within similar limits.

Table 4.1. Results on the analysis on the mismeasured T_1 state transitions of NGLG1

Transition	Obs. val MHz	$\nu_{obs}-\nu_{cal}$ S=0.540 MHz	$\delta\hat{y}i$ MHz	$\nu_{obs}-\nu_{cal}$ S=0.036 MHz	$\delta\hat{y}i$ MHz	Remark
$1_{1,1}-0_{0,0}$	29228.865	0.128	0.106	0.117	0.018	✓
$4_{1,4}-4_{0,4}$	20300.415	0.037	0.065	0.051	0.024	✓
$8_{1,7}-8_{0,8}$	23072.529	-2.317	0.070	-2.412	0.012	
$9_{1,9}-9_{0,9}$	18360.781	-10.115	0.072	-10.042	0.017	
$12_{1,11}-12_{0,12}$	25839.015	-0.728	0.307	-1.013	0.021	
$13_{1,13}-13_{0,13}$	16060.401	0.278	0.425	0.271	0.024	✓

Table 4.2. Mismeasured transitions of Allylamine

Transition	State	Rotamer form
$10_{1,9}-10_{0,10}$	Ground	NGLG1
$8_{1,7}-8_{0,8}$		
$9_{1,9}-9_{0,9}$	T1	NGLG1
$12_{1,11}-12_{0,12}$		
$4_{1,4}-3_{1,3}$		
$12_{1,12}-12_{0,12}$	T1	NGLT
$14_{1,14}-14_{0,14}$		
$4_{1,3}-4_{0,4}$	T2	NGLT
$8_{1,7}-8_{0,8}$		

GENERAL DISCUSSION - NGLG1

The molecule NGLG1 is a near prolate symmetric top with all the three components of dipole moment being nonzero [μ_a = 0.169 D, μ_b = 0.807 D and μ_c = 0.829 D]. So all the three types of transitions are expected in the rotational spectrum of the molecule. The observed spectrum consists of 44 transitions of the ground state, 27 transitions of the T_1 vibrational state and also 27 transitions of the T_2 vibrational state.

The results of the fit of these transitions are given in Tables 4.3, 4.5 and 4.7 and the rotational and centrifugal distortion constants are given in Tables 4.4, 4.6 and 4.8.

Since the microwave measurements of this molecule were limited to $\Delta\tau \leq 2$, only the transitions with $\Delta\tau \leq 2$ were predicted in the frequency region 5-40 GHz. Q-branch transitions were predicted up to J=26 and R-branch transitions up to J=7 only.*

Q-branch Transitions

The three Q-branch series, which occur in the region of interest, belong to a, b and c-types. The a-type and c-type series correspond to $\Delta\tau = 1$ whereas the b-type series corresponds to $\Delta\tau = 2$.

----

*Since transitions with values of J higher than these are not observed.

(i) $J_{1,J-1}-J_{1,J}$ series - This series belongs to a-type. For all the three states (Ground, T_1 and T_2) lines of interest lie between J=9 and J=25. None of the transitions of this series has been reported so far.

For ground state these lines lie between 5377.724 MHz and 38602.748 MHz, for T_1 state between 5278.444 MHz and 37909.726 MHz and for T_2 state between 5247.647 MHz and 37407.035 MHz.

The transition frequencies as well as the C.D. corrections of the lines belonging to this series increase with the increase in rotational quantum number. The frequencies and C.D. corrections of these lines are shown in Table 4.9.

(ii) $J_{1,J-1}-J_{0,J}$ series - This series belongs to b-type. For all the three states (ground, T_1 and T_2), the lines of interest lie between J=1 and J=22. Most of the transitions belonging to this series have been reported[46] earlier.

For the ground state, these lines lie between 20953.052 MHz and 39857.880 MHz. Transitions up to J=15 of this series have been reported[46] earlier. Transition corresponding to J=2 of this series, i.e. $2_{1,1}-2_{0,2}$ was reported by Botskor et al.[7] at 20715.098 MHz. This, however, seems to be wrong, as it is predicted presently at 21073.254 MHz. The T_1 state lines lie between 20937.673 MHz and 39441.649 MHz. Almost all the

transitions up to J=15 except those with J=4, 5 and 7 of this state have been reported[46] earlier. The T_2 state lines lie between 20942.079 MHz and 39336.687 MHz. Almost all the transitions up to J=14 except those with J=1, 4 and 5 of this series have been reported[46] earlier.

The frequencies of the transitions belonging to this series increase with the increase in the rotational quantum number. The C.D. corrections are negative for lower J values but become positive with the increase of J and then increase with the increase in the rotational quantum number. The frequencies and C.D. corrections for these lines are shown in Table 4.10.

(iii) $J_{1,J}-J_{0,J}$ series – This series belongs to c-type. For all the three states (ground, T_1 and T_2), the lines of interest lie between J=1 and J=26. Most of the transitions belonging to this series have been reported[46] earlier.

For ground state, these lines lie between 20833.661 MHz and 7144.234 MHz. All the transitions except $2_{1,2}-2_{0,2}$ transition of this series have been reported[46] earlier. The transition $2_{1,2}-2_{0,2}$ has been predicted presently at 20715.060 MHz.

For T_1 state, these lines lie between 20820.482 MHz and 7284.683 MHz. All the lines up to J=14 of this series except the one corresponding to J=10 have been reported[46] earlier. This line however has been predicted now at 17846.797 MHz.

For T_2 state, these lines lie between 20825.538 MHz and 7318.888 MHz. All the lines up to J=14 of this series have been reported[46] earlier.

The frequencies of these transitions decrease with the increase in the rotational quantum number. The C.D. corrections are negative for lower J values but become positive with the increase of J and then increase with the increase in the rotational quantum number up to J=9 of the ground state, up to J=10 of the T_1 state and up to J=11 of the T_2 state; and beyond these values of J the C.D. corrections decrease with the increase in the rotational quantum number and finally change sign at J=14 for the ground state, at J=15 for T_1 state and at J=17 for T_2 state. The frequencies and C.D. corrections for these lines are shown in Table 4.11.

Comparing the results of Tables 4.9, 4.10 and 4.11, it can be seen that the a-type, Q-branch series is highly distorted and the c-type is least distorted.

R-branch Transitions

Out of the eight series of this type possible with $J \le 7$ seven belong to a-type and one to b-type.

a-type Series

(i) $J_{1,J}-J-1_{0,J-1}$ series - Only two lines of each state corresponding to J=1 and 2 fall between 5 and 40 GHz for this

series. Both of these transitions have been reported[46] earlier in ground state, but only a transition corresponding to $J=1$ has been reported[46] in T_1 and T_2 states. The frequencies and C.D. corrections for these lines as calculated presently are shown in Table 4.12.

(ii) $J_{1,J-1}-J-1_{0,J-1}$ series - Only two lines for each of the states corresponding to $J=1$ and $J=2$ are expected below 40 GHz for this series. Both of these transitions have been reported[46] earlier in the ground state but only those corresponding to $J=1$ have been reported[46] in both T_1 and T_2 states. The results of the present calculation for these lines are shown in Table 4.13.

(iii) $J_{0,J}-J-1_{0,J-1}$ series - Four lines which fall below 40 GHz from $J=1$ to $J=4$ of this series have been predicted in this work but none of these has been reported earlier. The frequencies and C.D. corrections for these lines are shown in Table 4.14.

(iv) $J_{2,J-2}-J-1_{2,J-3}$ series - Only two lines corresponding to $J=3$ and $J=4$ of this series are expected below 40 GHz and these have been predicted in this work but none of these has been reported earlier. The frequencies and C.D. corrections for these lines are shown in Table 4.15.

(v) $J_{1,J-1}-J-1_{1,J-2}$ series - Only three lines corresponding to $J=2,3$ and 4 of this series occur below 40 GHz. These have been

predicted in present work for all the states but none has been
reported earlier. The frequencies and C.D. corrections as
calculated now for these lines are shown in Table 4.16.

(vi) $J_{2,J-1}-J-1_{2,J-2}$ series - The two lines of this series
which fall below 40 GHz, corresponding to J=3 and J=4
have been predicted in this work for all the states
but none has been reported so far. The frequencies and the
C.D. corrections for these lines are shown in Table 4.17.

(vii) $J_{1,J}-J-1_{1,J-1}$ series - Only three lines corresponding
to J=2, 3 and 4 of this series which fall below 40 GHz have
been predicted presently but none has so far been reported.
The frequencies and C.D. corrections for these lines are
shown in Table 4.18.

b-type Series

(i) $J_{0,J}-J-1_{1,J-1}$ series - Only four lines from J=4 to J=7
of this series are expected in the region of interest. These
have been predicted in this work but none of them has been
reported so far for any state. The frequencies and C.D. cor-
rections for these lines are shown in Table 4.19.

Other R-branch Transitions

Two transitions $4_{3,1}-3_{3,0}$ and $4_{3,2}-3_{3,1}$ belonging to
a-type have also been predicted in the frequency region studied.
The frequencies and C.D. distortion corrections for these lines
are shown in Table 4.20.

GENERAL DISCUSSION - NGLT

The molecule NGLT is a near prolate symmetric molecule with all the three components of dipole moment being nonzero [$\mu_a = 0.766$ D, $\mu_b = 0.700$ D, $\mu_c = 0.290$ D], hence we expect the microwave spectrum of this molecule to be very crowded with all the three types of transitions.

The observed spectrum consists of 77 transitions of the ground state, 40 transitions of T_1 vibrational state and 27 transitions of T_2 vibrational state. Tables 4.21, 4.23 and 4.25 give the results of the fit on these transitions.

Rotational and centrifugal distortion constants for different states are shown in Tables 4.22, 4.24, and 4.26.

All the Q-branch transitions up to J=29 and R-branch transitions up to J=7* have been predicted within $\Delta\tau \leq 2$, in the frequency region 5-40 GHz.

Q-branch Transitions -

Three Q-branch series have been predicted in the frequency region 5-40 GHz and up to J=29. These three series belong to a, b and c-types. The a- and c-type series are with $\Delta\tau = 1$ and b-type series has $\Delta\tau = 2$.

---

*Since transitions with values of J higher than these are not observed.

(i) $J_{1,J-1}-J_{1,J}$ series – This series belongs to a-type and for all the three states, the lines of interest lie between J=12 and J=29 in the frequency region studied. This series has not been reported so far.

For ground state these lines lie between 5874.699 MHz and 32988.396 MHz, for T_1 state these lines lie between 5768.746 MHz and 32439.501 MHz and for T_2 state between 5769.746 MHz and 32336.995 MHz. The frequencies as well as the C.D. corrections of these lines increase with the increase in the rotational quantum number. The frequencies and the C.D. corrections for these lines are shown in Table 4.27.

(ii) $J_{1,J-1}-J_{0,J}$ series – This series is a b-type series. Most of the transitions belonging to this series have been reported[47] earlier. For all the states the series starts at J=1 and in the frequency region studied ends at J=28.

For ground state, the series starts at 19801.774 MHz and ends at 39420.757 MHz. All transitions except $28_{1,27}-28_{0,28}$ of this series have been reported[47] earlier.

For T_1 state, the series starts at 19866.244 MHz and ends at 39080.309 MHz. The series has been reported[47] earlier up to J=20, except $4_{1,3}-4_{0,4}$; $5_{1,4}-5_{0,5}$ and $6_{1,5}-6_{0,6}$ transitions.

For T_2 state, the series starts at 19929.303 MHz and ends at 39071.663 MHz. Only eight transitions up to J=18 of this series have been reported[47] earlier.

The frequencies of the transitions belonging to this series increase with the increase in the rotational quantum number, while the C.D. corrections are negative for lower J values but become positive with the increase in the rotational quantum number, and then increase with the increase in rotational quantum number. The frequencies and the C.D. corrections of the lines belonging to this series are shown in Table 4.28.

(iii) $J_{1,J} - J_{0,J}$ series - This series belongs to c-type. For all the three states the lines of interest lie between J=1 and J=29. Most of the lines belonging to this series have been reported[47] earlier.

For the ground state these lines lie between 19726.722 MHz and 8115.070 MHz. All the transitions of the series in this state have already been reported.[47]

For T_1 state these lines lie between 19792.492 MHz and 8297.129 MHz. Only a few transitions up to J=14 of this series have been reported[47] earlier.

For the T_2 state these lines lie between 19855.551 MHz and 8370.329 MHz. The transitions from J=6 to J=19 of this state, excepting $7_{1,7} - 7_{0,7}$; $16_{1,16} - 16_{0,16}$ have been reported[47] earlier.

The frequencies of these transitions decrease with the increase in the rotational quantum number. The C.D. corrections are negative for lower J values but become positive and increase with the increase in the rotational quantum number up to $J=9$ of the ground state, up to $J=10$ of the T_1 and also up to $J=10$ of the T_2 state and then decrease with the increase in the rotational quantum number and finally change sign at $J=13$ of the ground state, at $J=14$ of both the T_1 and T_2 states and then increase with the increase in the rotational quantum number. The frequencies and C.D. corrections for these lines are shown in Table 4.29.

Comparing the results of Tables 4.27, 4.28 and 4.29, it can be seen that in the Q-branch, a-type series is the most distorted one whereas the c-type series is the least distorted.

R-branch Transitions

Out of the eight series of this branch possible with $J \leq 7$, seven belong to a-type and one belongs to b-type.

a-type Series

(i) $J_{1,J}-J-1_{0,J-1}$ series - Only two lines corresponding to $J=1$ and $J=2$ for each of the states (ground, T_1 and T_2) occur below 40 GHz in this series. These lines have already been reported[47] in the ground and the T_1 state but none so in the T_2 state. The frequencies and C.D. corrections for these lines as calculated presently are shown in Table 4.30.

(ii) $J_{1,J-1}-J-1_{0,J-1}$ series — Only two lines corresponding to J=1 and J=2 of each of the states (the ground, T_1 and T_2) are expected below 40 GHz for this series. These lines in ground state and the line corresponding to J=2 of the T_1 state have been reported[47] earlier but none of the T_2 state lines has been reported so far. The frequencies and C.D. corrections for these lines are shown in Table 4.31.

(iii) $J_{0,J}-J-1_{0,J-1}$ series — Four lines from J=1 to J=4 of this series occur below 40 GHz. All these lines in ground state and lines from J=1 to J=3 in T_1 and T_2 states of this series have already been reported.[47] The results of the present calculation for these lines are shown in Table 4.32.

(iv) $J_{2,J-2}-J-1_{2,J-3}$ series — Only two lines corresponding to J=3 and J=4 of this series would occur below 40 GHz but only ground state line corresponding to J=3 has been reported[47] so far. The frequencies and C.D. corrections for these lines as calculated presently are shown in Table 4.33.

(v) $J_{1,J-1}-J-1_{1,J-2}$ series — Only three lines corresponding to J=2,3 and 4 of this series occur below 40 GHz for all the three states. All these lines except $4_{1,3}-3_{1,2}$ of T_2 state have already been reported.[47] The frequencies and C.D. corrections for these lines as calculated now are shown in Table 4.34.

(vi) $J_{2,J-1}-J-1_{2,J-2}$ series - The two lines corresponding to J=3 and J=4 of this series fall below 40 GHz for all the states but only $3_{2,2}-2_{2,1}$ line of ground state has been reported[47] so far. The frequencies and C.D. corrections for these lines are shown in Table 4.35.

(vii) $J_{1,J}-J-1_{1,J-1}$ series - Three lines from J=2 to J=4 of this series which fall below 40 GHz have been predicted. All these lines except $3_{1,3}-2_{1,2}$ line of the ground state and the T_2 state have been reported[47] earlier. The frequencies and C.D. corrections for these lines are shown in Table 4.36.

b-type Series

(i) $J_{0,J}-J-1_{1,J-1}$ series - Five lines from J=3 to J=7 of this series are expected in the region of interest and have been predicted in the frequency region studied. Lines from J=3 to J=6 of ground state and from J=3 to J=4 of T_1 state have already been reported[47]. The frequencies and C.D. corrections for these lines are shown in Table 4.37.

Other R-branch Transitions

Two transitions $4_{3,1}-3_{3,0}$ and $4_{3,2}-3_{3,1}$ belonging to a-type have also been predicted in the frequency region studied. The frequencies and C.D. corrections for these lines

(vi) $J_{2,J-1} - J-1_{2,J-2}$ series - The two lines corresponding to J=3 and J=4 of this series fall below 40 GHz for all the states but only $3_{2,2}-2_{2,1}$ line of ground state has been reported[47] so far. The frequencies and C.D. corrections for these lines are shown in Table 4.35.

(vii) $J_{1,J} - J-1_{1,J-1}$ series - Three lines from J=2 to J=4 of this series which fall below 40 GHz have been predicted. All these lines except $3_{1,3}-2_{1,2}$ line of the ground state and the T_2 state have been reported[47] earlier. The frequencies and C.D. corrections for these lines are shown in Table 4.36.

b-type Series

(i) $J_{0,J} - J-1_{1,J-1}$ series - Five lines from J=3 to J=7 of this series are expected in the region of interest and have been predicted in the frequency region studied. Lines from J=3 to J=6 of ground state and from J=3 to J=4 of T_1 state have already been reported[47]. The frequencies and C.D. corrections for these lines are shown in Table 4.37.

Other R-branch Transitions

Two transitions $4_{3,1}-3_{3,0}$ and $4_{3,2}-3_{3,1}$ belonging to a-type have also been predicted in the frequency region studied. The frequencies and C.D. corrections for these lines are shown in Table 4.38.

Different sets of values of the physical quantities are expected for NGLG1 and NGLT because the important amine partial dipole moment and the nuclear quadrupole coupling tensors have very different orientations with respect to the heavy atom frame of each conformer. This becomes clear from Table 4.39.

The previously missing lines of higher vibrational states corresponding to different series have been predicted with certainty now, so these lines can be easily found.

The results can be further improved if the predicted Q-branch a-type series are observed and included in the fit with the variation in the rotational constant A allowed. A large number of Q-branch b-type and Q-branch c-type transitions have been reported earlier and it has been found that the rotational constants B and C are well determined. Thus the observation of Q-branch a-type series which unlike Q-branch b-type and Q-branch c-type series starts at higher rotational quantum numbers, will improve the results further as well as the rotational constant A.

The uncertainty in the rotational constant A is clear from a-type observed transitions (only R-branch transitions were reported earlier) which deviate comparatively more from the observed values.

Another Q-branch, a-type series has also been predicted (not given here) for both the forms of allylamine studied.

This series $(J_{2,J-2}-J_{2,J-1})$ starts at $J=22$ for NGLG1 form
and at $J=28$ for NGLT form. NGLG1 series lies between 5-10
GHz and NGLT series lies between 5-6 GHz. This series has
been predicted with very large standard deviation which can
however be improved upon if $J_{1,J-1}-J_{1,J}$ Q-branch a-type
series is observed, and a better value of A determined
therefore is used.

Table 4.3. Microwave spectrum of ground state of NGLG1

Std dev = 0.261 MHz

Transition	Calculated freq. MHz	Observed freq.* MHz	C.D. Correction MHz
$1_{1,0}-0_{0,0}$	29339.337	29339.212	-0.022
$1_{1,1}-1_{0,1}$	20833.661	20833.649	-0.059
$1_{1,0}-1_{0,1}$	20953.052	20953.098	-0.057
$3_{1,2}-3_{0,3}$	21254.539	21254.612	0.716
$5_{1,4}-5_{0,5}$	21805.457	21805.425	2.303
$6_{1,5}-6_{0,6}$	22178.607	22178.567	3.505
$7_{1,6}-7_{0,7}$	22619.867	22619.804	5.060
$8_{1,7}-8_{0,8}$	23131.934	23131.880	7.043
$9_{1,8}-9_{0,9}$	23717.863	23717.828	9.546
$9_{1,9}-9_{0,9}$	18340.134	18340.017	3.106
$10_{1,10}-10_{0,10}$	17807.324	17807.139	3.060
$10_{1,9}-10_{0,10}$ ‡	24381.040	24380.015	12.678
$11_{1,10}-11_{0,11}$	25125.161	25125.207	16.567
$11_{1,11}-11_{0,11}$	17235.701	17235.540	2.731
$12_{1,12}-12_{0,12}$	16629.337	16629.190	2.069
$12_{1,11}-12_{0,12}$	25954.189	25954.338	21.359
$13_{1,12}-13_{0,13}$	26872.317	26872.587	27.224
$13_{1,13}-13_{0,13}$	15992.603	15992.470	1.029
$14_{1,13}-14_{0,14}$	27883.905	27884.418	34.350

*Observed transition frequencies are corresponding to the observations of Botskor et al.[46]

‡ Transitions not included in the fit.

Table 4.3 (...Contd.)

$15_{1,14}-15_{0,15}$	28993.414	28992.830	42.951
$1_{1,1}-0_{0,0}$	29219.946	29219.820	-0.024
$2_{1,2}-1_{0,1}$	37486.793	37486.800	-0.037
$2_{1,1}-1_{0,1}$	37844.987	37845.200	-0.012
$2_{1,1}-2_{0,2}^{*\ddagger}$	21073.254	20715.098	0.243
$3_{1,3}-3_{0,3}$	20538.093	20538.086	0.609
$4_{1,3}-4_{0,4}$	21498.084	21498.034	1.389
$4_{1,4}-4_{0,4}$	20303.886	20303.985	1.082
$5_{1,5}-5_{0,5}$	20013.941	20013.891	1.599
$6_{1,6}-6_{0,6}$	19670.141	19670.020	2.114
$7_{1,7}-7_{0,7}$	19274.749	19275.380	2.574
$14_{1,14}-14_{0,14}^{\ddagger}$	15330.129	15329.959	-0.420
$8_{1,8}-8_{0.8}^{\ddagger}$	18830.409	18830.369	2.925
$15_{1,15}-15_{0,15}$	14646.763	14646.630	-2.301
$16_{1,16}-16_{0,16}$	13947.507	13947.390	-4.622
$17_{1,17}-17_{0,17}$	13237.452	13237.387	-7.375
$18_{1,18}-18_{0,18}$	12521.703	12521.662	-10.539
$19_{1,19}-19_{0,19}$	11805.298	11805.265	-14.078
$20_{1,20}-20_{0,20}$	11093.125	11093.076	-17.939
$21_{1,21}-21_{0,21}$	10389.836	10389.794	-22.062
$22_{1,22}-22_{0,22}$	9699.771	9700.730	-26.375
$23_{1,23}-23_{0,23}$	9026.891	9026.830	-30.800
$24_{1,24}-24_{0,24}$	8374.712	8374.645	-35.255
$25_{1,25}-25_{0,25}$	7746.266	7746.160	-39.659
$26_{1,26}-26_{0,26}$	7144.234	7143.900	-43.935

‡ Transitions not included in the fit.

* Wrongly reported transition.

Table 4.4.   Rotational and centrifugal distortion constants
of the ground state of NGLG1

<div>

Watson's determinable parameters

$A'' = 25086.54$ MHz

$B'' = 4252.82$ MHz

$C'' = 4133.43$ MHz

$\tau_1 = 123.30996$ KHz

$\tau_2 = -20.05883$ KHz

$\tau_3 = 6.80856$ MHz[b]

$\tau'_{aaaa} = -286.38259$ KHz

$\tau'_{bbbb} = -49.95033$ KHz

$\tau'_{cccc} = -56.43834$ KHz

</div>

<div>

Kivelson-Wilson's derived parameters[c]

$A' = 25086.517$ MHz

$B' = 4251.9116$ MHz

$C' = 4134.4230$ MHz

$\tau'_{bbcc} = -46.01784$ KHz

$\tau'_{ccaa} = -1.81674$ MHz

$\tau'_{aabb} = 1.98607$ MHz

</div>

Moments of Inertia

$I_a = 20.145305$ amu $\overset{\circ}{A}^2$ [a]

$I_b = 118.833150$ amu $\overset{\circ}{A}^2$

$I_c = 122.265528$ amu $\overset{\circ}{A}^2$

$\Delta = -16.712927$ amu $\overset{\circ}{A}^2$ [d]

---

[a] The conversion factor $= 505376.$ MHz amu $\overset{\circ}{A}^2$

[b] The value of τ_3 is set using the planarity condition and is not, strictly speaking, a determinable parameter.

[c] These parameters are calculated from A'', B'', C'', τ_1, τ_2 and τ_3 and thus obey the planarity conditions used to calculate τ_3.

[d] Inertia defect $\Delta = I_c - I_a - I_b$.

Table 4.5. Microwave spectrum of the T_1 state of NGLG1

Std dev = 0.036 MHz

Transition	Calculated freq MHz	Observed freq.* MHz	C.D. Correction MHz
$1_{1,0}-1_{0,1}$	20937.673	20937.680	-0.327
$1_{1,1}-1_{0,1}$	20820.482	20820.448	-0.328
$1_{1,0}-0_{0,0}$	29345.940	29346.021	-0.090
$2_{1,1}-2_{0,2}$	21055.650	21055.621	-0.033
$2_{1,2}-2_{0,2}$	20704.057	20704.142	-0.056
$3_{1,2}-3_{0,3}$	21233.562	21233.548	-0.014
$3_{1,3}-3_{0,3}$	20530.322	20530.320	0.329
$5_{1,5}-5_{0,5}$	20015.632	20015.612	1.323
$6_{1,5}-6_{0,6}$	22140.139	22140.126	3.171
$6_{1,6}-6_{0,6}$	19677.945	19677.929	1.858
$7_{1,7}-7_{0,7}$	19289.487	19289.447	2.357
$8_{1,8}-8_{0,8}$	18852.809	18852.784	2.772
$9_{1,8}-9_{0,9}$	23649.267	23649.282	9.144
$10_{1,9}-10_{0,10}$	24299.131	24299.108	12.251
$11_{1,10}-11_{0,11}$	25028.105	25028.097	16.116
$11_{1,11}-11_{0,11}$	17284.338	17284.350	2.988
$12_{1,12}-12_{0,12}$	16687.375	16687.378	2.554
$13_{1,12}-13_{0,13}$	26738.959	26738.944	26.730
$14_{1,13}-14_{0,14}$	27729.133	27729.155	33.843
$14_{1,14}-14_{0,14}$	15407.081	15407.099	0.684

*The observed transition frequencies are corresponding to the observations of Botskor et al.[46]

Table 4.5 (...Contd.)

$15_{1,14}-15_{0,15}$	28814.892	28814.900	42.443
$1_{1,1}-0_{0,0}^{\ddagger}$	29228.748	29228.865	-0.092
$4_{1,4}-4_{0,4}^{\ddagger}$	20300.364	20300.415	0.800
$8_{1,7}-8_{0,8}^{\ddagger}$	23074.941	23072.529	6.665
$9_{1,9}-9_{0,9}^{\ddagger}$	18370.823	18360.781	3.050
$12_{1,11}-12_{0,12}^{\ddagger}$	25840.028	25839.015	20.885
$13_{1,13}-13_{0,13}^{\ddagger}$	16060.130	16060.401	1.796

‡Transitions not included in the least square fit.

Table 4.6.   Rotational and centrifugal distortion constants
of T_1 state of NGIG1

Watson's determinable parameters		Kivelson-Wilson's derived parameters[c]	
A''	= 25083.42 MHz	A'	= 25083.441 MHz
B''	= 4262.61 MHz	B'	= 4263.1112 MHz
C''	= 4145.42 MHz	C'	= 4145.1100 MHz
τ_1	= 424.90369 KHz	τ'_{bbcc}	= 42.24223 KHz
τ_2	= 82.50945 KHz	τ'_{ccaa}	= 1.00255 MHz
τ_3	= -9.47154 MHz[b]	τ'_{aabb}	= -619.88993 KHz
τ'_{aaaa}	= -1.26112 MHz		
τ'_{bbbb}	= 51.30126 KHz		
τ'_{cccc}	= 45.19271 KHz		

Moments of Inertia

$$I_a = 20.147811 \text{ amu } Å^2 \text{ [a]}$$

$$I_b = 118.560225 \text{ amu } Å^2$$

$$I_c = 121.911893 \text{ amu } Å^2$$

$$\Delta = -16.796142 \text{ amu } Å^2 \text{ [d]}$$

---

[a] The conversion factor = 505376. MHz amu $Å^2$

[b] The value of τ_3 is set using the planarity condition and is not, strictly speaking, a determinable parameter.

[c] These parameters are calculated from A'', B'', C'', τ_1, τ_2 and τ_3 and thus obey the planarity conditions used to calculate τ_3.

[d] Inertia defect $\Delta = I_c - I_a - I_b$.

Table 4.7. Microwave spectrum of T_2 state of NGIG1

Std dev = 0.126 MHz

Transition	Calculated freq. MHz	Observed freq.* MHz	C.D. Correction MHz
$1_{1,1}-0_{0,0}$	29252.273	29252.490	-0.257
$1_{1,0}-0_{0,0}$	29368.814	29369.115	-0.256
$2_{1,2}-2_{0,2}$	20709.768	20709.752	-0.070
$4_{1,4}-4_{0,4}$	20308.350	20308.290	0.850
$1_{1,1}-1_{0,1}$	20825.538	20825.480	-0.352
$2_{1,1}-2_{0,2}$	21059.404	21059.321	-0.054
$3_{1,2}-3_{0,3}$	21236.320	21236.177	0.406
$3_{1,3}-3_{0,3}$	20537.012	20537.042	0.337
$5_{1,5}-5_{0,5}$	20025.226	20025.291	1.441
$6_{1,5}-6_{0,6}$	22137.605	22137.524	3.006
$6_{1,6}-6_{0,6}$	19689.443	19689.529	2.079
$7_{1,6}-7_{0,7}$	22567.706	22567.493	4.405
$7_{1,7}-7_{0,7}$	19303.168	19303.248	2.723
$8_{1,7}-8_{0,8}$	23066.620	23066.433	6.162
$8_{1,8}-8_{0,8}$	18868.929	18868.981	3.330
$9_{1,9}-9_{0,9}$	18389.606	18389.657	3.848
$9_{1,8}-9_{0,9}$	23637.253	23637.123	8.359
$10_{1,10}-10_{0,10}$	17868.425	17868.409	4.221
$10_{1,9}-10_{0,10}$	24282.836	24282.772	11.095
$11_{1,10}-11_{0,11}$	25006.405	25006.920	14.496

*The observed transition frequencies are corresponding to the observations of Botsker et al.[46]

Table 4.7 (...Contd.)

$11_{1,11} - 11_{0,11}^{\ddagger}$	17308.944	17308.285	4.390
$12_{1,12} - 12_{0,12}$	16715.032	16714.969	4.293
$12_{1,11} - 12_{0,12}$	25813.267	25813.340	18.716
$13_{1,13} - 13_{0,13}$	16090.841	16090.839	3.867
$13_{1,12} - 13_{0,13}$	26705.969	26706.083	23.947
$14_{1,14} - 14_{0,14}$	15440.775	15440.847	3.051
$14_{1,13} - 14_{0,14}$	27689.250	27689.233	30.420

$\ddagger$Transition not included in the least square fit.

Table 4.8. Rotational and centrifugal distortion constants of T_2 state of NGLG1

Watson's determinable parameters		Kivelson-Wilson's derived parameters[c]	
A'' =	25097.48 MHz	A' =	25097.472 MHz
B'' =	4271.59 MHz	B' =	4272.2451 MHz
C'' =	4155.05 MHz	C' =	4154.5148 MHz
τ_1 =	233.92696 KHz	τ'_{bbcc} =	-15.77095 KHz
τ_2 =	22.45613 KHz	τ'_{ccaa} =	1.31007 MHz
τ_3 =	8.35686 MHz[b]	τ'_{aabb} =	-1.07037 MHz
τ'_{aaaa} =	-1.43995 MHz		
τ'_{bbbb} =	-32.38502 KHz		
τ'_{cccc} =	-36.55118 KHz		

Moments of Inertia

I_a = 20.136523 amu Å^2 [a]

I_b = 118.310979 amu Å^2

I_c = 121.629342 amu Å^2

Δ = -16.818160 amu Å^2 [d]

[a] The conversion factor = 505376. MHz amu Å^2

[b] The value of τ_3 is set using planarity condition and is not strictly speaking, a determinable parameter.

[c] These parameters are calculated from A'', B'', C'', τ_1, τ_2 and τ_3 and thus obey the planarity conditions used to calculate τ_3.

[d] Inertia defect $\Delta = I_c - I_a - I_b$.

Table 4.9. Transitions of the $J_{1,J-1}-J_{1,J}$ series of NG1G1

Transition	Ground state		T_1 State		T_2 state	
	Calculated freq. MHz	C.D. Correction MHz	Calculated freq. MHz	C.D. Correction MHz	Calculated freq. MHz	C.D. Correction MHz
$9_{1,8}-9_{1,9}$	5377.724	6.440	5278.444	6.094	5247.647	4.511
$10_{1,9}-10_{1,10}$	6573.716	9.619	6452.334	9.113	6414.411	6.874
$11_{1,10}-11_{1,11}$	7889.460	13.836	7743.767	13.127	7697.960	10.105
$12_{1,11}-12_{1,12}$	9324.852	19.291	9152.653	18.331	9098.235	14.423
$13_{1,12}-13_{1,13}$	10879.715	26.194	10678.830	24.934	10615.127	20.080
$14_{1,13}-14_{1,14}$	12553.776	34.770	12322.052	33.155	12248.475	27.368
$15_{1,14}-15_{1,15}$	14346.651	45.253	14081.971	43.244	13998.044	36.625
$16_{1,15}-16_{1,16}$	16257.825	57.884	15958.117	55.439	15863.520	48.236
$17_{1,16}-17_{1,17}$	18286.629	72.912	17949.879	70.002	17844.494	62.638
$18_{1,17}-18_{1,18}$	20432.219	90.586	20056.484	87.202	19940.452	80.328
$19_{1,18}-19_{1,19}$	22693.552	111.158	22276.979	107.314	22150.755	101.865
$20_{1,19}-20_{1,20}$	25069.365	134.871	24610.207	130.617	24474.628	127.872

Table 4.9 (...Contd.)

$21_{1,20}-21_{1,21}$	27558.144	161.964	27054.782	157.390	26911.148	159.047
$22_{1,21}-22_{1,22}$	30158.109	192.657	29609.313	187.910	29459.225	196.163
$23_{1,22}-23_{1,23}$	32867.184	227.156	32271.174	222.452	32117.588	240.070
$24_{1,23}-24_{1,24}$	35682.974	265.638	35038.894	261.278	34884.776	291.705
$25_{1,24}-25_{1,25}$	38602.748	308.251	37909.726	304.637	37407.035	352.089

Table 4.10. Transition of the $J_{1,J-1}-J_{0,J}$ series of NGLG1

Transition	Ground State		T_1 state		T_2 state	
	Calculated freq. MHz	C.D. correction MHz	Calculated freq. MHz	C.D. correction MHz	Calculated freq. MHz	C.D. correction MHz
$1_{1,0}-1_{0,1}$	20953.052*	-0.057	20937.673*	-0.327	20942.079	-0.351
$2_{1,1}-2_{0,2}$	21073.254*‡	0.243	21055.650*	-0.033	21059.404*	-0.054
$3_{1,2}-3_{0,3}$	21254.539*	0.716	21233.562*	-0.014	21236.320*	0.406
$4_{1,3}-4_{0,4}$	21498.084*	1.389	21472.545	1.090	21473.942	1.050
$5_{1,4}-5_{0,5}$	21805.457*	2.303	21774.110	1.987	21773.754	1.904
$6_{1,5}-6_{0,6}$	22178.607*	3.505	22140.139*	3.171	22137.605*	3.006
$7_{1,6}-7_{0,7}$	22619.867*	5.060	22572.881	4.704	22567.706*	4.405
$8_{1,7}-8_{0,8}$	23131.934*	7.043	23074.941*	6.665	23066.620*	6.162
$9_{1,8}-9_{0,9}$	23717.863*	9.546	23649.267*	9.144	23637.253*	8.359
$10_{1,9}-10_{0,10}$	24381.040*	12.678	24299.131*	12.251	24282.836*	11.095
$11_{1,10}-11_{0,11}$	25125.161*	16.567	25028.105*	16.116	25006.905*	14.496
$12_{1,11}-12_{0,12}$	25954.189*	21.359	25840.028*	20.885	25813.267*	18.716

*Observed transitions
‡Wrongly reported transition.

Table 4.10 (...Contd.)

$13_{1,12}-13_{0,13}$	26872.317*	27.224	26738.959*	26.730	26705.969*	23.947
$14_{1,13}-14_{0,14}$	27883.905*	34.350	27729.133*	33.843	27689.250*	30.420
$15_{1,14}-15_{0,15}$	28993.414*	42.951	28814.892*	42.443	28767.484	38.415
$16_{1,15}-16_{0,16}$	30205.332	53.262	30000.614	52.769	29545.118	48.269
$17_{1,16}-17_{0,17}$	31524.081	65.536	31290.633	65.086	31226.598	60.379
$18_{1,17}-18_{0,18}$	32953.922	80.047	32689.143	79.601	32616.290	75.215
$19_{1,18}-19_{0,19}$	34498.851	97.080	34200.105	96.858	34118.389	93.323
$20_{1,19}-20_{0,20}$	36162.489	116.932	35827.143	116.941	35736.834	115.331
$21_{1,20}-21_{0,21}$	37947.979	139.901	37573.441	140.263	37475.215	141.961
$22_{1,21}-22_{0,22}$	39857.880	166.282	39441.649	167.164	39336.687	174.025

*Observed transitions

Table 4.11. Transitions of the $J_{1,J}-J_{0,J}$ series of NGLG1

Transition	Ground state		T_1 state		T_2 state	
	Calculated freq. MHz	C.D. Correction MHz	Calculated freq. MHz	C.D. Correction MHz	Calculated freq. MHz	C.D. Correction MHz
$1_{1,1}-1_{0,1}$	20833.661*	-0.059	20820.482*	-0.328	20825.538*	-0.352
$2_{1,2}-2_{0,2}$	20715.060	0.218	20704.057*	-0.056	20709.768*	-0.070
$3_{1,3}-3_{0,3}$	20538.093*	0.609	20530.322*	0.329	20537.012*	0.337
$4_{1,4}-4_{0,4}$	20303.886*	1.082	20300.364*	0.800	20308.350*	0.850
$5_{1,5}-5_{0,5}$	20013.941*	1.599	20015.632*	1.323	20025.226*	1.441
$6_{1,6}-6_{0,6}$	19670.141*	2.114	19677.945*	1.858	19689.443*	2.079
$7_{1,7}-7_{0,7}$	19274.749*	2.574	19289.487*	2.357	19303.168*	2.723
$8_{1,8}-8_{0,8}$	18830.409*	2.925	18852.809*	2.772	18868.929*	3.330
$9_{1,9}-9_{0,9}$	18340.134*	3.106	18370.823*	3.050	18389.606*	3.848
$10_{1,10}-10_{0,10}$	17807.324*	3.060	17846.797	3.138	17868.425*	4.221
$11_{1,11}-11_{0,11}$	17235.701*	2.731	17284.338*	2.988	17308.944*	4.390
$12_{1,12}-12_{0,12}$	16629.337*	2.069	16687.375*	2.554	16715.032*	4.293
$13_{1,13}-13_{0,13}$	15992.603*	1.029	16060.130*	1.796	16090.841*	3.867

*Observed transitions.

Table 4.11. Transitions of the $J_{1,J}-J_{0,J}$ series of NGLG1

Transition	Ground state		T_1 state		T_2 state	
	Calculated freq. MHz	C.D. Correction MHz	Calculated freq. MHz	C.D. Correction MHz	Calculated freq. MHz	C.D. Correction MHz
$1_{1,1}-1_{0,1}$	20833.661*	-0.059	20820.482*	-0.328	20825.538*	-0.352
$2_{1,2}-2_{0,2}$	20715.060	0.218	20704.057*	-0.056	20709.768*	-0.070
$3_{1,3}-3_{0,3}$	20538.093*	0.609	20530.322*	0.329	20537.012*	0.337
$4_{1,4}-4_{0,4}$	20303.886*	1.082	20300.364*	0.800	20308.350*	0.850
$5_{1,5}-5_{0,5}$	20013.941*	1.599	20015.632*	1.323	20025.226*	1.441
$6_{1,6}-6_{0,6}$	19670.141*	2.114	19677.945*	1.858	19689.443*	2.079
$7_{1,7}-7_{0,7}$	19274.749*	2.574	19289.487*	2.357	19303.168*	2.723
$8_{1,8}-8_{0,8}$	18830.409*	2.925	18852.809*	2.772	18868.929*	3.330
$9_{1,9}-9_{0,9}$	18340.134*	3.106	18370.823*	3.050	18389.606*	3.848
$10_{1,10}-10_{0,10}$	17807.324*	3.060	17846.797	3.138	17868.425*	4.221
$11_{1,11}-11_{0,11}$	17235.701*	2.731	17284.338*	2.988	17308.944*	4.390
$12_{1,12}-12_{0,12}$	16629.337*	2.069	16687.375*	2.554	16715.032*	4.293
$13_{1,13}-13_{0,13}$	15992.603*	1.029	16060.130*	1.796	16090.841*	3.867

*Observed transitions.

Table 4.11 (...Contd.)

$14_{1,14}-14_{0,14}$	15330.129*	-0.420	15407.081*	0.684	15440.775*	3.051*
$15_{1,15}-15_{0,15}$	14646.763*	-2.301	14732.920	-0.802	14759.440	1.790
$16_{1,16}-16_{0,16}$	13947.507*	-4.622	14042.497	-2.670	14031.598	0.033
$17_{1,17}-17_{0,17}$	13237.452*	-7.375	13340.754	-4.916	13332.104	-2.259
$18_{1,18}-18_{0,18}$	12521.703*	-10.539	12632.659	-7.522	12675.838	-5.113
$19_{1,19}-19_{0,19}$	11805.298*	-14.078	11923.126	-10.456	11957.634	-8.342
$20_{1,20}-20_{0,20}$	11093.125*	-17.939	11216.936	-13.674	11252.206	-12.541
$21_{1,21}-21_{0,21}$	10389.836*	-22.062	10518.659	-17.126	10554.067	-17.086
$22_{1,22}-22_{0,22}$	9699.771*	-26.375	9832.577	-20.746	9877.462	-22.138
$23_{1,23}-23_{0,23}$	9026.891*	-30.800	9162.617	-24.466	9206.298	-27.636
$24_{1,24}-24_{0,24}$	8374.712*	-35.255	8512.286	-28.216	8554.089	-33.506
$25_{1,25}-25_{0,25}$	7746.266*	-39.659	7804.637	-31.923	7923.909	-39.658
$26_{1,26}-26_{0,26}$	7144.234*	-43.935	7284.683	-35.494	7318.888	-45.987

*Observed transitions.

Table 4.12. Transitions of the $J_{1,J}-1^{-1}0_{,J-1}$ series of NGlGl

Transition	Ground state		T_1 state		T_2 state	
	Calculated freq. MHz	C.D. Correction MHz	Calculated freq. MHz	C.D. Correction MHz	Calculated freq. MHz	C.D. Correction MHz
$1_{1,1}-0_{0,0}$	29219.946*	-0.024	29228.748*	-0.092	29252.273*	-0.257
$2_{1,2}-1_{0,1}$	37486.793*	-0.037	37520.304	0.704	37562.581	-0.049

*Observed transitions

Table 4.13. Transitions of the $J_{1,J-1}-1_{0,J-1}$ series of NGlGl

Transition	Ground state		T_1 state		T_2 state	
	Calculated freq. MHz	C.D. Correction MHz	Calculated freq. MHz	C.D. Correction MHz	Calculated freq. MHz	C.D. Correction MHz
$1_{1,0}-0_{0,0}$	29339.337*	-0.022	29345.940*	-0.090	29368.814*	-0.256
$2_{1,1}-1_{0,1}$	37844.987*	-0.012	37871.977	0.727	37912.216	-0.034

*Observed transitions

Table 4.14. Transitions of the $J_{0,J}-J-1_{0,J-1}$ series of MGlG1

Transition	Ground state		T_1 state		T_2 state	
	Calculated freq. MHz	C.D. Correction MHz	Calculated freq. MHz	C.D. correction MHz	Calculated freq. MHz	C.D. Correction MHz
$1_{0,1}-0_{0,0}$	8386.285	0.035	8408.266	0.237	8426.735	0.095
$2_{0,2}-1_{0,1}$	16771.733	-0.255	16816.327	0.760	16852.813	0.020
$3_{0,3}-2_{0,2}$	25155.509	-1.195	25223.975	1.858	25277.577	-0.392
$4_{0,4}-3_{0,3}$	33536.773	-3.112	33631.003	3.816	33700.372	-1.312

Table 4.15. Transitions of the $J_{2,J-2} - J-1_{2,J-3}$ series of NGIG1

Transition	Ground state		T_1 state		T_2 state	
	Calculated freq. MHz	C.D. Correction MHz	Calculated freq. MHz	C.D. Correction MHz	Calculated freq. MHz	C.D. Correction MHz
$3_{2,1} - 2_{2,0}$	25161.346	0.550	25229.621	3.558	25283.140	1.270
$4_{2,2} - 3_{2,1}$	33548.942	-0.783	33642.759	6.089	33711.871	0.812

Table 4.16. Transitions of the $J_{1,J-1} - J-1_{1,J-2}$ series of NGIG1

Transition	Ground state		T_1 state		T_2 state	
	Calculated freq. MHz	C.D. Correction MHz	Calculated freq. MHz	C.D. Correction MHz	Calculated freq. MHz	C.D. Correction MHz
$2_{1,1} - 1_{1,0}$	16891.935	0.045	16934.303	1.053	16970.137	0.317
$3_{1,2} - 2_{1,1}$	25336.793	-0.722	25401.887	2.321	25454.494	0.069
$4_{1,3} - 3_{1,2}$	33780.318	-2.438	33869.986	4.477	33937.394	-0.668

Table 4.17. Transitions of the $J_{2,J-1}-1_{2,J-2}$ series of NGLG1

Transition	Ground state		T_1 state		T_2 state	
	Calculated freq. MHz	C.D. Correction MHz	Calculated freq. MHz	C.D. Correction MHz	Calculated freq. MHz	C.D. Correction MHz
$3_{2,2}-2_{2,1}$	25160.076	1.326	25225.518	1.428	25281.332	1.412
$4_{2,3}-3_{2,2}$	33548.033	3.425	33635.467	3.725	33709.803	3.617

Table 4.18. Transitions of the $J_{1,J}-1_{1,J-1}$ series of NGLG1

Transition	Ground state		T_1 state		T_2 state	
	Calculated freq. MHz	C.D. Correction MHz	Calculated freq. MHz	C.D. Correction MHz	Calculated freq. MHz	C.D. Correction MHz
$2_{1,2}-1_{1,1}$	16653.182	0.072	16698.994	0.124	16736.901	0.161
$3_{1,3}-2_{1,2}$	24979.350	0.016	25048.060	0.062	25104.860	0.052
$4_{1,4}-3_{1,3}$	33304.984	-0.218	33396.635	-0.124	33472.327	-0.182

Table 4.19. Transitions of the $J_{0,J}-J-1_{1,J-1}$ series of NGLG1

Transition	Ground state		T_1 state		T_2 state	
	Calculated freq. MHz	C.D. Correction MHz	Calculated freq. MHz	C.D. Correction MHz	Calculated freq. MHz	C.D. Correction MHz
$4_{0,4}-3_{1,3}$	12998.680	-3.721	13100.681	3.488	13163.160	-1.648
$5_{0,5}-4_{1,4}$	21610.803	-7.415	21736.842	6.120	21812.188	-3.760
$6_{0,6}-5_{1,5}$	30274.480	-12.785	30426.744	10.?25	30512.197	-6.798
$7_{0,7}-6_{1,6}$	38986.992	-20.116	39168.365	15.839	39260.927	-10.905

Table 4.20. Some isolated R-branch transitions of NGLG1

Transition	Ground state		T_1 state		T_2 state	
	Calculated freq. MHz	C.D. Correction MHz	Calculated freq. MHz	C.D. Correction MHz	Calculated freq. MHz	C.D. Correction MHz
$4_{3,1}-3_{3,0}$	33548.117	2.098	33642.013	8.904	33711.439	3.901
$4_{3,2}-3_{3,1}$	33547.001	3.212	33643.147	7.765	33710.127	5.211

Table 4.21. Microwave spectrum of ground state of NGLT

Std dev = 0.403 MHz

Transition	Calculated freq. MHz	Observed freq.* MHz	C. D. Correction MHz
$29_{1,29}-29_{0,29}$	8115.070	8115.081	-112.183
$28_{1,28}-28_{0,28}$	8630.551	8630.580	-102.414
$27_{1,27}-27_{0,27}$	9158.693	9158.630	-92.556
$27_{1,26}-27_{0,27}$	37823.504	37823.896	426.526
$26_{1,26}-26_{0,26}$	9697.486	9697.228	-82.738
$26_{1,25}-26_{0,26}$	36310.608	36310.553	366.675
$25_{1,25}-25_{0,25}$‡	10244.635	10244.330	-73.087
$25_{1,24}-25_{0,25}$	34880.545	34880.404	313.631
$24_{1,24}-24_{0,24}$‡	10798.079	10797.674	-63.726
$24_{1,23}-24_{0,24}$	33531.904	33531.646	266.868
$23_{1,23}-23_{0,23}$‡	11355.345	11354.841	-54.767
$23_{1,22}-23_{0,23}$	32262.739	32262.455	225.863
$22_{1,22}-22_{0,22}$‡	11913.922	11913.301	-46.311
$22_{1,21}-22_{0,22}$	31070.963	31070.741	190.102
$21_{1,21}-21_{0,21}$‡	12471.224	12470.488	-38.442
$21_{1,20}-21_{0,21}$	29954.317	29954.100	159.086
$20_{1,20}-20_{0,20}$‡	13024.615	13023.712	-31.230
$20_{1,19}-20_{0,20}$	28910.410	28910.295	132.334
$19_{1,19}-19_{0,19}$‡	13571.445	13570.605	-24.726
$19_{1,18}-19_{0,19}$	27936.755	27936.715	109.389
$18_{1,18}-18_{0,18}$‡	14109.075	14108.176	-18.962

*Observed transition frequencies are corresponding to the observations of Botskor et al.[40]
‡Transitions not included in the fit.

Table 4.21 (...Contd.)

$18_{1,17}-18_{0,18}$	27030.811	27030.907	89.822
$17_{1,17}-17_{0,17}$ ‡	14634.899	14634.016	-13.952
$17_{1,16}-17_{0,17}$	26190.016	26190.128	73.235
$16_{1,16}-16_{0,16}$ ‡	15146.376	15145.509	-9.691
$16_{1,15}-16_{0,16}$	25411.817	25412.027	59.257
$15_{1,15}-15_{0,15}$ ‡	15641.044	15640.141	-6.161
$15_{1,14}-15_{0,15}$	24693.704	24693.950	47.553
$14_{1,14}-14_{0,14}$ ‡	16116.545	16115.739	-3.324
$14_{1,13}-14_{0,14}$	24033.232	24033.663	37.816
$13_{1,13}-13_{0,13}$ ‡	16570.634	16569.854	-1.134
$13_{1,12}-13_{0,13}$	23428.045	23428.549	29.769
$12_{1,12}-12_{0,12}$ ‡	17001.195	17000.664	0.468
$12_{1,11}-12_{0,12}$	22875.894	22876.381	23.168
$11_{1,11}-11_{0,11}$ ‡	17406.250	17405.673	1.549
$11_{1,10}-11_{0,11}$	22374.653	22375.175	17.793
$10_{1,10}-10_{0,10}$ ‡	17783.966	17783.556	2.182
$10_{1,9}-10_{0,10}$	21922.334	21922.781	13.451
$9_{1,9}-9_{0,9}$ ‡	18132.661	18132.328	2.443
$9_{1,8}-9_{0,9}$	21517.093	21517.592	9.974
$9_{1,9}-8_{2,6}$	14406.498	14406.990	-19.569
$8_{1,8}-8_{0,8}$ ‡	18450.807	18450.597	2.408
$8_{1,7}-8_{0,8}$	21157.241	21157.723	7.216
$7_{1,7}-7_{0,7}$	18737.031	18736.846	2.153
$7_{1,6}-7_{0,7}$	20841.250	20841.740	5.051

‡ Transitions not included in the fit.

Table 4.21 (...Contd.)

$6_{1,6}-6_{0,6}$ ‡	18990.116	18990.130	1.751
$6_{1,5}-6_{0,6}$	20567.756	20568.196	3.372
$6_{0,6}-5_{1,5}$ ‡	31090.831	31089.576	-3.180
$5_{1,5}-5_{0,5}$ ‡	19209.001	19209.040	1.269
$5_{1,4}-5_{0,5}$	20335.560	20335.979	2.088
$5_{1,4}-4_{2,3}$	16803.542	16803.204	-4.415
$5_{0,5}-4_{1,4}$ ‡	22526.398	22525.584	-1.667
$4_{1,3}-4_{0,4}$	20143.636	20144.077	1.126
$4_{1,4}-4_{0,4}$ ‡	19392.780	19393.000	0.768
$4_{0,4}-3_{0,3}$ ‡	33537.076	33536.415	-0.267
$4_{1,3}-3_{1,2}$ ‡	33689.586	33688.922	0.434
$4_{1,4}-3_{1,3}$ ‡	33388.435	33388.467	-0.518
$4_{0,4}-3_{1,3}$ ‡	13996.375	13995.240	-0.568
$3_{1,2}-3_{0,3}$	19991.125	19991.504	0.425
$3_{1,3}-3_{0,3}$	19540.701	19540.866	0.301
$3_{2,1}-2_{2,0}$ ‡	25157.283	25156.214	1.818
$3_{2,2}-2_{2,1}$ ‡	25155.824	25156.214	1.214
$3_{0,3}-2_{0,2}$ ‡	25153.818	25153.334	0.063
$3_{1,2}-2_{1,1}$ ‡	25267.600	25267.142	0.549
$3_{0,3}-2_{1,2}$ ‡	5501.653	5500.896	0.151
$2_{1,1}-2_{0,2}$	19877.343	19877.455	-0.066
$2_{1,2}-2_{0,2}$	19652.165	19652.428	-0.089
$2_{1,1}-1_{0,1}$	36647.036	36646.878	0.106
$2_{1,2}-1_{0,1}$	36421.858	36421.804	0.078

‡ Transitions not included in the fit.

Table 4.21 (...Contd.)

$2_{1,2}-1_{1,1}$	16694.673	16694.807	-0.017
$2_{0,2}-1_{0,1}$	16769.693	16769.306	0.167
$2_{1,1}-1_{1,0}$	16845.262	16844.953	0.472
$1_{1,0}-1_{0,1}$	19801.774	19802.133	-0.366
$1_{1,1}-1_{0,1}$	19726.722	19726.937	-0.367
$1_{1,1}-0_{0,0}$	28111.713	28111.890	-0.247
$1_{0,1}-0_{0,0}$	8384.991	8384.856	0.121
$1_{1,0}-0_{0,0}$	28186.765	28187.105	-0.245

‡ Transitions not included in the fit.

Table 4.22. Rotational and centrifugal distortion constants of the ground state of NGLT

Watson's determinable parameters	Kivelson-Wilson's derived parameters[c]
$A'' = 23957.05$ MHz	$A' = 23957.045$ MHz
$B'' = 4229.96$ MHz	$B' = 4229.515$ MHz
$C'' = 4154.91$ MHz	$C' = 4155.486$ MHz
$\tau_1 = 253.78012$ KHz	$\tau'_{bbcc} = -9.28617$ KHz
$\tau_2 = 24.85182$ KHz	$\tau'_{ccaa} = -889.95927$ KHz
$\tau_3 = 657.88984$ KHz[b]	$\tau'_{aabb} = 1.15302$ MHz
$\tau'_{aaaa} = -1.47810$ MHz	
$\tau'_{bbbb} = -8.43832$ KHz	
$\tau'_{cccc} = -15.97124$ KHz	

Moments of Inertia

$$I_a = 21.095085 \text{ amu } \mathring{A}^2 \text{ [a]}$$

$$I_b = 119.475360 \text{ amu } \mathring{A}^2$$

$$I_c = 121.633441 \text{ amu } \mathring{A}^2$$

$$\Delta = -18.937004 \text{ amu } \mathring{A}^2 \text{ [d]}$$

---

[a] The conversion factor = 505376. MHz amu $\mathring{A}^2$

[b] The value of τ_3 is set using the planarity condition and is not strictly speaking, a determinable parameter.

[c] These parameters are calculated from A'', B'', C'', τ_1, τ_2 and τ_3 and thus obey the planarity conditions used to calculate τ_3.

[d] Inertia defect $\Delta = I_c - I_a - I_b$.

Table 4.22. Rotational and centrifugal distortion constants
of the ground state of NGLT

Watson's determinable parameters		Kivelson-Wilson's derived parameters[c]	
A'' =	23957.05 MHz	A' =	23957.045 MHz
B'' =	4229.96 MHz	B' =	4229.515 MHz
C'' =	4154.91 MHz	C' =	4155.486 MHz
τ_1 =	253.78012 KHz	τ'_{bbcc} =	-9.28617 KHz
τ_2 =	24.85182 KHz	τ'_{ccaa} =	-889.95927 KHz
τ_3 =	657.88984 KHz[b]	τ'_{aabb} =	1.15302 MHz
τ'_{aaaa} =	-1.47810 MHz		
τ'_{bbbb} =	-8.43832 KHz		
τ'_{cccc} =	-15.97124 KHz		

Moments of Inertia

$$I_a = 21.095085 \text{ amu Å}^2 \text{[a]}$$

$$I_b = 119.475360 \text{ amu Å}^2$$

$$I_c = 121.633441 \text{ amu Å}^2$$

$$\Delta = -18.937004 \text{ amu Å}^2 \text{[d]}$$

---

[a] The conversion factor = 505376. MHz amu Å^2

[b] The value of τ_3 is set using the planarity condition and is not strictly speaking, a determinable parameter.

[c] These parameters are calculated from A'', B'', C'', τ_1, τ_2 and τ_3 and thus obey the planarity conditions used to calculate τ_3.

[d] Inertia defect $\Delta = I_c - I_a - I_b$.

Table 4.23. The microwave spectrum of T_1 state of NGLT

Std. dev = 0.128 MHz

Transition	Calculated freq. MHz	Observed[*] freq. MHz	C.D. Correction MHz
$1_{0,1}-0_{0,0}$	8397.245	8397.170	0.095
$1_{1,0}-1_{0,1}$	19866.244	19866.288	-0.216
$2_{0,2}-1_{0,1}$	16794.134	16793.933	0.040
$2_{1,2}-1_{1,1}$	16720.612	16720.718	0.062
$2_{1,1}-2_{0,2}$	19940.491	19940.585	0.076
$7_{1,6}-7_{0,7}$	20886.913	20886.895	4.731
$8_{1,7}-8_{0,8}$	21196.933	21196.860	6.638
$2_{1,1}-1_{1,0}$	16868.382	16868.165	0.332
$9_{1,8}-9_{0,9}$	21549.855	21549.814	9.043
$10_{1,9}-10_{0,10}$	21947.137	21947.113	12.053
$11_{1,11}-11_{0,11}$	22390.393	22390.422	15.796
$12_{1,11}-12_{0,12}$	22881.388	22881.447	20.421
$13_{1,12}-13_{0,13}$	23422.032	23422.164	26.106
$14_{1,13}-14_{0,14}$	24014.373	24014.520	33.056
$15_{1,14}-15_{0,15}$	24660.589	24660.712	41.512
$16_{1,15}-16_{0,16}$	25362.969	25362.952	51.751
$17_{1,16}-17_{0,17}$	26123.910	26123.582	64.092
$18_{1,17}-18_{0,18}^{\dagger}$	26945.886	26945.040	78.902
$19_{1,18}-19_{0,19}^{\dagger}$	27831.440	27832.678	96.595

[*]Observed transition frequencies are corresponding to the observations of Botskor et al.[47]

[†]Transitions not included in the fit.

Table 4.23 (...Contd.)

$20_{1,19}-20_{0,20}$	28783.154	28783.225	117.642
$1_{1,1}-0_{0,0}$	28189.737	28189.772	-0.122
$2_{1,2}-1_{0,1}$	36513.354	36513.270	0.094
$2_{1,1}-1_{0,1}$	36734.625	36734.506	0.116
$2_{1,2}-2_{0,2}$	19719.220	19719.292	0.055
$3_{1,2}-2_{1,1}$	25302.089	25302.079	0.142
$3_{0,3}-2_{0,2}$	25190.310	25190.273	-0.317
$3_{1,3}-2_{1,2}$	25080.714	25080.735	0.016
$3_{0,3}-2_{1,2}^{\dagger}$	5471.089	5471.700	-0.372
$3_{1,2}-3_{0,3}$	20052.271	20052.091	0.536
$4_{1,4}-3_{1,3}^{\dagger}$	33440.357	33436.965	-0.432
$4_{0,4}-3_{1,3}$	13975.739	13975.650	-1.569
$4_{1,3}-3_{1,2}$	33735.214	33735.407	-0.474
$6_{1,6}-6_{0,6}$	19068.536	19068.680	1.995
$7_{1,7}-7_{0,7}$	18819.762	18819.620	2.506
$8_{1,8}-8_{0,8}$	18538.385	18538.415	2.927
$9_{1,9}-9_{0,9}$	18225.583	18225.640	3.196
$10_{1,10}-10_{0,10}$	17882.685	17882.668	3.247
$11_{1,11}-11_{0,11}$	17511.165	17511.085	3.010
$12_{1,12}-12_{0,12}^{\dagger}$	17112.642	17107.689	2.413
$14_{1,14}-14_{0,14}^{\dagger}$	16241.769	16243.350	-0.156

†Transitions not included in the fit.

Table 4.24. T_1 state rotational and centrifugal distortion constants of NGLT

Watson's determinable parameters		Kivelson-Wilson's derived parameters[c]	
A''	= 24028.16 MHz	A' = 24028.152 MHz	
B''	= 4235.45 MHz	B' = 4235.9017 MHz	
C''	= 4161.70 MHz	C' = 4161.3658 MHz	
τ_1	= 219.70376 KHz	τ'_{bbcc} = -15.27099 KHz	
τ_2	= 20.89681 KHz	τ'_{ccaa} = 903.38986 KHz	
τ_3	= 9.28363 MHz[b]	τ'_{aabb} = -668.41510 KHz	
τ'_{aaaa}	= -897.18011 KHz		
τ'_{bbbb}	= -26.50925 KHz		
τ'_{cccc}	= -32.19877 KHz		

Moments of Inertia

$$I_a = 21.032655 \text{ amu } \text{Å}^2 \text{[a]}$$

$$I_b = 119.320497 \text{ amu } \text{Å}^2$$

$$I_c = 121.434990 \text{ amu } \text{Å}^2$$

$$\Delta = -18.918162 \text{ amu } \text{Å}^2 \text{[d]}$$

---

[a] The conversion factor = 505376. MHz amu Å^2

[b] The value of τ_3 is set using the planarity condition and is not, strictly speaking, a determinable parameter

[c] These parameters are calculated from A'', B'', C'', τ_1, τ_2 and τ_3 and thus obey the planarity conditions used to calculated τ_3.

[d] Inertia defect $\Delta = I_c - I_a - I_b$.

Table 4.25. The microwave spectrum of T_2 state of NGLT

std. dev = 0.711 MHz

Transition	Calculated freq. MHz	Observed* freq. MHz	C.D. Correction MHz
$1_{0,1}-0_{0,0}$	8407.848	8407.720	0.118
$1_{1,0}-1_{0,1}$	19929.303	19930.248	-1.017
$2_{0,2}-1_{0,1}$	16815.381	16815.138	0.126
$2_{1,1}-1_{1,0}$	16889.658	16889.371	0.448
$3_{0,3}-2_{0,2}$	25222.281	25221.954	-0.089
$3_{1,2}-2_{1,1}$	25334.105	25333.754	0.418
$4_{1,3}-4_{0,4}$ ‡	20265.262	20266.454	0.530
$4_{1,4}-3_{1,3}$	33482.614	33482.440	-0.396
$6_{1,6}-6_{0,6}$	19131.782	19131.870	1.412
$8_{1,7}-8_{0,8}$ ‡	21260.536	21261.952	6.471
$8_{1,8}-8_{0,8}$	18601.671	18601.430	2.442
$9_{1,9}-9_{0,9}$	18288.863	18288.440	2.752
$10_{1,10}-10_{0,10}$	17945.935	17945.387	2.840
$11_{1,11}-11_{0,11}$	17574.362	17573.614	2.638
$12_{1,12}-12_{0,12}$	17175.766	17175.202	2.080
$13_{1,12}-13_{0,13}$	23486.221	23487.216	27.018
$13_{1,13}-13_{0,13}$	16751.914	16751.184	1.101

*Observed transition frequencies are corresponding to the observations of Botskor et al.[47]

‡ Transition not included in the fit.

Table 4.25 (...Contd.)

$14_{1,14}-14_{0,14}$	16304.709	16304.154	-0.359
$15_{1,14}-15_{0,15}$	24724.629	24724.950	42.707
$15_{1,15}-15_{0,15}$	15836.190	15835.636	-2.355
$16_{1,15}-16_{0,16}$	25426.698	25426.496	52.922
$17_{1,16}-17_{0,17}$	26187.074	26186.176	65.047
$17_{1,17}-17_{0,17}$	14843.964	14844.072	-8.131
$18_{1,17}-18_{0,18}$	27008.145	27009.068	79.358
$18_{1,18}-18_{0,18}$	14324.899	14325.415	-11.971
$19_{1,19}-19_{0,19}$	13793.773	13794.877	-16.465
$2_{1,2}-1_{1,1}$	16741.825	16741.950	-0.115

Table 4.26. Rotational and centrifugal distortion constants of T_2 state of NGLT

Watson's determinable parameters

$A'' = 24097.31$ MHz

$B'' = 4240.74$ MHz

$C'' = 4166.99$ MHz

$\tau_1 = 254.99196$ KHz

$\tau_2 = 21.40973$ KHz

$\tau_3 = 2.50891$ MHz [b]

$\tau'_{aaaa} = -4.08951$ MHz

$\tau'_{bbbb} = -15.13286$ KHz

$\tau'_{cccc} = -21.44358$ KHz

Kivelson-Wilson derived parameters [c]

$A' = 24097.303$ MHz

$B' = 4240.2136$ MHz

$C' = 4167.6511$ MHz

$\tau'_{bbcc} = -14.49948$ KHz

$\tau'_{ccaa} = -1.05281$ MHz

$\tau'_{aabb} = 1.32230$ MHz

Moments of Inertia

$I_a = 20.972299$ amu $\mathring{A}^2$ [a]

$I_b = 119.171654$ amu $\mathring{A}^2$

$I_c = 121.280828$ amu $\mathring{A}^2$

$\Delta = -18.863125$ amu $\mathring{A}^2$ [d]

---

[a] The conversion factor = 505376. amu $\mathring{A}^2$

[b] The value of τ_3 is set using the planarity condition and is not, strictly speaking, a determinable parameter

[c] These parameters are calculated from A'', B'', C'', τ_1, τ_2 and τ_3 and thus obey the planarity conditions used to calculate τ_3.

[d] Inertia defect $\Delta = I_c - I_a - I_b$.

Table 4.27. Transitions of the $J_{1,J-1}-J_{1,J}$ series of NGLT

Transition	Ground state		T_1 state		T_2 state	
	Calculated freq. MHz	C.D. correction MHz	Calculated freq. MHz	C.D. correction MHz	Calculated freq. MHz	C.D. correction MHz
$12_{1,11}-12_{1,12}$	5874.699	22.700	5768.746	18.008	5769.746	19.034
$13_{1,12}-13_{1,13}$	6857.411	30.904	6733.154	24.724	6734.308	25.916
$14_{1,13}-14_{1,14}$	7916.687	41.140	7772.604	33.212	7773.840	34.507
$15_{1,14}-15_{1,15}$	9052.660	53.714	8887.246	43.784	8888.439	45.062
$16_{1,15}-16_{1,16}$	10265.492	68.949	10077.227	56.782	10078.180	57.856
$17_{1,16}-17_{1,17}$	11555.117	87.186	11342.685	72.585	11343.111	73.177
$18_{1,17}-18_{1,18}$	12921.734	108.784	12683.750	91.608	12683.246	91.329
$19_{1,18}-19_{1,19}$	14365.310	134.115	14001.534	114.305	14096.560	112.627
$20_{1,19}-20_{1,20}$	15885.795	163.564	15593.135	141.172	15588.982	137.399
$21_{1,20}-21_{1,21}$	17483.094	197.528	17161.627	172.747	17154.384	165.985
$22_{1,21}-22_{1,22}$	19157.041	236.413	18806.057	209.615	18794.576	198.732
$23_{1,22}-23_{1,23}$	20907.394	280.630	20526.441	252.407	20509.299	235.992

Table 4.27 (...Contd.)

$24_{1,23}-24_{1,24}$	22733.825	330.594	22322.759	301.804	22298.212	278.123
$25_{1,24}-25_{1,25}$	24635.911	386.718	24194.949	358.537	24160.836	325.485
$26_{1,25}-26_{1,26}$	26613.122	449.413	26142.906	423.391	26096.795	378.435
$27_{1,26}-27_{1,27}$	28664.812	519.081	28166.471	497.205	28105.304	437.325
$28_{1,27}-28_{1,28}$	30790.207	596.111	30265.429	580.870	30185.663	502.498
$29_{1,28}-29_{1,29}$	32988.396.	680.873	32439.501	675.338	32336.995	574.287

Table 4.28. Transitions of the $J_{1,J-1}-J_{0,J}$ series of NGLT

Transition	Ground state		T_1 state		T_2 state	
	Calculated freq.	C.D. correction	Calculated freq.	C.D. correction	Calculated freq.	C.D. correction
$1_{1,0}-1_{0,1}$	19801.774*	-0.366	19866.244*	-0.216	19929.303*	-1.017
$2_{1,1}-2_{0,2}$	19877.343*	-0.066	19940.491*	0.076	20003.580	-0.695
$3_{1,2}-3_{0,3}$	19991.125*	0.425	20052.271*	0.536	20115.403	-0.189
$4_{1,3}-4_{0,4}$	20143.636*	1.126	20202.069	1.189	20265.262*	0.530
$5_{1,4}-5_{0,5}$	20335.560*	2.088	20390.539	2.073	20453.810	1.500
$6_{1,5}-6_{0,6}$	20567.756*	3.372	20618.495	2.234	20681.860	2.770
$7_{1,6}-7_{0,7}$	20841.250*	5.051	20886.913*	4.731	20950.390	4.403
$8_{1,7}-8_{0,8}$	21157.241*	7.216	21196.933*	6.638	21260.536*	6.471
$9_{1,8}-9_{0,9}$	21517.093*	9.974	21549.855*	9.043	21613.595	9.065
$10_{1,9}-10_{0,10}$	21922.334*	13.451	21947.137*	12.053	22011.013	12.286
$11_{1,10}-11_{0,11}$	22374.653*	17.793	22390.393*	15.796	22454.407	16.256
$12_{1,11}-12_{0,12}$	22875.894*	23.168	22881.388*	20.421	22945.513	21.114
$13_{1,12}-13_{0,13}$	23428.045*	29.769	23422.032*	26.106	23486.221*	27.018

*Observed transitions.

Table 4.28.(...Contd.)

$14_{1,13}-14_{0,14}$	24033.232*	37.816	24014.373*	33.056	24078.549	34.148
$15_{1,14}-15_{0,15}$	24693.704*	47.553	24660.589*	41.512	24724.629*	42.707
$16_{1,15}-16_{0,16}$	25411.817*	59.257	25362.969*	51.751	25426.698*	52.922
$17_{1,16}-17_{0,17}$	26190.016*	73.235	26123.910*	64.092	26187.074*	65.047
$18_{1,17}-18_{0,18}$	27030.811*	89.822	26945.886*	78.902	27008.145*	79.358
$19_{1,18}-19_{0,19}$	27936.755*	109.389	27831.440*	96.595	27692.333	96.162
$20_{1,19}-20_{0,20}$	28910.410*	132.334	28783.154*	117.542	28642.079	115.789
$21_{1,20}-21_{0,21}$	29954.317*	159.086	29803.627	142.572	29859.805	138.597
$22_{1,21}-22_{0,22}$	31070.963*	190.102	30895.446	171.974	30947.885	164.965
$23_{1,22}-23_{0,23}$	32262.739*	225.863	32061.156	206.506	32108.612	195.296
$24_{1,23}-24_{0,24}$	33531.904*	266.868	33303.230	246.890	33344.156	230.010
$25_{1,24}-25_{0,25}$	34880.545*	313.691	34624.037	293.920	34656.535	269.544
$26_{1,25}-26_{0,26}$	36310.608*	366.675	36025.819	348.459	36047.561	314.341
$27_{1,26}-27_{0,27}$	37823.504*	426.526	37510.600	411.443	37518.931	364.851
$28_{1,27}-28_{0,28}$	39420.757	493.697	39080.309	483.875	39071.663	421.522

*Observed transitions.

Table 4.29. Transitions of the $J_{1,J}-J_{0,J}$ series of NGLA

Transition	Ground state		T₁ state		T₂ state	
	Calculated freq. MHz	C.D. Correction MHz	Calculated freq. MHz	C.D. correction MHz	Calculated freq. MHz	C.D. Correction MHz
$1_{1,1}-1_{0,1}$	19726.722*	-0.367	19792.492	-0.218	19855.551	-1.019
$2_{1,2}-2_{0,2}$	19652.165*	-0.089	19719.220*	0.055	19782.306	-0.719
$3_{1,3}-3_{0,3}$	19540.701*	0.301	19609.677	0.442	19672.800	-0.293
$4_{1,4}-4_{0,4}$	19392.780*	0.768	19464.300	0.918	19527.465	0.230
$5_{1,5}-5_{0,5}$	19209.001*	1.269	19283.676	1.450	19346.884	0.814
$6_{1,6}-6_{0,6}$	18990.116*	1.751	19068.536*	1.995	19131.782*	1.412
$7_{1,7}-7_{0,7}$	18737.031*	2.153	18819.762*	2.506	18883.036	1.974
$8_{1,8}-8_{0,8}$	18450.807*	2.408	18538.385*	2.927	18601.671*	2.442
$9_{1,9}-9_{0,9}$	18132.661*	2.443	18225.583*	3.196	18288.863*	2.752
$10_{1,10}-10_{0,10}$	17783.966*	2.182	17882.685*	3.247	17945.935*	2.840
$11_{1,11}-11_{0,11}$	17406.250*	1.549	17511.165*	3.010	17574.362*	2.638
$12_{1,12}-12_{0,12}$	17001.195*	0.468	17112.642*	2.413	17175.766*	2.080
$13_{1,13}-13_{0,13}$	16570.634*	-1.134	16688.878	1.382	16751.914*	1.101
$14_{1,14}-14_{0,14}$	16116.545*	-3.324	16241.769*	-0.156	16304.709*	-0.359

*Observed transitions

Table 4.29 (...Contd.)

$15_{1,15}-15_{0,15}$	15641.044*	-6.161	15773.342	-2.272	15836.190*	-2.355
$16_{1,16}-16_{0,16}$	15146.376*	-9.691	15285.742	-5.032	15348.517	-4.934
$17_{1,17}-17_{0,17}$	14634.899*	-13.952	14781.224	-8.493	14843.964*	-8.131
$18_{1,18}-18_{0,18}$	14109.075*	-18.962	14262.136	-12.766	14324.895*	-11.971
$19_{1,19}-19_{0,19}$	13571.445*	-24.726	13730.906	-17.710	13793.773*	-16.465
$20_{1,20}-20_{0,20}$	13024.615*	-31.230	13190.019	-23.530	13253.097	-21.610
$21_{1,21}-21_{0,21}$	12471.224*	-38.442	12642.000	-30.176	12705.421	-27.389
$22_{1,22}-22_{0,22}$	11913.922*	-46.311	12089.389	-37.641	12153.309	-33.767
$23_{1,23}-23_{0,23}$	11355.345*	-54.767	11534.715	-45.592	11599.312	-40.696
$24_{1,24}-24_{0,24}$	10798.079*	-63.726	10920.472	-54.914	11045.944	-48.113
$25_{1,25}-25_{0,25}$	10244.635*	-73.087	10429.088	-64.618	10495.649	-55.942
$26_{1,26}-26_{0,26}$	9697.486*	-82.738	9832.913	-74.932	9950.765	-64.094
$27_{1,27}-27_{0,27}$	9158.693*	-92.556	9344.129	-85.762	9413.627	-72.474
$28_{1,28}-28_{0,28}$	8630.551*	-102.414	8814.880	-96.996	8885.999	-80.977
$29_{1,29}-29_{0,29}$	8115.070*	-112.183	8297.129	-108.511	8370.329	-89.498

*Observed transitions.

Table 4.30. Transitions of the $J_{1,J-1}-J-1_{0,J-1}$ series of NGLT

Transition	Ground state		T_1 state		T_2 state	
	Calculated freq. MHz	C.D. correction MHz	Calculated freq. MHz	C.D. correction MHz	Calculated freq. MHz	C.D. correction MHz
$1_{1,1}-0_{0,0}$	28111.713*	-0.247	28189.737*	-0.122	28263.400	-0.900
$2_{1,2}-1_{0,1}$	36421.858*	0.078	36513.354*	0.094	36597.687	-0.593

*Observed transitions

Table 4.31. Transitions of the $J_{1,J-1}-J-1_{0,J-1}$ series of NGLT

Transition	Ground state		T_1 state		T_2 state	
	Calculated freq. MHz	C.D. correction MHz	Calculated freq. MHz	C.D. correction MHz	Calculated freq. MHz	C.D. correction MHz
$1_{1,0}-0_{0,0}$	28186.765*	-0.245	28263.489	-0.121	28337.151	-0.899
$2_{1,1}-1_{0,1}$	36647.036*	0.106	36734.625*	0.116	36818.960	-0.569

*Observed transitions.

Table 4.32. Transitions of the $J_{0,J}-J-1_{0,J-1}$ series of NGLT

Transition	Ground state		T_1 state		T_2 state	
	Calculated freq. MHz	C.D. Correction MHz	Calculated freq. MHz	C.D. Correction MHz	Calculated freq. MHz	C.D. Correction MHz
$1_{0,1}-0_{0,0}$	8384.991*	0.121	8397.245*	0.095	8407.848*	0.118
$2_{0,2}-1_{0,1}$	16769.693*	0.167	16794.134*	0.040	16815.381*	0.126
$3_{0,3}-2_{0,2}$	25153.818*	0.063	25190.310*	-0.317	25222.281*	-0.089
$4_{0,4}-3_{0,3}$	33537.076*	-0.267	33585.416	-1.128	33628.233	-0.636

*Observed transitions

Table 4.33. Transitions of the $J_{2,J-2}-1_{2,J-3}$ series of NGLT

Transition	Ground state		T_1 state		T_2 state	
	Calculated freq. MHz	C.D. Correction MHz	Calculated freq. MHz	C.D. Correction MHz	Calculated freq. MHz	C.D. Correction MHz
$3_{2,1}-2_{2,0}$	25157.283*	1.818	25193.599	1.326	25225.790	1.780
$4_{2,2}-3_{2,1}$	33543.529	2.076	33591.498	1.604	33634.663	1.854

*Observed transitions

Table 4.34. Transitions of the $J_{1,J-1}-1_{1,J-2}$ series of NGLT

Transition	Ground state		T_1 state		T_2 state	
	Calculated freq. MHz	C.D. Correction MHz	Calculated freq. MHz	C.D. Correction MHz	Calculated freq. MHz	C.D. Correction MHz
$2_{1,1}-1_{1,0}$	16845.262*	0.472	16868.382*	0.332	16889.658*	0.448
$3_{1,2}-2_{1,1}$	25267.600*	0.549	25302.089*	0.142	25334.105*	0.418
$4_{1,3}-3_{1,2}$	33689.586*	0.434	33735.214*	-0.474	33778.092	0.082

*Observed transitions

Table 4.35. Transitions of the $J_{2,J-1}-J-1_{2,J-2}$ series of NGLT

Transition	Ground state		T_1 state		T_2 state	
	Calculated freq. MHz	C.D. Correction MHz	Calculated freq. MHz	C.D. Correction MHz	Calculated freq. MHz	C.D. Correction MHz
$3_{2,2}-2_{2,1}$	25155.824*	1.214	25192.754	1.304	25224.504	1.314
$4_{2,3}-3_{2,2}$	33542.484	3.168	33591.612	3.180	33634.013	3.250

*Observed transitions

Table 4.36. Transitions of the $J_{1,J}-J-1_{1,J-1}$ series of NGLT

Transition	Ground state		T_1 state		T_2 state	
	Calculated freq. MHz	C.D. Correction MHz	Calculated freq. MHz	C.D. Correction MHz	Calculated freq. MHz	C.D. Correction MHz
$2_{2,1}-1_{1,1}$	16694.673*	-0.017	16720.612*	0.062	16741.825*	-0.115
$3_{1,3}-2_{1,2}$	25041.690	-0.213	25080.714*	0.016	25112.450	0.012
$4_{1,4}-3_{1,3}$	33388.435*	-0.518	33440.357*	-0.432	33482.614*	-0.396

*Observed transitions.

Transition	Ground state		T$_1$ state		T$_2$ state	
	Calculated freq. MHz	C.D. Correction MHz	Calculated freq. MHz	C.D. Correction MHz	Calculated freq. MHz	C.D. Correction MHz
$3_{0,3}-2_{1,2}$	5501.653*	0.151	5471.089*	-0.372	5439.975	0.630
$4_{0,4}-3_{1,3}$	13996.375*	-0.568	13975.739*	-1.569	13955.434	0.344
$5_{0,5}-4_{1,4}$	22526.398*	-1.667	22514.793	-3.461	22505.455	-1.860
$6_{0,6}-5_{1,5}$	31090.831*	-3.180	31087.311	-6.165	31089.140	-3.997
$7_{0,7}-6_{1,6}$	39688.631	-5.133	39692.200	-9.755	39705.444	-6.822

*Observed transitions.

Table 4.38. Some isolated R-branch transitions of NGLT

Transition	Ground state		T$_1$ state		T$_2$ state	
	Calculated freq. MHz	C.D. Correction MHz	Calculated freq. MHz	C.D. Correction MHz	Calculated freq. MHz	C.D. Correction MHz
$4_{3,1}-3_{3,0}$	33544.899	4.993	33592.968	3.956	33636.294	4.965
$4_{3,2}-3_{3,1}$	33543.178	6.713	33590.868	6.054	33634.702	6.355

Table 4.39.   Rotational and Centrifugal distortion constants
of Allylamine in their ground state

Constant	Value for NGLG1	Value for NGLT
Watson's determinable parameters		
A''	25086.54 MHz	23957.05 MHz
B''	4252.82 MHz	4229.96 MHz
C''	4133.43 MHz	4154.91 MHz
τ_1	123.30996 KHz	253.78012 KHz
τ_2	-20.05883 KHz	24.85182 KHz
τ_3	6.80856 MHz	657.88984 KHz
τ'_{aaaa}	-286.38259 KHz	-1.47810 MHz
τ'_{bbbb}	-49.95033 KHz	-8.43832 KHz
τ'_{cccc}	-56.43834 KHz	-15.97124 KHz
Kivelson-Wilson's parameters		
A'	25086.517 MHz	23957.045 MHz
B'	4251.9116 MHz	4229.515 MHz
C'	4134.4230 MHz	4155.486 MHz
τ'_{bbcc}	-46.01784 KHz	-9.28617 KHz
τ'_{ccaa}	-1.81674 MHz	-889.95927 KHz
τ'_{aabb}	1.98607 MHz	1.15302 MHz
Moments of Inertia and Inertia Defect		
I_a	20.145305 amu $Å^2$	21.095085 amu $Å^2$
I_b	118.833150 amu $Å^2$	119.475360 amu $Å^2$
I_c	122.265528 amu $Å^2$	121.633441 amu $Å^2$
	-16.712927 amu $Å^2$	-18.937004 amu $Å^2$

Table 4.39. Rotational and Centrifugal distortion constants of Allylamine in their ground state

Constant	Value for NGLG1	Value for NGLT
Watson's determinable parameters		
A''	25086.54 MHz	23957.05 MHz
B''	4252.82 MHz	4229.96 MHz
C''	4133.43 MHz	4154.91 MHz
τ_1	123.30996 KHz	253.78012 KHz
τ_2	-20.05883 KHz	24.85182 KHz
τ_3	6.80856 MHz	657.88984 KHz
τ_{aaaa}	-286.38259 KHz	-1.47810 MHz
τ'_{bbbb}	-49.95033 KHz	-8.43832 KHz
τ'_{cccc}	-56.43834 KHz	-15.97124 KHz
Kivelson-Wilson's parameters		
A'	25086.517 MHz	23957.045 MHz
B'	4251.9116 MHz	4229.515 MHz
C'	4134.4230 MHz	4155.486 MHz
τ'_{bbcc}	-46.01784 KHz	-9.28617 KHz
τ'_{ccaa}	-1.81674 MHz	-889.95927 KHz
τ'_{aabb}	1.98607 MHz	1.15302 MHz
Moments of Inertia and Inertia Defect		
I_a	20.145305 amu Å^2	21.095085 amu Å^2
I_b	118.833150 amu Å^2	119.475360 amu Å^2
I_c	122.265528 amu Å^2	121.633441 amu Å^2
	-16.712927 amu Å^2	-18.937004 amu Å^2

CONCLUSIONS

The present study will be very helpful in the following ways:

1.   The centrifugal distortion correction value is large at higher rotational quantum numbers, hence the centrifugal distortion constants will be very helpful for the further study of the spectra at higher rotational quantum numbers.

2.   The centrifugal distortion analysis will be of use in obtaining further support for the assignment of the observed spectra.

3.   Before information on the molecular structure can be obtained, the spectral constants A'', B'', C'' must be corrected for the contribution of distortion. By means of planar relations three values of rotational constants A, B, C can be obtained from different sets* of τ's. The values quoted in Table A for distortion free rotational constants A, B, C have been obtained by using the values extracted from τ_1 and τ_{cccc}, via the planar relations. This gives results which are intermediate between the two sets (extracted from τ_1, τ_2 and τ_2, τ_{cccc}) of rotational constants. Hence with these values of rotational constants the already known structure of the molecule will be refined.

4.   The problem of determining molecular force field has been a subject of keen interest.[48-53] The force constants

─────────────

*Different sets give different values of τ_{abab}, difference between them reflects the breakdown in planarity conditions.

have been calculated theoretically by Coulson et al.[54] and
Anderson[55]. The distortion constants depend explicitly on
the elements of the inverse force field constant matrix. In
particular, under the assumption of small oscillations

$$\tau_{\alpha\alpha\alpha\alpha} = R_{\alpha} \sum_{i,j} J_{\alpha\alpha}^{(i)} J_{\alpha\alpha}^{(j)} F_{ij}^{-1} \quad (\alpha = a, b \text{ or } c)$$

where $R_{\alpha} = -\dfrac{A_{\alpha}^2}{RI_{\alpha}^2}$, $R = \dfrac{10^{-22}}{2h}$ and $A_{\alpha} = \dfrac{h}{8\pi^2 I_{\alpha}}$

is the rotational constant in MHz, F_{ij}^{-1} are the elements of
inverse force constants matrix and $J_{\alpha\alpha}^{(i)} = \dfrac{\partial I_{\alpha\alpha}}{\partial S_i}$ have been
given by Kivelson and Wilson.[20]

So the above study will be helpful for the determination
of force field constants and hence the vibrational frequencies
and Coriolis coupling constants. The importance of supplementing
the vibrational frequency data with vibration-rotation data
has been pointed out by Duncan and Mills.[56-57]

<u>Table A.</u> Ground state rotational constants (distortion free)

	Molecule	Value in MHz
(i)	HNO_3	A = 13010.966
		B = 12099.860
		C = 6260.702
(ii)	DNO_3	A = 12970.519
		B = 11312.726
		C = 6035.038
(iii)	N_2F_4	A = 5576.182
		B = 3189.399
		C = 2813.184
(iv)	NGLG1	A = 25088.484
		B = 4253.212
		C = 4131.473
(v)	NGLT	A = 23958.204
		B = 4230.674
		C = 4153.748

REFERENCES

1. S. C. Wang, Phys. Rev. 34, 243 (1929).

2. R. S. Mulliken, Phys. Rev. 59, 873 (1941).

3. J. H. Van Vleck, Phys. Rev. 33, 467 (1929).

4. B. S. Ray, Zeits. F. Physik 78, 74 (1932).

5. C. H. Townes and A. L. Schawlow, 'Microwave Spectroscopy' McGraw Hill Book Co. (1955).

6. G. W. King, R. M. Hainer and Paul C. Cross, J. Chem. Phys. 11, 27 (1943).

7. M. T. Emerson and D. F. Eggers, Jr., J. Chem. Phys. 37, 251 (1962).

8. H. H. Nielsen, Phys. Rev. 60, 794 (1941).

9. H. H. Nielsen, Phys. Rev. 61, 540 (1942).

10. H. H. Nielsen, Rev. Mod. Phys. 23, 90 (1951).

11. W. H. Shaffer and H. H. Nielsen, Phys. Rev. 56, 188 (1939).

12. W. H. Shaffer and R. P. Schuman, J. Chem. Phys. 12, 504 (1944).

13. R. B. Lawrance and M. W. P. Strandberg, Phys. Rev. 83, 363 (1951).

14. E. B. Wilson, Jr., J. Chem. Phys. 4, 313 (1936).

15. E. B. Wilson, Jr., J. Chem. Phys. 4, 526 (1936).

16. E. B. Wilson, Jr., J. Chem. Phys. 4, 260 (1936).

17. E. B. Wilson, Jr., J. Chem. Phys. 5, 617 (1937).

18. Walter Gordy and Robert L. Cook, 'Microwave Molecular Spectra', Interscience Publishers (1970).

19. A. P. Aleksandrov and M. R. Aliev, J. Mol. Spect. 47, 1 (1973).

20. D. Kivelson and E. B. Wilson, Jr., J. Chem. Phys. 20, 1575 (1952).

21. Z. I. Slawsky and D. M. Dennison, J. Chem. Phys. 7, 509 (1939).

22. J. K. G. Watson, J. Chem. Phys. 45, 1360 (1966).

23. J. K. G. Watson, J. Chem. Phys. 48, 181 (1968).

24. J. K. G. Watson, J. Chem. Phys. 47, 1935 (1967).

25. J. K. G. Watson, J. Chem. Phys. 48, 4517 (1968).

26. W. H. Kirchhoff, J. Mol. Spect. 41, 333 (1972).

27. D. Kivelson and E. B. Wilson, Jr., J. Chem. Phys., 21, 1229 (1953).

28. R. E. Hillger and M. W. P. Strandberg, Phys. Rev. 83, 575 (1951).

29. D. W. Posener and M. W. P. Strandberg, Phys. Rev. 95, 374 (1954).

30. Louis Pierce, Nicholas Di Cianni and Robert H. Jackson, J. Chem. Phys. 38, 730 (1963).

31. R. M. Hainer, P. C. Cross and G. W. King, J. Chem. Phys. 17, 826 (1949).

32. M. D. Harmony, 'Introduction to Molecular Energies and Spectra', Holt, Rinehart and Winston, Inc. (1972).

33. H. C. Allen and P. C. Cross, 'Molecular Vib-Rotors', John Wiley and Sons, Inc. (1963).

34. D. M. Dennison, Rev. Mod. Phys. 3, 280 (1931).

35. D. J. Millen and J. R. Morton, Chem. and Ind. 954 (1956).

36. D. J. Millen and J. R. Morton, J. Chem. Soc. 1523 (1960).

37. A. P. Cox and J. M. Riveros, J. Chem. Phys. 42, 3106 (1965).

38. J. W. Fleming, Chem. Phys. Letters 25, 553 (1974).

39. D. R. Lide, Jr. and D. E. Mann, J. Chem. Phys. 31, 1129 (1959).

40. E. Hirota, J. Chem. Phys. $\underline{42}$, 2071 (1965).

41. S. Kondo, E. Hirota and Y. Morino, J. Mol. Spect. $\underline{28}$, 471 (1968).

42. E. Hirota, J. Mol. Spect. $\underline{35}$, 9 (1970).

43. A. N. Murty and R. F. Curl, Jr., J. Chem. Phys. $\underline{46}$, 4176 (1967).

44. K. V. L. N. Sastry, S. C. Das, W. V. F. Brooks and A. Bhaumic, J. Mol. Spect. $\underline{31}$, 54 (1969).

45. G. Roussy, J. Demaison, I. Botskor and H. D. Rudolph, J. Mol. Spect. $\underline{38}$, 535 (1971).

46. I. Botskor, H. D. Rudolph and G. Roussy, J. Mol. Spect., $\underline{53}$, 15 (1974).

47. I. Botskor, H. D. Rudolph and G. Roussy, J. Mol. Spect. $\underline{52}$, 457 (1974).

48. D. Kivelson, J. Chem. Phys. $\underline{22}$, 904 (1954).

49. L. Pierce, J. Chem. Phys., $\underline{24}$, 139 (1956).

50. M. G. K. Pillai and R. F. Curl, Jr., J. Chem. Phys., $\underline{37}$, 2921 (1962).

51. R. L. Cook, J. Chem. Phys., $\underline{42}$, 2927 (1965).

52. G. E. Herberich, R. H. Jackson and D. J. Millen, J. Chem. Soc. (A) 336 (1966).

53. A. M. Mirri and E. Mazzariol, Spectrochim. Acta $\underline{22}$, 785 (1966).

54. C. A. Coulson and B. M. Deb, Int. J. Quant. Chem. Symp. $\underline{V}$, 411 (1971).

55. A. B. Anderson, J. Chem. Phys. $\underline{58}$, 381 (1973).

56. J. L. Duncan and I. M. Mills, Spectrochimica Acta $\underline{20}$, 523 (1964).

57. J. L. Duncan and I. M. Mills, Spectrochimica Acta $\underline{20}$, 1089 (1964).

APPENDIX

· The microwave spectrum of Difluoramine (NF_2H) was studied by Lide (J. Chem. Phys. <u>38</u>, 456 (1963)) who reported the microwave spectrum of the molecule up to J=19 in the frequency region 15-36 GHz. In fitting the data to the rigid rotator formula, he found that there is discrepancy between observed and calculated values of several MHz even at fairly low J values. He found that the Q-branch transition frequencies can be fitted satisfactorily (within ±14 MHz) by introducing a single term of the form $-D_{JK} K_{-1}^2 J (J+1)$. However, good agreement was not found for the R-branch transitions. For example, the value for the $9_{2,7}-8_{3,5}$ (R-branch) transition differed by 33 MHz from the observed value.

The molecule NF_2H is a near prolate symmetric top with allowed b- and c-type rotational transitions, nineteen transitions were observed by Lide which make the centrifugal distortion analysis possible for this molecule. The analysis of the spectrum was performed in the same lines as discussed in Chapter 2 of the thesis. The results of the analysis are shown in Table A1 and the rotational and centrifugal distortion constants are given in Table A2 along with the distortion free rotational constants. It is gratifying to note from the table A1 that the agreement between the observed and the calculated values from the present study has come to within $\pm$ 0.06 MHz.

Table A1. Microwave spectrum of NF_2H

Std. dev = 0.035 MHz

Transition	Observed freq. MHz	Calculated freq. MHz	Obs-cal freq. MHz	C.D. Correction MHz
$3_{0,3}-2_{1,2}$	19583.52	19583.522	-0.002	-0.683
$3_{0,3}-2_{1,1}$	15088.89	15088.905	-0.015	-0.513
$4_{1,4}-4_{0,4}$	35523.72	35523.702	0.018	1.144
$4_{0,4}-3_{1,2}$	32497.20	32497.218	-0.018	-2.422
$5_{1,5}-5_{0,5}$	32241.07	32241.062	0.008	2.778
$6_{1,6}-5_{2,3}$	26234.22	26234.247	-0.027	-4.235
$6_{1,6}-6_{0,6}$	28653.12	28653.121	-0.001	5.001
$6_{1,6}-5_{2,4}$	24705.13	24705.103	0.027	-3.361
$7_{1,6}-6_{2,5}$	33895.25	33895.260	-0.010	-18.696
$7_{1,7}-7_{0,7}$	24928.93	24928.989	-0.059	7.735
$7_{1,6}-6_{2,4}$	30861.65	30861.627	0.023	-16.408
$8_{1,8}-8_{0,8}$	21237.18	21237.172	0.008	10.778
$9_{2,7}-8_{3,6}$	22429.00	22429.013	-0.013	8.910
$9_{1,9}-9_{0,9}$	17728.35	17728.287	0.063	13.834
$9_{2,7}-8_{3,5}$	22778.60	22778.575	0.025	8.175
$10_{1,10}-9_{2,8}$	27046.08	27046.083	-0.003	18.233
$17_{2,16}-17_{1,16}$*	36008.70	36008.703	-0.003	155.277
$18_{2,17}-18_{1,17}$	29946.50	29946.533	-0.033	164.200
$19_{2,18}-19_{1,18}$	24567.50	24567.466	0.034	168.244

*This line was written as $17_{2,16}-17_{1,17}$.

Table A2. Rotational and centrifugal distortion constants of NF_2H

Watson's determinable parameters			Kivelson-Wilson's derived parameters		
A''	=	53019.806 MHz	A'	=	53019.781 MHz
B''	=	10895.809 MHz	B'	=	10895.832 MHz
C''	=	9307.5468 MHz	C'	=	9307.5898 MHz
τ_1	=	84.096 KHz	τ'_{bbcc}	=	-48.915 KHz
τ_2	=	-17.498 KHz	τ'_{ccaa}	=	46.735 KHz
τ_3	=	2.183 MHz	τ'_{aabb}	=	86.275 KHz
τ'_{aaaa}	=	3.64289 MHz			
τ'_{bbbb}	=	-78.81664 KHz			
τ'_{cccc}	=	-33.5131 KHz			

Distortion free rotational constants

$$A = 53019.768 \text{ MHz}$$

$$B = 10895.819 \text{ MHz}$$

$$C = 9307.610 \text{ MHz}$$